

Gas Phase Acetoxylation of Methyl Aromatics to their Corresponding Esters over PdSb/TiO₂ Catalysts: Activation, Steady-State Operation, Deactivation and Regeneration



Dissertation
zur
Erlangung des akademischen Grades
doctor rerum naturalium (Dr. rer. nat.)
der Mathematisch-Naturwissenschaftlichen Fakultät
der Universität Rostock

vorgelegt von

M.Sc. Neetika Madaan

geboren am 13.04.1984 in Neu Delhi, Indien

aus Rostock

Rostock : 02.08.2011

Name: Neetika Madaan

Defense date: 20th December 2011 at 14:00 hr (Tuesday)

Defense place: Likat Seminarraum, Universität Rostock

Thesis Title: Gas Phase Acetoxylation of Methyl Aromatics to their Corresponding Esters over PdSb/TiO₂ Catalysts: Activation, Steady-State Operation, Deactivation and Regeneration

Referees

1. Prof. Dr. Angelika Brückner

Leibniz Institute for Catalysis
University Rostock
Albert Einstein Str 29a
18059, Rostock
Germany

2. Dr. habil. Andreas Martin

Leibniz Institute for Catalysis
University Rostock
Albert Einstein Str 29a
18059, Rostock
Germany

3. Prof. Dr. Erhard Kemnitz

Institut für Chemie
Humboldt-University in Berlin
Brook-Taylor-Str. 2
12489 Berlin-Adlershof
Germany

Declaration

I hereby declare that the work presented in this thesis entitled, "Gas Phase Acetoxylation of Methyl Aromatics to their Corresponding Esters over PdSb/TiO₂ Catalysts: Activation, Steady-State Operation, Deactivation and Regeneration" is entirely original and was carried out by me independently at Leibniz Institute for Catalysis, Germany under the supervision of Dr. habil. Andreas Martin, Supervisor and Dr. V.N. Kalevaru, Project leader. I further declare that this thesis has not formed the basis for the award of any degree or diploma, fellowship or similar title of any University or Institution.

Date : 02.08.2011

Leibniz Institute for Catalysis

University Rostock, Rostock

Germany

(Neetika Madaan)

Abstract

Partial oxidation reactions using oxygen as oxidant are of great scientific and economic interest. There are several challenges involved in controlling the oxidation path towards the desired product and the sustainable availability of a large number of oxygenates resp. One such example is the selective oxidation of toluene (Tol) to benzyl acetate (BA) belonging to the reaction type of acetoxylation that takes place in the presence of acetic acid and oxygen. Acetoxylation of simple olefins like ethylene to vinyl acetate and propylene to allyl acetate are very well known and important commercial processes. The extension of this work from simple olefins to aromatics is an interesting reaction from both the academic and industrial points of view. BA is a fruity smell ester, which is commonly used in perfumery, food, cosmetic industries etc. Even more, BA can be easily hydrolysed to the highly demanded benzyl alcohol. Benzyl alcohol is widely used in various chemical industries but unfortunately at the moment it is manufactured through the environmental unfriendly route of chlorination of toluene via benzyl chloride and subsequent hydrolysis.

The selective gas phase oxidation of toluene to benzyl acetate has been found to proceed effectively over supported PdSb/TiO₂ catalysts. Thus, PdSb/TiO₂ is taken as a model catalyst for all the studies in this thesis. From the research reported on the PdSb system used in the present acetoxylation reaction, it was found that these catalysts need a long induction period (10-12 h) to reach maximum and stable performance but however suffers with fast deactivation due to the accumulation of carbon. One of the factors found to influence the catalytic activity of PdSb and to reach the induction period was the Pd particle size. Pd particles size of about 50-100 nm was found to be necessary to show better activity in this reaction. However, long induction period, low initial activity and easy deactivation were some of the common problems related to this system.

In view of this, the thesis aimed at the preparation, characterization, and catalytic testing with varying reaction parameters to overcome the above mentioned problems. Catalysts are subjected to various thermal pre-treatment atmospheres to check their influence on the stability of the catalyst. Reaction conditions were optimized with the main goal to obtain highly active and selective catalysts. Furthermore a detail study on the deactivation and regeneration of the catalysts is presented to improve the economic worth of the system. Extension of this reaction with various substituted toluene to produce corresponding esters was also studied.

Catalyst samples with 10 wt% Pd and 16 wt% Sb (10Pd16Sb/TiO₂ (anatase)) were prepared using a two step impregnation technique. In the first step Sb₂O₃ is impregnated

over the titania (anatase) support, and in the second step the solid obtained from the first step was impregnated over PdCl_2 . The catalyst thus obtained was subjected to suitable thermal treatment before catalyst testing. Heterogeneously catalyzed acetoxylation runs in the gas phase were performed in a micro catalytic fixed-bed, vertical and tubular Hastelloy[®] C reactor (length 250 mm; i.d. 9.4 mm). The product stream was analyzed on-line by gas chromatography (Shimadzu GC-2010) using a WCOT-fused silica capillary column (60 m, 0.32 mm) and a FID detector equipped with a methaniser. Highly purified (> 99.99) gases were used for thermal treatment and for catalytic tests. The nature of the catalysts was investigated by using different characterization methods such as ICP-OES, C.H.N.S, TG-DTA, XRD, BET surface area, XPS, TEM, etc.

Different thermal pre-treatment procedures with respect to temperature and atmosphere showed a clear influence on the catalytic performance. $10\text{Pd}16\text{Sb}/\text{TiO}_2$ catalyst pre-treated in the reactor at $300\text{ }^\circ\text{C}/2\text{h}/\text{air}$ showed low initial activity which increased with time up to a toluene conversion (X-Tol) of 65 % and a yield of BA (Y-BA) of 54 %, but its performance started to deactivate quickly. Deactivation of the catalyst is accounted due to carbon deposits and agglomeration of the particles during the reaction. $10\text{Pd}16\text{Sb}/\text{TiO}_2$ catalysts were also treated externally at $600\text{ }^\circ\text{C}$ in air, He and in $10\%\text{H}_2/\text{He}$. Catalytic results obtained revealed that samples treated under helium showed long-term stability (up to 25 h on-stream) compared to other calcined catalysts. Significant change in the distribution of Pd and Sb was also observed with time depending on thermal pre-treatment given. Homogeneously intermixed particles with Pd : Sb ratio of 3-5 was noticed in helium pre-treated catalyst, whereas inhomogeneous distribution of Pd and Sb was seen in air pre-treated catalyst. Surface characterization by XPS showed that the extent of reduction of oxidised Pd species during the course of the reaction also found to depend upon the thermal pre-treatment given to the fresh catalyst. The more stable helium calcined catalysts showed slow reduction of the surface PdO_x species.

The reaction parameters including temperature, feed rates of toluene, acetic acid, oxygen content and gas hourly space velocity for the acetoxylation of toluene to benzyl acetate were optimized. The aim was to improve the conversion of toluene and selectivity of benzyl acetate (S-BA) with minimum formation of by products. The optimization of the testing results revealed that a reaction temperature of $210\text{ }^\circ\text{C}$ and molar ratio of toluene : acetic acid : oxygen : inert gas was set to 1 : 4 : 3 : 16 with a gas hourly space velocity of 2688 h^{-1} were most suitable.

The $10\text{Pd}16\text{Sb}/\text{TiO}_2$ solid calcined in He showed a stable performance up to 25 h on-stream. However, afterwards the catalyst underwent rapid deactivation afterwards down

to X-Tol = 18 % and Y-BA = 12 %. A significant loss of oxidised Pd from the surface and coke deposition was believed to be the main reason for the loss of catalytic activity. The deactivated catalysts were then treated in air for 2 h to burn-off carbon at four different temperatures in the range from 250 to 400 °C. Treatment of the deactivated catalysts at 250 °C and 300 °C in air was effective in restoring the lost activity of the catalysts, whereas higher temperatures of 350 °C and 400 °C treated catalysts could not restore the lost activity. The nature of the regenerated catalysts was studied in detail to understand the difference in the performance of catalysts treated below 300 °C and above that. Catalysts treated at 300 °C in air was effective mainly in two ways such as i) restoration of enough oxidised Pd species on the surface and ii) removal of carbon deposits. As a result, the catalyst could easily regain its activity. In contrast, the catalysts treated at 350 °C and above failed to restore oxidised Pd. Additionally, a surface loss of Sb and total Pd was also observed at 350 °C and above due to the possible migration of Sb and Pd to deeper layers and the formation of carbides which in turn also affected the activity.

The effect of the reaction pressure on the performance of 10Pd16Sb/TiO₂ calcined in helium was also tested. Reaction pressure ranging from 1-10 bar showed marked improvement on the performance of the catalyst. The conversion of toluene increased from 34 to 75 % and the selectivity of the product increased from 74 to 100 % when the reaction pressure rose from 1 bar to 6 bar. However, reaction pressure beyond 6 bar showed some detrimental effect on the selectivity of the catalyst. Furthermore, it was found that the pressure has a pronounced effect on the long-term stability of the sample. The catalyst treated at lower pressure showed comparable long-term stability to the one treated at higher pressure. TEM analysis gave evidence for the formation of pure big Pd particles of size ~100 nm, and smaller particles (2 nm) containing mainly Sb for the higher pressure treated samples. A distinct separation of Pd and Sb distribution was observed at 6 and 8 bar, whereas at lower pressure Pd and Sb was spread together throughout, in the particle sizes ranging from 2 to 100 nm. Even more, surface analysis showed the faster reduction of oxidised Pd at higher reaction pressure (4 bar and above), which leads to the generation of Pd^{δ-} species. These Pd^{δ-} species are known to be detrimental for the stability of the catalyst in the acetoxylation reaction. The best reaction pressure to obtain the highest performance (X-Tol = 75 % and S-BA = 100 %) of the catalysts was found to be 6 bar.

One of the thesis goals was an extension of the acetoxylation of toluene to other derivatives of toluene. Thus, catalytic runs were carried out using various substituents in ortho, meta and para positions with varying electron withdrawing and/or donating groups (-Cl, -F, -OMe, -Me) using 10Pd16Sb/TiO₂ catalyst. Surprisingly, the derivatives of

toluene were found to be not active in this catalytic system. DFT calculations indicated that the substituted toluenes are not easily adsorbed on the Pd(111) catalyst surface under the reaction conditions applied compared to toluene and therefore no further reaction was possible.

Zusammenfassung

Partialoxidationen sind von großem Interesse, da sie es oft ermöglichen in lediglich einem Oxidationsschritt mit umweltfreundlichen und leicht zugänglichen Oxidationsmitteln wie Sauerstoff das gewünschte Produkt zu erhalten. Eine wichtige Gruppe der Partialoxidationen sind Acetoxylierungen, bei denen aus Kohlenwasserstoffen in Gegenwart von Essigsäure und Sauerstoff Acetate gebildet werden. Lange bekannt und wichtige industrielle Prozesse sind Acetoxylierungen von einfachen Olefinen wie Ethen zu Vinylacetat und Propen zu Allylacetat. Von akademischem und auch industriellem Interesse ist der Übergang von einfachen Olefinen zu Aromaten als Ausgangsstoff. Aus diesem Grunde wurde in dieser Arbeit die Acetoxylierung von Toluol zu Benzylacetat näher untersucht.

Benzylacetat ist ein fruchtig riechender Ester, der u. a. in der Parfüm-, Lebensmittel- und Kosmetikindustrie verwendet wird. Außerdem kann das hergestellte Benzylacetat leicht zu Benzylalkohol hydrolysiert werden, was ein wichtiges Lösungsmittel in der Farben-, Lack- und Tintenindustrie ist. Heutzutage wird Benzylalkohol über die Chlorierung von Toluol hergestellt; ein Prozess, der durch die Freisetzung von großen Mengen von HCl und der Bildung des krebserzeugenden Zwischenproduktes Benzylchlorid die Umwelt sehr stark belastet.

In früheren Arbeiten wurde gezeigt, dass die selektive Oxidation von Toluol zu Benzylacetat effektiv an PdSb/TiO₂-Katalysatoren abläuft. Daher wurde dieses System exemplarisch in dieser Arbeit für weiter führende verwendet. Ein Nachteil dieser Katalysatoren waren lange Induktionszeiten von 10 h bis 12 h und die schnelle Desaktivierung aufgrund von Kohlenstoffablagerungen. Die katalytische Aktivität und auch die Induktionszeit wurden dabei u. a. durch die Größe der Pd-Partikel beeinflusst. Erst Pd-Partikel mit einer Größe zwischen 50 und 100 nm sind ausreichend aktiv. Ziel der vorliegenden Arbeit war deshalb, durch eine Optimierung der Reaktionsbedingungen die lange Induktionszeit zu verkürzen und eine Desaktivierung zu vermeiden. Ein weitere Zielsetzung war es, für die desaktivierten Katalysatoren eine geeignete Regenerationsprozedur zu entwickeln.

Die Katalysatorproben mit 10 Gew.-% Pd und 16 Gew.-% Sb (10Pd16Sb/TiO₂ (Anatas)) wurden über eine zweistufige Imprägnierung hergestellt. Im ersten Schritt wurde der TiO₂-Träger mit Sb₂O₃ und im zweiten Schritt der dabei erhaltene Feststoff mit einem Pd-Precursor imprägniert. Der resultierende Katalysator wurde anschließend einer passenden thermischen Vorbehandlung unterzogen. Die Austestung zur heterogen katalysierten Acetoxylierung in der Gasphase wurde in einem Festbettreaktor (Länge 250 mm, Innendurchmesser 9,4 mm) durchgeführt. Der Produktstrom wurde

über on-line Gaschromatographie (Shimadzu GC-2010) mit Hilfe einer WCOT-Quarzglas-Kapillarsäule (60 m, 0,32 mm) und einem FID mit integriertem Methanisator analysiert. Für die thermische Vorbehandlung und die katalytischen Austestungen wurden hochreine Gase (>99,99) verwendet. Die Katalysatoren wurden mit Hilfe verschiedener Charakterisierungsmethoden untersucht wie z. B. ICP-OES, C.H.N.S., TG-DTA, XRD, BET-Oberflächenbestimmung, XPS und TEM.

Bei verschiedenen thermischen Vorbehandlungen, die sich in Temperatur und Atmosphäre unterschieden, konnte ein deutlicher Einfluss auf die katalytischen Eigenschaften gefunden werden. Der 10Pd16Sb/TiO₂ Katalysator, der im Reaktor unter Luft bei 300 °C für 2 Stunden aktiviert wurde, zeigte eine geringere Anfangsaktivität, die sich mit der Zeit zu einem Toluolumsatz (X-Tol) von 65 % und einer Ausbeute an Benzylacetat (Y-BA) von 54 % erhöhte. Nach Erreichen dieser Maximalwerte desaktivierte der Katalysator schnell. Die Desaktivierung des Katalysators ist auf Kohlenstoffablagerungen und Agglomeration der Partikel während der Reaktion zurückzuführen. Weitere 10Pd16Sb/TiO₂ Katalysatoren wurden extern bei 600 °C unter Luft, He bzw. 10 % H₂/He vorbehandelt. Die in der He Atmosphäre vorbehandelten Proben zeigten im Gegensatz zu den anderen Katalysatoren eine Langzeitstabilität von bis zu 25 Stunden Laufzeit. Deutliche Unterschiede in der Verteilung von Pd und Sb konnten in Abhängigkeit der Vorbehandlung beobachtet werden. Bei den He vorbehandelten Proben wurden Mischpartikel mit einem Pd : Sb-Verhältnis von 3-5 gefunden, während die Vorbehandlung in Luft zu einer uneinheitlichen Verteilung von Pd und Sb führte. Die Charakterisierung der Oberfläche mittels XPS zeigte, dass auch die Reduktionsgeschwindigkeit der oxidierten Pd-Spezies während der Reaktion von der thermischen Vorbehandlung des Katalysators abhängt. Bei den stabileren, unter He kalzinierten Katalysatoren tritt nur eine langsame Reduktion der PdOx-Spezies an der Oberfläche auf.

Verschiedene Reaktionsparameter wie Druck, Feed-Zusammensetzung und Temperatur wurden für die Acetoxylierung von Toluol zu Benzylacetat mit dem Ziel optimiert den Toluol-Umsatz und die Benzylacetat-Selektivität (S-BA) zu erhöhen und die Bildung von Nebenprodukten zu minimieren. Die Optimierung der Reaktionsbedingungen zeigte, dass eine Reaktionstemperatur von 210 °C und ein Stoffmengenverhältnis von Toluol : Essigsäure : Sauerstoff : Inertgas mit 1 : 4 : 3 : 16 bei einer Raumgeschwindigkeit von 2688 h⁻¹ am besten geeignet waren.

Der unter Helium kalzinierte 10Pd16Sb/TiO₂-Feststoff war bis zu 25 h Laufzeit stabil. Anschließend desaktivierte der Katalysator und Umsätze bzw. Ausbeuten gingen auf 18 und 12 % zurück. Analytische Untersuchungen an den desaktivierten Proben ergaben, dass der Verlust der Aktivität einhergeht mit einer deutlichen Abnahme des Anteils von

oxidiertem Pd und der Ablagerung von Kohlenstoff auf der Katalysatoroberfläche. Die desaktivierten Proben wurden daher für 2 h bei vier verschiedenen Temperaturen zwischen 250 °C und 400 °C in Luft behandelt, um Kohlenstoff zu entfernen. Die Behandlung von desaktivierten Katalysatoren bei 250 °C und 300 °C war erfolgreich, um die Aktivität wieder herzustellen, wohingegen eine Vorbehandlung bei höheren Temperaturen bei 350 und 400 °C nicht erfolgreich war. Die regenerierten Katalysatoren wurden detailliert untersucht, um diese Unterschiede zu verstehen. Bei Katalysatoren, die bei 300 °C behandelt wurden, wurde Pd auf der Oberfläche reoxidiert und der Kohlenstoff entfernt, wodurch der Katalysator seine verlorene Aktivität wieder erlangte. Bei Katalysatoren, die bei höheren Temperaturen als 300 °C behandelt wurden, gelang die Oxidation des Palladiums nicht. Zusätzlich wurde ein Verlust von Oberflächen-Sb und -Pd bei Temperaturen von 350 °C und darüber beobachtet. Mögliche Ursache ist die Migration von Sb und Pd in tiefere Schichten und/oder die Bildung von Carbiden, welche auch die Aktivität der Katalysatoren beeinflussen.

Ebenfalls wurde der Einfluss des Reaktionsdruckes auf den in He vorbehandelten 10Pd16Sb/TiO₂ getestet. Der Reaktionsdruck im Bereich von 1 bis 10 bar zeigte einen deutlichen Einfluss auf die Leistungsfähigkeit des Katalysators. Der Umsatz von Toluol erhöhte sich von 34 auf 75 % und die Selektivität zum gewünschten Produkt Benzylacetat von 74 auf sogar 100 % bei einer Drucksteigerung von 1 auf 6 bar. Ein Reaktionsdruck oberhalb von 6 bar zeigte dagegen einen nachteiligen Effekt auf die Selektivität des Katalysators. Weiterhin wurde gefunden, dass der Reaktionsdruck einen deutlichen Einfluss auf die Stabilität der katalytischen Leistungsfähigkeit mit der Laufzeit hat. Die bei niedrigeren Drücken genutzten Proben zeigten eine bessere Stabilität als solche, die bei höheren Drücken eingesetzt wurden. Grund ist die schnellere Ablagerung von Kohlenstoffspezies bei höheren Drücken. Die TEM Analyse ergab, dass sich reine Pd Partikel in der Größe von ca. 100 nm und kleinere Partikel (2 nm), die hauptsächlich Sb enthalten, bei höheren Drücken bilden. Dagegen war bei niedrigeren Drücken Pd und Sb immer gemeinsam in Partikeln zwischen 2 und 100 nm zu finden. Zusätzlich war in der Oberflächenanalyse eine schnellere Reduktion des oxidierten Pd bei höheren Drücken (≥ 4 bar) zu beobachten, welche zur Bildung sogenannter Pd^{δ-} Spezies führte. Diese sind bekanntermaßen schädlich für die Katalysatorstabilität in der Acetoxylierung. Der am besten geeignete Reaktionsdruck lag bei 6 bar; bei diesem Reaktionsdruck wurde ein Toluol-Umsatz von 75 % bei einer 100 %igen Selektivität zu BA erreicht.

Weiterhin wurde im Laufe der Arbeiten versucht, die Acetoxylierung an Toluolderivaten durchzuführen. Hierzu wurden katalytische Versuche mit unterschiedlichen Substituenten in ortho-, meta- und para-Position durchgeführt. Dabei

wurden sowohl elektronenziehende als auch -schiebende Substituenten (-Cl, -F, -OMe, -Me) eingesetzt. Überraschenderweise wurde für alle Toluolderivate keine Aktivität festgestellt. Zum Verständnis dieses Verhaltens wurden Berechnungen mit Hilfe der Differential-Funktional-Theorie (DFT) durchgeführt. Abschätzungen ergaben, dass substituierte Toluole unter den gewählten Reaktionsbedingungen nicht auf einer Pd(111) Oberfläche adsorbieren können. Dadurch sind eine weitere Reaktion der Toluolderivate und die Bildung der gewünschten Acetate nicht möglich.

Dedicated
To my beloved parents....

Acknowledgements

This work has been conducted from July 2008 until July 2011 in the research group of “Heterogeneous Catalytic Processes” at Leibniz Institute for Catalysis (LIKAT) at the University Rostock, Germany.

First and foremost, I would like to extend my utmost gratitude and thankfulness to my supervisor **Dr. habil. Andreas Martin**, for giving me an opportunity to work on this project. I am obliged for his patience, motivation, enthusiasm, and immense knowledge. His perpetual energy and liveliness spirit guided me all the time of research and during writing of this thesis. In addition, he was always accessible and willing to help his students with their research. I appreciate all his contributions of time, ideas, and funding to make my Ph.D. experience productive and stimulating. In every sense, none of this work would have been possible without him.

I am truly grateful to **Dr. V.N. Kalevaru**, for his outstanding assistance and numerous scientific discussions. I am thankful to him for guiding me and teaching the research skills. His excellent knowledge, perception and personal experience have a great impact on my thesis. I am obliged for his patience with my flaws and for believing in me and encouraging me throughout this study.

My most sincere thanks go to **Prof. Angelika Brückner**, her wide knowledge and her logical way of thinking have provided a strong basis for the present thesis. She has always tried to put me and my work on the right track. I thank her for her valuable support and guidance to make my goals achievable.

Special thanks to **Dr. Jörg Radnik**, I deeply admire his persistent and meticulous attitude. I am grateful to his valuable support and assistance throughout this work. His insightful discussions and suggestions about the research are highly valued.

It is also my pleasure to thank **Prof. Bernhard Lücke** for his ready assistance whenever required.

In addition my thanks go to Analytical staff members of the LIKAT for their timely assistance, who have involved in the analytics of this work particularly: Dr. U. Bentrup, Dr. M. Schneider and Dr. M.-M. Pohl.

I would like to thank Marek Checkinski, Creative Quantum, for carrying out DFT calculations.

I also like to extend my thanks to all the members of Dr. habil. A. Martin's group for directly or indirectly extending their help during the work.

My time at LIKAT was made enjoyable in large part due to many of my friends and work buddies that became a part of my life. I am grateful to all friends, Suresh, Martina, Piyali, Hanh, Hanan, Ailing, Naresh, Shoubhik, Tobias, who have spent their precious time for my backpacking and for being stress busters. Thanks for our memorable parties, barbecues, night outs and trips around and making my stay here fun-filled and pleasurable.

My lovely friends back home, who were just a “phone-call away” at any odd hour of time, Amrita, Kanika, Megha, Pulkit, Rika, Samudra, Simmi, Smita warmth of their love and understanding has always given me immense strength.

Finally, I would like to deeply thank my parents and family members for pampering me and showering unconditional love on me throughout. Their unflagging love and encouragement in all my pursuits living far away from them is so much treasured. And most of all for my loving, supportive, and patient fiancé Stanislav, whose faithful support and companionship throughout my Ph.D. work is so appreciated. Thank you.

Neetika Madaan

Plan of the thesis

The content of the present thesis is divided into eight chapters on the basis of a general introduction to acetoxylation, literature survey, experimental part, characterization techniques and performance of catalysts subjected to different conditions.

- Chapter 1** deals with the introduction about catalysis in general and palladium catalysis in particular. A literature survey on oxidation and acetoxylation reaction displaying some concepts on catalytic applications is given. Objectives of the thesis are also presented.
- Chapter 2** explains the impregnation method of titania supported PdSb catalyst preparation, basic characterization techniques, details on experimental set up procedures and evaluation of the catalysts for gas phase reactions are described.
- Chapter 3** includes the catalytic data obtained by subjecting the 10Pd16Sb/TiO₂ catalysts under varying the thermal pre-treatment (air, He, 10%H₂/He). Catalytic performance of those catalysts under each atmosphere is described and evaluated with the help of BET surface area, XRD, TEM, XPS etc. in detail.
- Chapter 4** demonstrates the catalytic data from the optimization of the reaction parameters (T, GHSV, toluene, acetic acid and oxygen concentration). The influence of each parameter on the performance is discussed.
- Chapter 5** presents a broad study of the deactivation and regeneration of the 10Pd16Sb/TiO₂ catalysts. Optimization of regeneration conditions for the deactivated catalysts with different temperatures (250-400 °C) and duration are also given. These catalysts are characterized by BET surface area, ICP, XRD, TGA, DTA, XPS, TEM etc. at different stages of reaction.
- Chapter 6** shows the catalytic data obtained by studying the effect of varying reaction pressure on the catalytic activity. The reaction pressure is varied from 1 to 10 bar. The performance of such testing along with the nature of the catalysts is described herein.
- Chapter 7** describes the catalytic results obtained by testing the gas phase acetoxylation on various substituted toluenes in presence of acetic acid and oxygen.
- Chapter 8** summarizes the results of the investigations; an outlook for future research on the gas phase acetoxylation reaction is given.

Content

1	Introduction and Literature Survey	1
1.1	Catalysis – Science and global market segment.....	2
1.2	Palladium metal in catalysis	3
1.3	Palladium in oxidation catalysis	4
1.4	Palladium in acetoxylation.....	5
1.5	Deactivation and regeneration of the palladium catalysts	10
1.6	Objectives of the thesis	12
2	Experimental Methods and Equipments	13
2.1	Methods of catalyst preparation	14
2.1.1	Preparation of the 10Pd16Sb/TiO ₂ catalysts.....	15
2.2	Catalyst Characterization	16
2.2.1	Thermal analysis (TA)	17
2.2.2	Carbon analysis	17
2.2.3	Inductively coupled plasma optical emission spectroscopy (ICP-OES)	17
2.2.4	BET surface area and pore size distribution	18
2.2.5	X-ray diffraction (XRD).....	19
2.2.6	X-ray photoelectron spectroscopy (XPS)	20
2.2.7	Transmission electron microscopy (TEM)	20
2.3	Experimental Setup for catalytic tests	21
2.3.1	Calculations	23
2.4	Density Functional Theory studies	24
3	Effect of varying thermal pre-treatment on the activity and stability of 10Pd16Sb/TiO₂ catalysts	25
3.1	Studies on 10Pd16Sb/TiO ₂ catalyst pre-treated at 300 °C in air without external pre-treatment	26
3.1.1	Time-on-stream behaviour of 10Pd16Sb/TiO ₂ catalyst pre-treated in the reactor (in situ) without any external pre-treatment.....	26
3.1.2	Characterization of the 10Pd16Sb/TiO ₂ catalysts pre-treated at 300 °C in air at different stages of the reaction.....	27

3.1.2.1	BET surface areas and Elemental analysis	27
3.1.2.2	FT-IR studies	29
3.1.2.3	X-ray diffraction	29
3.1.2.4	Morphological studies: TEM, STEM-EDX.....	31
3.1.2.5	X-ray photoelectron spectroscopy	34
3.2	Effect of external pre-treatment (600 °C/4 h) and atmosphere (air, He and 10%H ₂ /He) on the stability of 10Pd16Sb/TiO ₂ solids.....	36
3.2.1	Time-on-stream behaviour of 10Pd16Sb/TiO ₂ catalysts subjected to pre calcination in air and He at 600 °C/4 h	37
3.2.2	Catalyst characterization of 10Pd16Sb/TiO ₂ catalyst treated in 600 °C air and helium.....	38
3.2.2.1	Elemental analysis and BET surface areas	38
3.2.2.2	X-ray diffraction studies	39
3.2.2.3	Transmission electron microscopy	40
3.2.2.4	X-ray photoelectron spectroscopy	41
3.3	Summary and Conclusions.....	43
4	Optimization of acetoxylation reaction conditions for 10Pd16Sb/TiO₂ - He calcined catalyst.....	45
4.1	Influence of reaction temperature.....	46
4.2	Influence of toluene feed rate and acetic acid : toluene feed.....	46
4.3	Influence of oxygen : toluene ratio and feed space velocity	47
4.4	Study of diffusion limitations in the system	48
4.5	Summary and Conclusions.....	50
5	Deactivation and Regeneration studies on using the 10Pd16Sb/TiO₂ - He calcined catalyst.....	53
5.1	Time-on-stream behaviour of the 10Pd16Sb/TiO ₂ - He catalyst.....	54
5.2	Characterization of the 10Pd16Sb/TiO ₂ - He catalyst at different stages of reaction.....	54
5.2.1	Elemental analysis and BET surface area.....	55
5.2.2	Carbon analysis.....	55
5.2.3	Transmission electron micrographs.....	56

5.2.4	X-ray photoelectron spectroscopy.....	57
5.3	Regeneration of 10Pd16Sb/TiO ₂ - He calcined catalyst.....	58
5.3.1	Carbon analysis	61
5.3.2	BET surface area and pore size distribution	61
5.3.3	X-ray diffraction.....	62
5.3.4	Transmission electron microscopy.....	64
5.3.5	X-ray photoelectron spectroscopy.....	65
5.3.6	Effect of regeneration time (2, 4 and 6 hours) at 300 °C in air	68
5.4	Summary and Conclusions	69
6	Effect of reaction pressure on the performance of 10Pd16Sb/TiO₂ - He catalyst.	71
6.1	Calculation of the dew point for the reaction mixture	72
6.2	Time-on-stream performance of the 10Pd16Sb/TiO ₂ - He catalyst with varying pressure.....	73
6.3	Characterization of catalysts used under different pressures	76
6.3.1	Extent of carbon formation on 10Pd16Sb/TiO ₂ - He catalyst with varying reaction pressure	77
6.3.2	BET surface area and pore size distribution	77
6.3.3	X-ray diffraction.....	79
6.3.4	Transmission electron microscopy.....	80
6.3.5	X-ray photoelectron spectroscopy.....	81
6.4	Summary and Conclusions	83
7	Acetoxylation of various substituted toluenes	85
7.1	Catalytic data for various substituted toluenes in the acetoxylation reaction	86
7.2	Potential reaction steps.....	88
7.3	Density Functional Theory studies	88
7.3.1	Evaluation of the properties/nature of the substrates without catalyst	89
7.3.1.1	Homolytic and hetrolytic C–H bond cleavage of toluene and its derivatives of the benzylic carbon	89
7.3.1.2	Thermodynamics of the reaction of the toluene and its derivatives to form products	91

7.3.2	Evaluation of the interaction of the substrates with Pd(111) catalyst surface	91
7.3.2.1	Adsorption studies of toluene and its derivatives on the Pd(111) surface	91
7.3.2.2	Cleavage of the C–H bond on the adsorbed toluene and its derivatives on the Pd(111) surface	94
7.4	Summary and Conclusions.....	95
8	Overall summary and outlook	97
9.	References	101

1 Introduction and Literature Survey

This chapter aims to introduce the scientific framework of this thesis. Various aspects about oxidation catalysis, the role of palladium in catalysis and in particular, in acetoxylation reactions are illuminated. The aim of the thesis is formulated focussing the research on the influence of reaction parameters, deactivation phenomena, regeneration procedures and influence of substituents on the toluene reactant conversion and product selectivity over PdSb/TiO₂ catalysts.

1.1 Catalysis – Science and global market segment

Catalysis as the science of the acceleration of chemical processes due to lowering of the reaction energy barrier is a key technology of the 21st century (Fig. 1). A catalyst is a substance which takes part in the reaction, affects the rate of reaction but is not consumed in it. It usually participates in various chemical transformations at different stages of the reaction, and may be inhibited, deactivated or destroyed by secondary processes (e.g. coking). Nature is filled with many catalysts in the form of enzymes; we deal with catalysis even in our day to day life. Many catalytic reactions are taking place inside a human body, which are vital for its sustenance. Catalysis is a highly interdisciplinary field with great challenges to scientists and engineers [1, 2]. The production of most industrially important chemicals involves catalysis. Estimates [3] indicate that 90 % of all commercially produced chemical products involve catalysts at some stage in the process of their manufacture. According to the BCC Research study [4] for all types of chemical catalysts, a total market of almost \$2.7 billion in 2010, growing at a compound annual growth rate of about 2.5 % to more than \$3 billion in 2015. World demand for overall chemical synthesis, petroleum refining and polymerization catalysts is expected to rise 6.3 % per year to \$17.2 billion in 2014 [5].

There are chiefly 3 fields for catalysis, namely bio-catalysis (reaction where the catalyst is an enzyme), homogeneous catalysis (the catalyst is in the same phase as the reactants) and heterogeneous catalysis (the catalyst is in different phase than reactants).

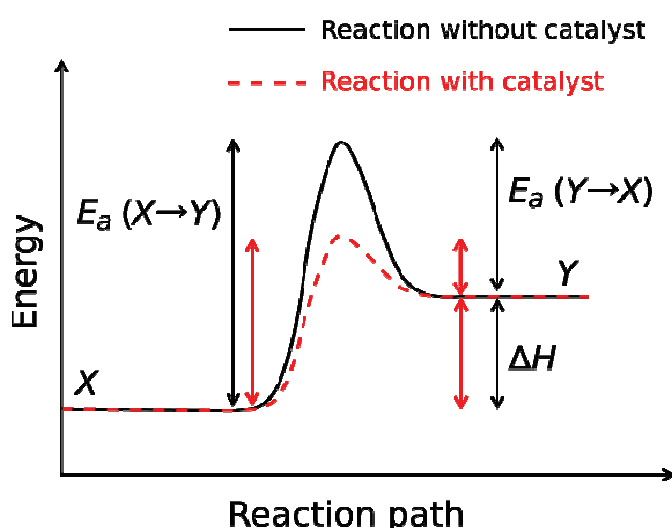


Fig. 1 The non-catalytic vs. catalytic pathway during a chemical reaction|

Among them, heterogeneous catalysis is of an integral importance to the world's economy. For example, heterogeneous catalysts have diverse industrial applications in

the chemical, food, pharmaceutical, automobile and petrochemical industries. Around 80 % of industrial catalytic processes are heterogeneous in nature. Heterogeneous catalysis is also finding new applications in emerging areas such as fuel cells, green chemistry, cleaning of waste and exhaust gas streams, nanotechnology and bio-refining / biotechnology [6].

One should note that during a catalytic reaction usually the following steps occur:

- i). Transport of reactants and energy from the bulk up to the catalyst pellet exterior surface
- ii). Transport of reactants and energy from the external surface into the porous pellet
- iii). Adsorption of reactants on the catalyst surface
- iv). Chemical reaction
- v). Desorption of products at the catalytic sites
- vi). Transport of products from the catalyst interior to the external surface of the pellet
- vii). Transport/diffusion of products into the bulk fluid

These above 7 steps decide the outcome of the catalytic reaction. Rate of a reaction is dependent on one of the steps which is slowest and is called as rate determining step. In the flowing sections we will deal with various catalysis aspects of only Pd metal.

1.2 Palladium metal in catalysis

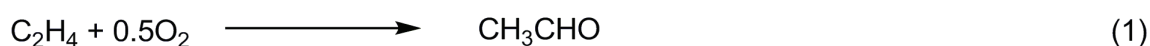
Palladium is a rare and lustrous silvery-white metal, which was discovered in 1803 by William Hyde Wollaston, an English Chemist. He named it after the asteroid Pallas. Naturally occurring palladium is composed of seven isotopes. Worldwide annual Pd production in June 2011 reached 6.8 M. oz. [7]. The Palladium deposits are extensively found in the Norite belt of the Bushveld igneous complex in the Transvaal, South Africa, USA, Ontario, Canada and in Russia. Nearly 80 % of the world palladium production is concentrated in mainly two countries: the Russian Federation and South Africa [8]. In early 2011, price of palladium has seen ranging between a low of US\$ 753 per ounce to a high of US\$ 858 per ounce [9].

Palladium metal/oxides are scientifically important materials that have found several applications in the field of catalysis. More stable and active catalysts were obtained by dispersing palladium on suitable supports of required physical properties. Palladium possesses variable oxidation states; 0, +1, +2, +4 oxidation states; the +4 oxidation state is rarely found. Until now a good numbers of valuable reactions in the homogeneous catalysis are carried out using Pd as a key catalyst [10-12], but beyond the scope of this thesis. In the heterogeneous catalysis the Pd is widely used for hydrogenation reactions [13-15], dehydrogenations, hydrodehalogenations [16-19] and petroleum cracking [20], water gas shift [21, 22], steam reforming [23-26] etc.

1.3 Palladium in oxidation catalysis

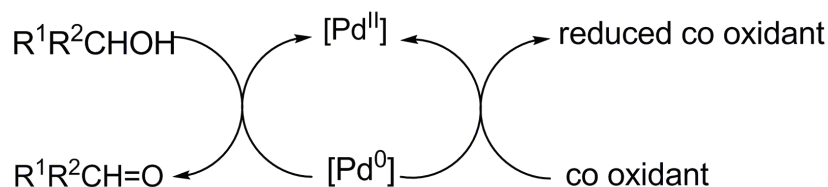
A direct and controlled partial oxidation of various hydrocarbons to get desired oxygenates is one of the greatest challenges in heterogeneous catalysis. The major problem in oxidation reactions is to prevent the further oxidation of the desired products into the unwanted by-products, e.g. the thermodynamically favoured carbon oxides. This difficulty can be overcome to a larger extent by carrying out controlled oxidation in presence of efficient catalyst and auxiliaries catching intermediate oxidation states. For example, the partially oxidized intermediate in ammoxidation of aromatics is quenched by ammonia to form a nitrile [27]. In acetoxylation, oxidation is carried out over Pd-containing solids and in presence of acetic acid which prevents the further oxidation.

Synthesis of acetaldehyde



Palladium, in its various forms is known to be an excellent catalytic component in different types of oxidation reactions. It is possibly the most active and versatile transition metal in use for various synthesis, catalyzing both oxidative and non-oxidative reactions.[28, 29]. A well-known example include the Wacker process [30] In Wacker process, ethylene and oxygen are treated by an acidified water solution of palladium and cupric chlorides which yields acetaldehyde (eq. 1).

The oxide state of Pd is used in a combustion catalyst, for example in the automotive catalyst and for the oxidation reactions [31, 32]. From the literature, it is also known that Pd based catalysts are used for oxidation reactions via Pd(II) catalysis [33-36]. Pd is generally very active even under ambient conditions [37-39] and in some reactions Pd is catalytically highly selective as well e.g. [40-45]. Palladium catalysed processes have also been widely studied for the oxidation of primary and secondary alcohols for e.g. [46, 47]. Reduction of Pd^{II} is to Pd⁰, and the restoration of oxidative species by the addition into the reaction of stoichiometric amounts of a co-oxidant is shown in the Scheme 1.

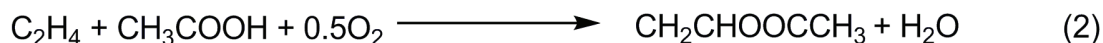


Scheme 1. Palladium based redox cycle for the oxidation of alcohols

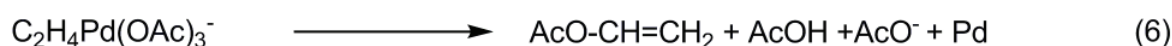
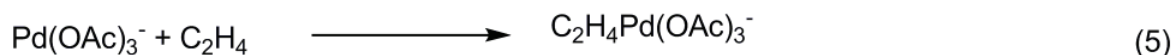
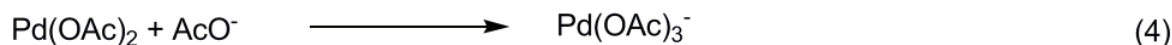
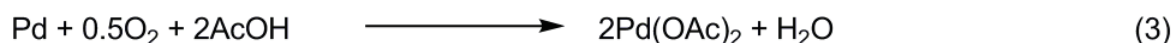
Additionally, Pd is unaffected by many chemical reagents. It was supported on many different carriers like titania, zirconia, alumina, alkaline earth salts, and carbonates, silica and other supports and was used widely for various investigations.

1.4 Palladium in acetoxylation

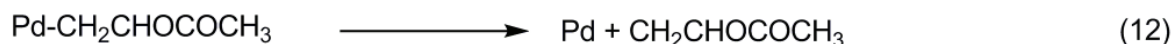
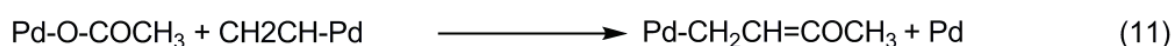
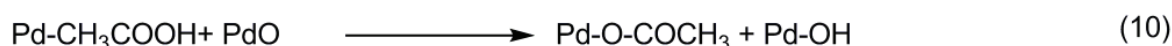
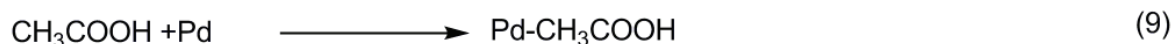
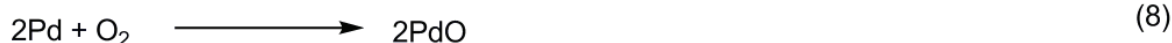
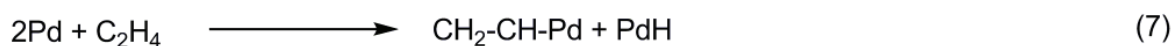
Acetoxylation reaction of ethylene to vinyl acetate



Acetoxylation reactions are the reactions in which a hydrogen atom is replaced by an acetate group in an oxidizing atmosphere with the formation of water. The reaction is applicable to vinyl, allyl, benzyl and aryl hydrogen. The most widely used chemistry is the acetoxylation of ethylene in the presence of oxygen over a palladium-based catalyst (eq. 2.). The commercial production of vinyl acetate monomer (VAM) involves a heterogeneous process [48, 49]. In the heterogeneous process, this reaction is catalyzed by metallic palladium. The overall reaction is the same as for the homogeneous process. The initial work on acetoxylation of ethylene and acetic acid to produce vinyl acetate was studied by Moiseev during the 1960's [50]. Moiseev's results claimed that the Wacker process for the manufacture of acetaldehyde could be altered in favour of the formation of vinyl acetate by using PdCl_2 as a catalyst. The technical acetoxylation process was developed by Knapsack and Hoechst [48] in cooperation with National distillers and Bayer [51]. Since the discovery of this process, extensive studies have been focused on improving the catalyst, which is reflected by the hundreds of patents [52, 53] in this field even nowadays, many patents are being filed every year. All catalyst employed are palladium based [49, 54]. Another metal such as gold [55] (e.g., Pd/Au/K at 0.56/0.25/2.9 wt%) [56] or cadmium [57, 58] (e.g., Pd/Cd/K at 2.1/2.0/2.4 wt%) [56] is added as moderator; an alkali metal salt is added in large access. Silica is generally used as a supporting material. The gold-based and cadmium-based catalysts are, respectively, eggshell-loaded or uniformly impregnated. Many other formulations are patented as well, but have proved to be less economic. This process is operated at 140 to about 190 °C and 5 to 12 atm pressure [49]. The temperature has to be raised over the time to compensate for the aging of the catalyst. In general, the reaction temperature is kept low to have less combustion. The space-time yield of vinyl acetate is increased with both the total pressure and the partial oxygen pressure. Considerable work regarding industrial application has been reported [59-66] on various Pd-based catalysts however, there is no consent regarding the reaction mechanism and the nature of the active sites/intermediates in VAM synthesis. In literature two mechanisms has been proposed on the generation of vinyl acetate from ethylene. One of the mechanism proposed is by Samanos et al. [67], this mechanism involves the coupling of ethylene directly with chemisorbed acetate. The resulting acetoxy ethyl-Pd intermediate is formed first and then it undergoes β -hydride elimination to form VAM.

Possible mechanistic route for the synthesis of vinyl acetate by Samanos et al.

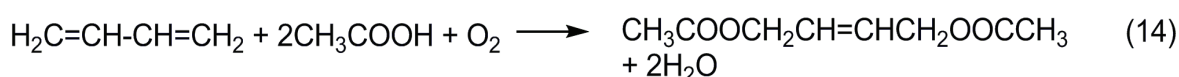
The other mechanism is proposed by Nakamura et.al [68]. They proposed that reaction involves the coupling of ethylene directly with chemisorbed acetate. The resulting acetoxy ethyl-Pd intermediate undergoes β -hydride elimination to form VAM.

Possible mechanistic route for the synthesis of vinyl acetate by Nakamura et al.

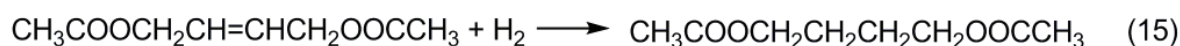
Apart from the olefin acetoxylation the Pd catalysed acetoxylation of dienes to produce corresponding esters has also gained more importance in synthetic chemistry. One such example is 1,4-butanediol, which is useful industrial product for producing polybutylenetetrathalate or as a raw material for making tetrahydrofuran, pyrrolidone, etc. It has been produced from acetylene [69], propylene [70], 1,3 butadiene [71].

Synthesis of 1,4-butanediol via acetoxylation of 1,3-butadiene

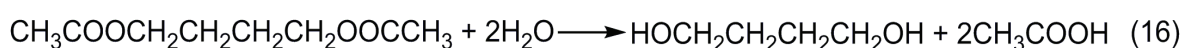
i) acetoxylation of 1,3-butadiene over noble metals for making 1,4-diacetoxybutene-2



ii) hydrogenation 1,4-diacetoxybutene-2 into 1,4-diacetoxybutane

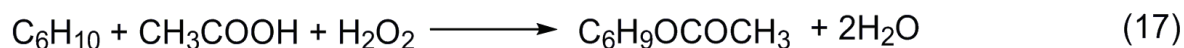


iii) hydrolysis of 1,4-diacetoxybutane into 1,4-butanediol

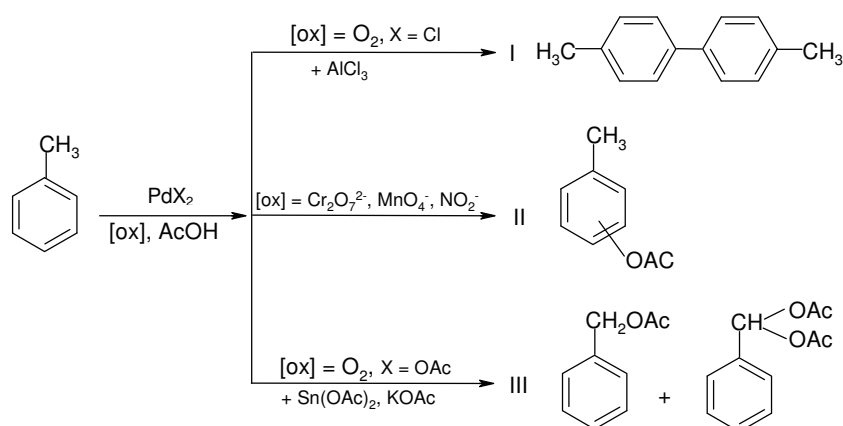


Shinohara [72] has studied the gas phase acetoxylation of 1,3-butadiene over Pd-KOAc and Sb, Bi and Te promoted Pd-KOAc catalysts. They reported the higher activity and selectivity (towards 1,4-diacetoxybutene-2, the desired product) by adding the promoter to Pd-KOAc catalyst compared to the Pd-KOAc.

Acetoxylation of cyclohexene to 2-cyclohexenyl acetate in presence of H_2O_2



Jia et al. [73] has studied the allylic acetoxylation of cyclohexene to produce 2-cyclohexenyl acetate using hydrogen peroxide in acetic acid over palladium(II) catalyst. They reported that the acetoxylation reaction competes with the epoxidation by the peracetic acid generated in situ in this system. The increase of the concentration of palladium catalyst and addition of benzoquinone enhance the acetoxylation considerably. According to them, the palladium-catalyzed acetoxylation of olefins using H_2O_2 as oxidant appears essentially as a metal centred nucleophilic attack by two nucleophiles, i.e. H_2O_2 and AcOH on the olefin co-ordinated to palladium in π or π -allyl mode, in competition with a non metal-centred epoxidation of the olefin by the peracetic acid generated in situ. Thus the selectivity of the reaction is strongly depending on the coordination mode (π or π -allyl), and the strength of the coordination of the olefins to Pd. A further aspect of this reaction supports from the ambivalent role of H_2O_2 , which can oxidize olefin to ketone, re-oxidize Pd^0 or Pd-H to Pd(II), or re-oxidize hydroquinone to benzoquinone.



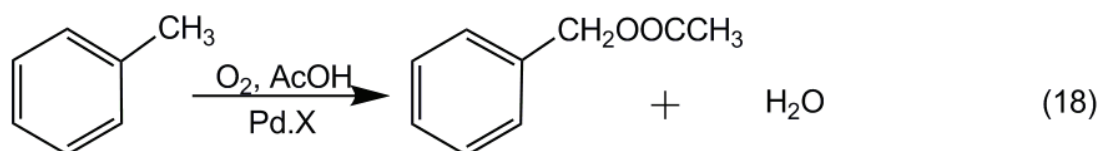
Scheme 2. Various routes for oxidation of toluene using palladium containing catalysts

Over the past two decades the Pd catalysed acetoxylation of alpha-olefins and alkyl aromatics hydrocarbons (toluene and various substituted toluenes as well) has become an increasingly attractive and, in some instances, the only route for the selective synthesis of vinylic, allylic or benzylic alcohols and esters [74-76]. Depending upon the reaction conditions and the nature of catalysts applied, the Pd catalysed oxidation of

toluene can be directed in three different ways such as i) the formation of bitolyls [77, 78], ii) tolyl acetates [79, 80], iii) benzyl acetate and benzylidene diacetate [76, 81-83] as shown in Scheme 2.

In this thesis acetoxylation of toluene (Tol) with acetic acid (AcOH) to benzyl acetate (BA) via gas phase oxidation will be reported in detail. Benzyl acetate is naturally found in plants such as jasmine, hyacinth, gardenias and azaleas. BA because of its fruity aroma is used chiefly in the perfume and food industry (for making chewing gum, gelatine desserts, candy, ice cream, etc.), it is also used in chemicals industry, notably as a solvent for cellulose acetate.

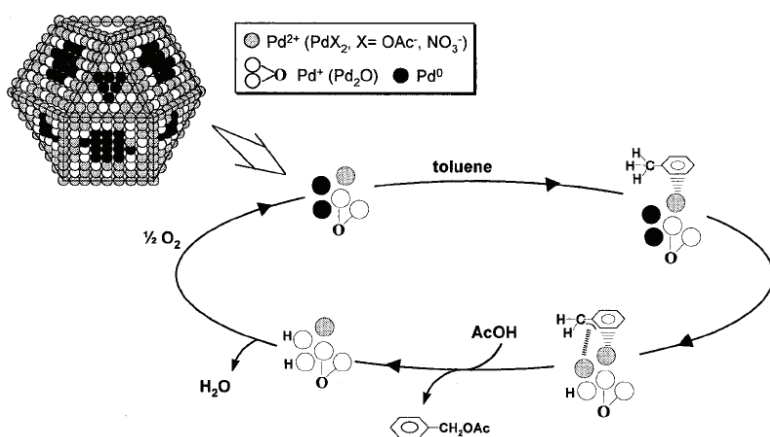
Acetoxylation of toluene to benzyl acetate



Global demand for benzyl acetate ranges from 5,000 to 10,000 tonnes/annum. Benzylic aldehydes, alcohols and its derivatives are widely used as end products and intermediates in the flavours and fragrances industry. Benzylic alcohol is used as a base chemical for the dilution of perfumes, as local anaesthetics and for applications in the textile industry. Benzylic alcohols may also serve as intermediates for the synthesis of insecticides, such as synthesis of permethrin by esterification of 3-phenoxybenzyl alcohols by a chrysanthemic acid derivative [84]; also the intermediates formed can be further used for various industrially important chemicals. Demand and consumption of such alcohols/esters got more importance in an industrialised world. Hence supply of the same becomes a necessity. In this context, using more effective and economic synthesis of such esters/alcohols by the means of catalysis will be of higher interests.

Many groups have been studying acetoxylation of toluene to produce benzyl acetate via single step in gas phase, but still the reaction route to produce benzyl acetate is not much understood and explored till now. Nothing more than suggestions have been reported from few authors, as it is often difficult to ascribe the mechanism. One of the mechanisms was proposed by a Japanese group, Kaneda et al., as shown in Scheme 3. [85]. They speculated a possible mechanism for the acetoxylation of Tol, catalyzed by the 8-shell Pd cluster. An ensemble of the cationic Pd species (Pd^+ and Pd^{2+}) and Pd^0 were found on the giant Pd surface and plays a vital role in this reaction. The initial step is a π -bond interaction between toluene and the cationic Pd^{2+} species. The second step is the rupture of the methyl C-H bond of toluene by a neighbouring Pd^0 to form a π -benzyl Pd adduct together with formation of a Pd-H species. This is followed by an

attack of CH_3COO^- anion on a benzylic position to yield benzyl acetates and H_2O . Pd atoms readily reacts with oxygen species of the neighbouring Pd_2O to give H_2O , regenerating the Pd^0 species. The Pd_2O species could be easily reformed by the dissociative adsorption of molecular oxygen on the surface of Pd^0 species. However detailed study on the reaction mechanism and the reaction pathway is still unknown.



Scheme 3. Proposed reaction mechanism for toluene acetoxylation with Pd catalyst [85].

From the literature [75, 81, 86], it is known that Pd based catalysts are widely used for acetoxylation reactions in general, and toluene acetoxylation in particular [87, 88]. Most of the work reported so far was carried out under liquid-phase conditions and in batch reactors in heterogeneous catalysis. However, there is not much success in the gas phase acetoxylation of toluene; very low yields of acetoxylation products were claimed [89]. Komatsu et al.[90] reported acetoxylation of toluene over different SiO_2 -supported inter-metallic Pd compounds like Pd_2Ge , Pd_5Ga_2 , Pd_3Pb , Pd_3Bi , etc. and only a maximum yield of BA around 7 % could be achieved. Very recently, our group [91-93] reported that PdSb supported on TiO_2 (anatase) has shown the best performance with 86 % selectivity of benzyl acetate (S-BA) at 68.5 % toluene conversion (X-Tol) in the direct gas phase acetoxylation. Catalyst showed low initial activity which increased gradually within the initial 10-12 h on-stream (induction period) to its maximum activity. Long induction period of around 10 h implies that catalyst started with low initial activity and it needs some 10 h to reach pinnacle of its performance. After acquiring its best activity, catalyst showed immediate deterioration of its performance, and displayed rapid deactivation. It was found that bigger Pd particles (50-100 nm) were generated during the course of the reaction starting from 5-10 nm in the fresh. These bigger (50-100 nm) particles were quite active and needed for the better performance of the catalyst. Deposition of carbonaceous yields generated during the course of the reaction was found to be the reason of rapid deactivation in the system. Therefore this study was undertaken to understand the limitations of this system i.e. to study and improve the

stability of the catalyst with time, additionally to investigate the reason behind the rapid deactivation of the catalyst.

1.5 Deactivation and regeneration of the palladium catalysts

One of the big problems in the heterogeneous catalysis is the declining catalytic performance with time. Most heterogeneous catalysts consists of highly expensive Pd and Pt, therefore it is very important to use these materials in highly economic way. Usually catalysts lifetime is limited; it can be for few minutes or can still be active up to few years. It is known that catalyst deactivation is a result of number of unwanted chemical and physical changes of the catalyst [94-96]. This physical or chemical phenomenon can be quite complex and can ultimately lead to the loss of active sites due to changes in the structure and state of the catalyst. The changes taking place in structure, morphology and valency of the active specie lead to the loss of activity. Albers et al. [97] have studied deactivation of Pd catalysts in detail, they stated that the effects like particle growth, coke deposition, coke transformation, and influence of supports and the valency changes on the solid surface are the important factors that lead to deactivation.

Some basic reasons of catalyst deactivation can be stated as follows:

(i) Poisoning of the catalyst (ii) Deposition on the surface of the catalyst which blocks the active centres (e. g., coking) (iii) Change in the phases of deposits on the surface e.g. coke transformation (iv) Particle growth, thermal effects and sintering of the catalyst lead to a loss of active surface area (v) Loss of components by evaporation (e.g. formation of volatile metal-carbonyls with CO) (vi) Valency changes of the active metal at the surface.

Sintering and the agglomeration of the particle lead to morphological changes on the catalyst. These physical changes are one of the main causes for a declining activity or in some cases have known to be fatal for the catalyst and leads even complete deactivation of the catalysts [98]. Some unwanted effects maybe avoided by using sufficient and controlled temperatures, ample impregnation agents and the appropriate support material, for e.g. Pd/TiO₂ catalysts showed sintering at 500 °C under the influence of hydrogen whereas Pd/Al₂O₃ catalysts were found to be more resistant under the same conditions [99]. In oxidation of methane, palladium-based catalysts are known to be widely used [100]. The palladium deterioration was explained by the metal sintering and the transformation in valency of the metals i.e. changes between PdOx and Pd⁰ state during the reaction [101]. One of the most common reasons for the catalyst deactivation is coking. Many different forms of C have been observed in different reactions. Some are deposited on the surface of the catalyst, some are transformed from one to another form of carbon or some are just generated during the

reaction. Some people have studied the formation of different types of coke formed on the catalyst at different temperatures. For example, Bludau et al.[102] have studied and confirmed the formation of different types of coke on the catalysts. They explained different carbonaceous forms are produced depending on the temperature of the reaction i.e. the type of coke formed below 200 °C is different from the other formed at temperature higher than 300 °C.

A better understanding of deactivation processes is very important and necessary which can help to avoid certain loss on the catalyst to some extent or to reverse the deactivation process to regain its activity by following appropriate regeneration procedure wherever it is possible. The regeneration of the catalyst can be highly beneficial from the economic point of view for e.g. investment costs for new catalyst; disposal and environmental costs can be avoided. Before trying to regenerate the catalyst, probable reason of deactivation, mechanism of deactivation, suitable condition and textural properties of the spent materials should be carefully studied. Regeneration of a catalyst also depends upon the reaction conditions under which catalyst was deactivated. Furthermore, regeneration only makes sense in cases where deactivation can be reverted, as in the case of coke deposition [103]. In most of the cases, temperature is one of the deciding factors; it can influence the stability of metallic phase and of the support. Higher temperature can cause de-structuring of the active phase, also sintering of the metallic phase may occur.

It is widely known that the palladium catalysts undergo deactivation due to carbon species, either by their accumulation on the surface, or by their interactions with the surface C species. In some cases restoration of the solid activity is successfully obtained by just burning of C deposits in the form of oxides. Whereas in the few deactivated catalysts, process of regeneration by burning of carbon or reducing the metal are not so helpful [104]. In such cases it cannot simply be attributed to the carbonaceous accumulation on the surface, but to their interaction with active sites of Pd on the surface and the strength of their bonding. Also many authors have reported [105-107] that it is difficult to regenerate the catalyst as it is not just about the C deposits. It is not easy to recover the shielded active sites and let them to interact with the reactant molecules [108]. It depends on various factors like the changes taking place on the structure, morphology, valency of the active component and the degree of unwanted/carbon particles deposited on the surface. The regeneration of used catalysts is a principle step in the evaluation of the eco-sustainability of several catalysts and its usage. Not only does the decreasing catalyst activity lead to a loss of productivity, it is also often accompanied by a lowering of the selectivity. Therefore, in the industrial

processes great efforts are made to avoid catalyst deactivation or to regenerate deactivated catalyst.

1.6 Objectives of the thesis

The present study is aimed to develop and enhance the performance of PdSb/TiO₂ solids in the gas phase heterogeneous-catalysed acetoxylation reaction. A meticulous and thorough approach is adopted to understand the behaviour of the catalyst in this system, which includes the following:

- i). To improve the catalyst properties, in terms of their economic application i.e. to raise low initial activity and to enhance the performance of the catalyst.
- ii). To optimize the reaction parameters for the acetoxylation of toluene to benzyl acetate, i.e. to study the effect of each component like toluene, acetic acid, oxygen, space velocity and temperature.
- iii). To check the long term activity with main focus on the stability of the catalyst. The key investigation of this study is to determine the causes and the type of deactivation.
- iv). To explore the regeneration pathway of the deactivated catalysts and to find out optimum regeneration conditions.
- v). To test the reaction pressure influence on activity and selectivity of the catalyst. This aspect was never checked before. PdSb/TiO₂ catalyst was subjected to varying reaction pressure of 1 to 10 bar.
- vi). To extend the present study to check the influence of different substituents with varying electronic properties on the acetoxylation performance using similar catalysts in order to synthesize their corresponding esters.

These catalytic systems will be characterized by different techniques such as TG-DTA, C.H.N.S, ICP, XRD, XPS, TEM, BET, FT-IR. The nature of the catalysts will be studied at different stages of the reaction and correlated with their acetoxylation activity and product selectivity.

The impact of different catalyst synthesis parameters, starting materials and co-components on the structure and performance of the active metal particles has been analyzed in more detail in the Ph.D. thesis of Suresh Gatla [109].

2 Experimental Methods and Equipments

In chapter 2, methods of catalyst preparation with details on impregnation method of preparation of PdSb supported on titania (anatase) are described. Various characterization techniques used in this thesis with their application are illustrated. Additionally, the experimental set-up for catalytic test runs and the procedure followed are presented.

2.1 Methods of catalyst preparation

Depending on the application, the catalysts are synthesized by different procedures in order to obtain particular size and shape. For example the slurry and the fluidized bed reactions require catalysts in the range of tens of micrometers, whereas fixed bed reactors need millimetre sized particles [110]. There are various techniques for manufacturing catalyst: (i) sol-gel method, (ii) impregnation method, (iii) slurry method, (iv) deposition - precipitation method, (v) electrostatic adsorption, (vi) co-precipitation

In this thesis, the impregnation method was adopted for the preparation of 10Pd16Sb supported on titania (supplied by Kronos, Germany) catalysts. Therefore only this method will be discussed in detail. In the Impregnation method, a certain volume of precursor solution containing the active phase is mixed with the solid support. Then this solid obtained is dried to remove the excess solvent. Impregnation can be classified in two categories according to the volume of solution added. Those are wet impregnation and incipient wetness impregnation. In wet impregnation, the solution is taken much in excess. Later the excess solid is separated and the excess solvent is removed by drying. In incipient wetness impregnation the amount of the solvent used is equal or even less than the pore volume of the support. The maximum loading is limited by the solubility of the precursor in the solution. Normally after above procedure catalyst is subjected to the following treatments (i) Drying and (ii) Calcination

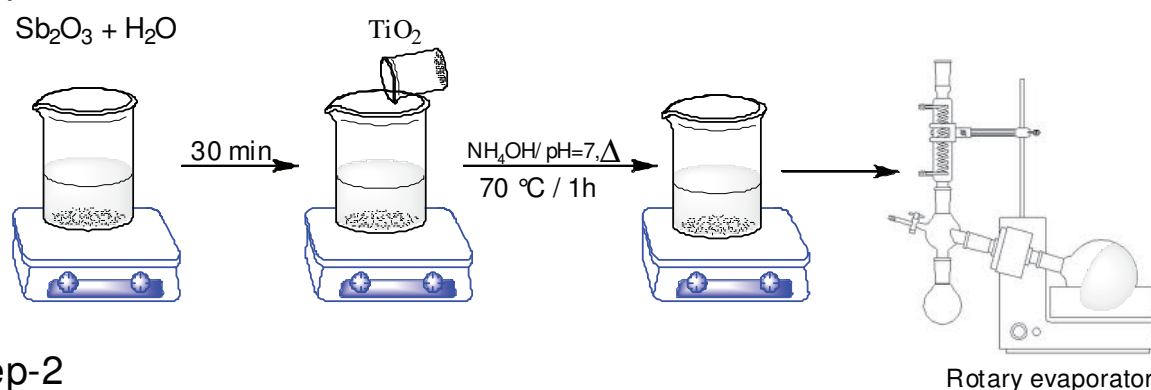
Drying means removal of solvent (usually water) from the pores of a solid. This is the usual step for eliminating excess solvents from the pores of the water. Sometimes, over heating can destroy the wanted structure of the catalyst. Therefore drying should be carried out carefully at optimum temperature [111]. The rate of evaporation should be slow and reversible to allow even redistribution of the active components on the surface of support.

Calcination is done after drying, which involves controlled heating without the formation of a liquid phase. It is usually carried out at temperatures higher than reaction temperature under varying atmospheres (i.e. inert, oxidising or reducing). Calcination involves chemical and physical changes of the metal in the catalyst such as decomposition of the impregnated metal precursor into oxide, alloys etc depending on the atmosphere, interaction between active sites and support, sintering of the support etc. [111]. During calcination the catalyst also solidifies into a final form, for example, amorphous into crystalline, therefore the surface and mechanical properties of the catalyst are derived mainly in this process.

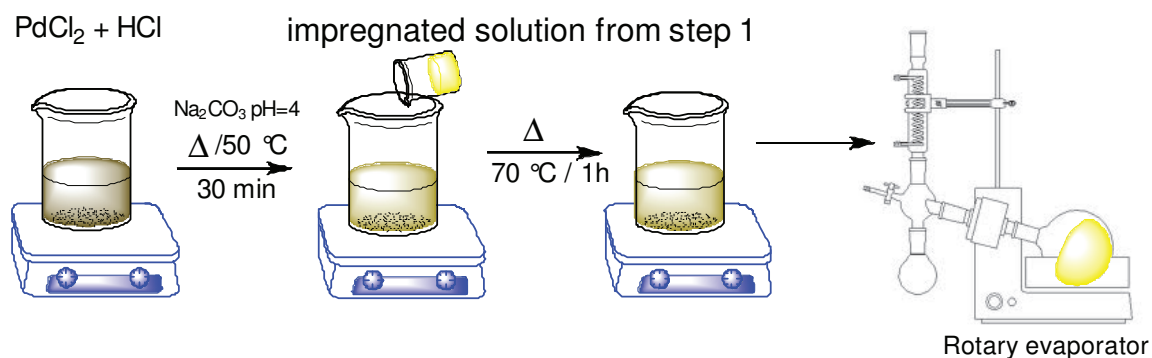
2.1.1 Preparation of the 10Pd16Sb/TiO₂ catalysts

10 wt% Pd and 16 wt% Sb on TiO₂ (anatase, Kronos) catalyst was prepared in two steps. In the first step, Sb₂O₃ (>99.9 % Sigma-Aldrich) powder was mixed in 20 ml distilled water and stirred for 30 min. Then TiO₂ was added to Sb₂O₃ slurry and was stirred for 1 h at ambient temperature. 25 % ammonia solution was added drop wisely to adjust pH = 7. The solution was heated up to 70 °C for 1 h, followed by solvent removal in a rotary evaporator. The solid obtained was dried at 120 °C for 16 h and calcined in air at 400 °C for 3 h. In the second step, PdCl₂ (>99.9 % Alfa) precursor was dissolved in dilute HCl. The solution obtained was cooled to room temperature and 1 N Na₂CO₃ (>99 % Alfa) solution was added to adjust the pH = 4. The solid prepared in step 1 was added to the above solution and stirred for 1 h, followed by solvent evaporation in a rotary evaporator. The resulting solid was dried at 120 °C for 16 h. Preparation details can be seen in [109, 112].

Step-1



Step-2



Scheme 4. Schematic representation of preparation of PdSb/TiO₂ catalysts

A list of catalysts used for various catalytic tests, different characterizations and their denotations are summarized in Table 1.

Table 1. List of catalysts and their denotation used in acetoxylation of toluene to benzyl acetate

No.	Catalyst at different stages	Denotation
1	10Pd16Sb/TiO ₂ -fresh (after 300 °C/2h in air ^a activation)	PdSb-f
2	10Pd16Sb/TiO ₂ -air ^a (used-5h)	PdSb-u5
3	10Pd16Sb/TiO ₂ -air ^a (used-11h)	PdSb-u11
4	10Pd16Sb/TiO ₂ -air ^a (used-15h)	PdSb-u15
5	10Pd16Sb/TiO ₂ -air ^a (used-33h)	PdSb-u33
6	10Pd16Sb/TiO ₂ -air ^b -fresh	PdSb-f(A)
7	10Pd16Sb/TiO ₂ -air ^b -(used-30h)	PdSb-u30(A)
8	10Pd16Sb/TiO ₂ -He ^c -fresh	PdSb-f(He)
9	10Pd16Sb/TiO ₂ -He ^c -(used-6h)	PdSb-u6(He)
10	10Pd16Sb/TiO ₂ -He ^c -(used-32h)	PdSb-u32(He)
11	10Pd16Sb/TiO ₂ -He ^c -(used-42h)	PdSb-u42(He)
12	10Pd16Sb/TiO ₂ -He ^c -(used-42h)-R*/300 °C/2h/air	PdSb-u42-r300(He)
13	10Pd16Sb/TiO ₂ -He ^c -(used-42h)-R*/300 °C/4h/air	PdSb-u42-r300-4(He)
14	10Pd16Sb/TiO ₂ -He ^c -(used-42h)-R*/300 °C/6h/air	PdSb-u42-r300-6(He)
15	10Pd16Sb/TiO ₂ -He ^c -(used-42h)-R*/350 °C/2h/air	PdSb-u42-r350(He)
16	10Pd16Sb/TiO ₂ -He ^c -(used-42h)-R*/400 °C/2h/air	PdSb-u42-r400(He)
17	10Pd16Sb/TiO ₂ -He ^c -(used-42h)-R*/300 °C/2h/air(used-7h)	PdSb-u42-r300-7(He)
18	10Pd16Sb/TiO ₂ -He ^c -(used-42h)-R*/350 °C/2h/air(used-7h)	PdSb-u42-r350-7(He)

^a in situ air activation in the reactor; ^b ex situ air calcination in the furnace; ^c ex situ helium calcination in the furnace; R* - Regenerated

2.2 Catalyst Characterization

Standard methods for characterization of fresh, used, deactivated and regenerated catalysts were used. The details are given below.

2.2.1 Thermal analysis (TA)

The TA has found wide importance in different disciplines of sciences. In chemistry, it is used for determining phase composition, hydration, polymerization, solvent retention, purity, melting, decomposition etc. Two most commonly used thermal methods are thermogravimetric analysis (TGA) and differential thermal analysis (DTA). Thermogravimetry can be defined as a technique whereby the weight of a substance, in heated or cooled environment at a controlled rate, is recorded as a function of time or temperature. Plots of weight change vs. temperature or time represents the products formed at different timings or temperatures. DTA is a technique in which the temperature difference between the sample and a thermally inert reference substance is continuously recorded as a function of furnace temperature or time. The thermal effects may be either endothermic or exothermic and are caused by physical phenomena such as fusion, crystalline structure inversions, boiling, vaporisation, sublimation and others. Some enthalpy effects are also caused by chemical reactions such as dissociation or decomposition, oxidation, dehydration, reduction, combination and displacement etc. In this manner endo and exothermal bands and peaks appearing on the thermograms give information regarding the detection of enthalpy changes. TG/DTA analysis was done with a TGA 92 (Setaram). The heating rate was 10 K/min till 700 °C in air flow.

2.2.2 Carbon analysis

For carbon analysis the samples are packed into lightweight containers of oxidisable metal like Sn and dropped into a vertical quartz tube, heated to 1050 °C. When sample is introduced, the helium stream is temporarily enriched with pure oxygen. The exothermic oxidation of Sn raises the temperatures to nearly 1700 °C at which a complete combustion of the sample takes place. The resulting combustion products pass through oxidation reagents (WO_3) to produce CO_2 , H_2O and NO_2 from the elemental carbon, hydrogen and nitrogen. In the present case only CO_2 and small amount of H_2O was released. These gases are then passed over Cu to remove excess oxygen and reduce the nitrogen oxides to elemental nitrogen. He is used as the carrier gas. The gas from the combustion reactor enters into the column, heated to 1900 °C. The components are eluted in the order N_2 , CO_2 , H_2O , and then measured by TCD. This analysis was done with the CHNS micro analyser TruSpec (Leco).

2.2.3 Inductively coupled plasma optical emission spectroscopy (ICP-OES)

This highly sensitive analytical technique for elemental determination is based on the principles of atomic emission. ICP-OES is a fast, multi-element technique, which permits the analysis of around 70 different chemical elements at the trace, minor and major concentration levels. ICP-OES has adequate sensitivity for most of the commonly

determined trace metals (for example Cu, Cr, Ni and Zn), superior performance to many other techniques for the more refractory elements (such as Ti, V, W) and allows the determination of some non-metals (including P, B etc). Most of the samples are handled in liquid form, either as aqueous or acidic solutions. Measuring gaseous samples, for the stable hydride gas-forming elements like As, Se and Sb is an important technique.

In ICP, a sample solution is introduced into the core of inductively coupled argon plasma (ICP). Sample solutions are converted to an aerosol of fine droplets by a rebuilding device such as a pneumatic nebulizer. This generates temperature of ca. 8000 °C. At this temperature all elements become thermally excited and emit light at their characteristic wavelengths. This light is collected by the spectrometer and resolves the light into a spectrum of its constituent wavelengths. Samples were analysed using ICP-OES: Perkin Elmer OPTIMA 3000XL using ICP–WinLAB software.

2.2.4 BET surface area and pore size distribution

Surface area determination is an important factor in predicting catalyst performance. The surface area measurements can be used to predict the efficiency of metal dispersion, porosity of catalyst as a method of assessing the efficiency of catalyst supports and promoters. There are several techniques like N₂ adsorption, mercury penetration etc. to estimate the total surface area and pore size distribution of porous materials in which BET (Brunauer, Emmett and Teller) is the most acceptable technique in determining surface area of solids by physical adsorption of gases at their boiling temperatures. The significance of the BET theory lies in its ability to determine the number of molecules required to form a monolayer of adsorbed gas on a solid surface despite the fact that a monomolecular layer is never actually formed. The BET equation is based on an extension of the Langmuir theory to multi layer adsorption. The basic equation to find out surface area is shown below

$$\frac{P}{V_{ads}(P_0 - P)} = \frac{1}{V_m C} + \frac{C-1}{V_m C} \cdot \frac{P}{P_0} \quad (19)$$

Where P = adsorption equilibrium pressure

P₀ = Saturated vapour pressure of adsorbate at its boiling point

V_{ads} = Volume at STP occupied by molecules adsorbed at pressure P

V_m = Volume of adsorbate required for a monolayer coverage

C = Constant related to heat of adsorption of adsorbate in 1st and subsequent layers.

According to BET method, a plot of P/V_{ads} (P₀ – P) Vs P/P₀ is a straight line (when P / P₀ is in the range of 0.05 to 0.30). The slope s = (C–1)/V_mC and intercept, I = 1/V_mC, knowing the slope (s) and intercept (I) permits the calculation of V_m (the number of gas

molecules adsorbed in a monolayer) which is used in calculating specific surface area of the catalyst by the following equation.

$$S = \frac{V_m N_A}{22414 W A_m} \quad (20)$$

Where V_m = monolayer volume in ml at STP

N_A = Avogadro number

W = weight of the catalyst sample (g)

A_m = Mean cross sectional area occupied by adsorbate molecule (e.g. for N_2 , it is 16.2 \AA^2)

The BET surface areas and pore size distribution were determined on a Nova, Quantachrome 4200e instrument by N_2 adsorption at 77 K. Prior to the measurements, the known amount of solid was evacuated for 2 h at 200 °C to remove moisture.

2.2.5 X-ray diffraction (XRD)

X-rays are electromagnetic radiation with typical photon energies in the range of 100 eV-100 keV. For diffraction applications, only short wavelength X-rays 1 keV-100 keV is used. As the wavelength of X-rays is comparable to the size of atoms, they are ideally suited for probing the structural arrangement of atoms and molecules in a wide range of materials. The energetic X-rays can penetrate deep into the materials and provide information about the bulk structure. The operative equation in X-ray diffraction is the Bragg equation:

$$n\lambda = 2d \sin \theta \quad (21)$$

where n is the order of a reflection ($n = 1, 2, 3, \dots$), λ the wavelength, d the distance between parallel lattice planes, and θ the angle between the incident beam and a lattice plane, known as the Bragg angle. With the d -values tabulated in decreasing order and the relative intensities recorded on a scale of 100 for the strongest line, the identification of the diffracting phases in the sample can be made. Agreements of the intensities as well as the d -values suggest the identity of phase and confirmation is obtained by reference to the compounds data from ASTM/JCPDS cards. With the analysis of X-ray diffraction line broadening (XLB) of the peak shape of one or more diffraction lines crystallite size can be calculated using the Scherrer equation

$$D_B = \frac{k\lambda}{\beta \cos \theta} \quad (22)$$

where D_B = mean crystallite diameter

K = Scherrer's constant

λ = X-ray wave length (1.5418 Å for CuK α radiation)

β = full width at half maximum (FWHM)

θ = diffraction angle

XRD patterns were recorded on a transmission powder diffractometer (STADIP, Stoe) with Cu K α radiation of 1.5406 Å; pattern examination was carried out using the inorganic powder database ICSD.

2.2.6 X-ray photoelectron spectroscopy (XPS)

Electrons of each element have characteristic binding energies. X-ray photons exciting a sample; cause the emission of core electrons. By detecting these electrons and plotting the counts of electrons versus the binding energy of these electrons will give the XP spectrum. The element characteristic set of peaks corresponds to the electron configuration, the peak area, and hence the numbers of detected electrons are proportional to the number of the specific element and therefore suitable to determine the amount in the sample. The origin of the detected electrons is the near-surface region, e.g. the top 5 to 10 nm. XPS is useful in determining the surface composition, valence states etc. Spectra were obtained by VG ESCALAB 220iXL instrument with Al K α radiation ($E = 1486.6$ eV).

2.2.7 Transmission electron microscopy (TEM)

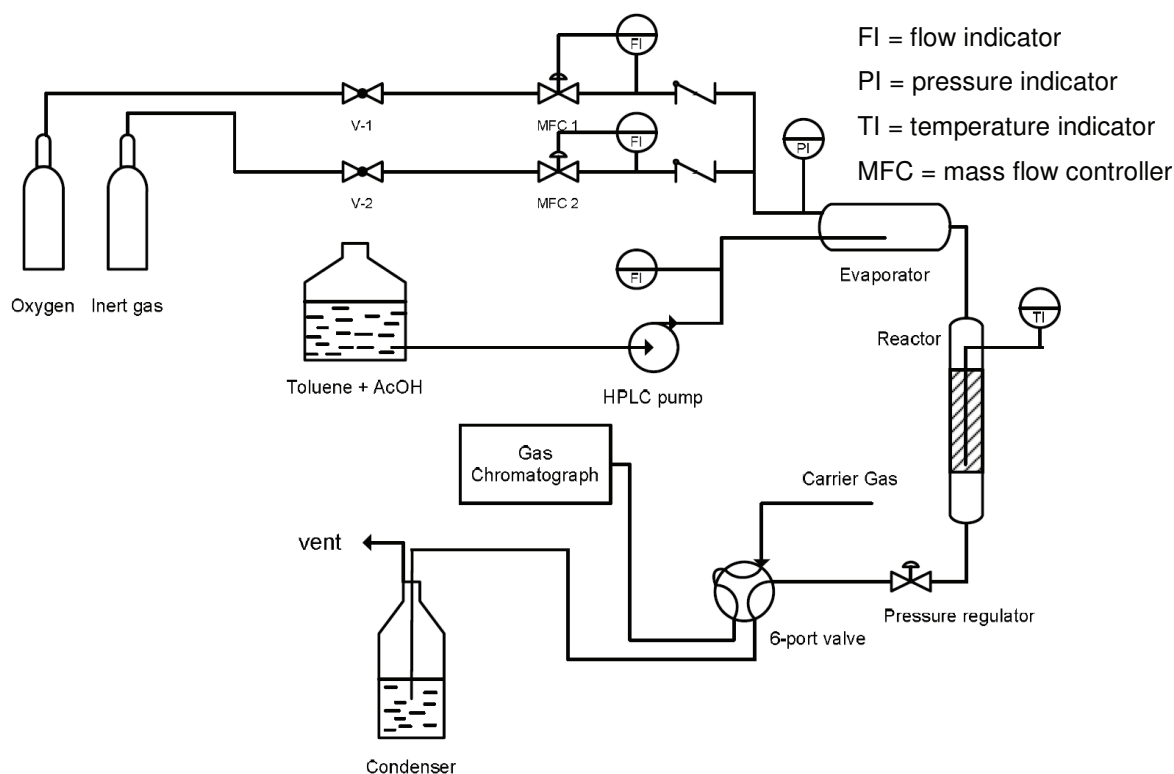
The TEM is useful for indicating the size of supported metal crystallites and change in their size, shape, distribution and position. It has now become capable of observing specimens at atomic resolution and is making valuable contribution to research and development of the industrial catalysts. In transmission electron microscope, a sample in the form of thin foil is irradiated by electrons having energy of hundred of eV. In the interior of the crystal the electrons are transmitted, scattered, or reflected. Electrons emitted by an electron gun pass through accelerator to the illumination system composed of two or more condenser magnetic lenses. After the interaction with the specimen the electrons enter the imaging system of the microscope, composed of the objective, intermediate and projector magnetic lens. The image is visualized on a fluorescent screen and recorded on a photographic film or on a CCD-camera. Objective lens is the most important lens of TEM, because its aberrations limit the resolution of the microscope. An electron diffraction pattern is formed in its back focal plane. A removable aperture situated in this plane is used to select different electron beams to form different images, thus manipulating the image contrast. The TEM measurements were performed at 200 kV on a JEM-ARM200F (JEOL) which is aberration-corrected by a CESCOR

(CEOS) for the scanning transmission (STEM) applications. The microscope is equipped with a JED-2300 (JEOL) energy-dispersive x-ray-spectrometer (EDXS) for chemical analysis. High-angle annular dark field (HAADF) and EDXS imaging was operated with spot size 6c and a 40 μm condenser aperture. TEM samples were prepared by depositing it on a holey carbon supported grid (mesh 300) and transferred to the microscope.

2.3 Experimental Setup for catalytic tests

One of the most common ways to carry out a heterogeneous catalyzed gas phase reaction is by passing reactants over a fixed solid phase catalyst. The arrangement of the fixed catalyst is generally called a fixed-bed and the respective reactor is called a fixed bed reactor [79]. The fixed bed reactors are commonly used to study the continuous flow processes especially for vapour or gas-phase reactions.

Acetoxylation runs were performed in a fixed bed tubular down-flow, micro-catalytic Hastelloy-C reactor (length 250 mm; i.d. 9.4 mm). The reaction gases like O_2 and 5% CH_4/N_2 (used as maker) were supplied from commercially available compressed gas cylinders and used without further purification. The flow rates of these gases were measured with mass flow controllers. The organic feed mixture of toluene and acetic acid was pumped to the reactor with a HPLC pump (Shimadzu LC 10Ai). The liquid reactant mixture was vaporised before it entered the reactor in a preheating zone provided on the top of the reactor. The molar ratios of the reactants, toluene/acetic acid/oxygen/inert gas were 1 : 4 : 3 : 16. About 1 ml (ca. 0.8 g) of catalyst particles (0.425-0.6 mm size) is loaded into the reactor and the reaction was performed mostly at 210 $^{\circ}\text{C}$ and 2 bar. The product stream was collected in a cold trap and analyzed off-line by gas chromatography (Shimadzu GC-2010) using an WCOT fused silica capillary column. The column outlet was connected to a methaniser (30% Ni/ SiO_2 catalyst) for conversion of carbon containing products into methane, detected by a Flame Ionization Detector (FID). Chromatographic separation involves the use of stationary phase and a mobile phase. Components of a mixture carried by the mobile phase in the column are differentially attracted by the stationary phase, and thus, move through the stationary phase at different rates and are analyzed by the detectors. WCOT column with a FID and was used to detect all components toluene, acetic acid, benzyl acetate and benzaldehyde. In addition, a methaniser was used to detect very small concentrations of CO and CO_2 in the reaction.



Scheme 5. Flow diagram of the acetoxylation set up (see Appendix Fig. A1 for details)

A FID detector operates with a mixture of hydrogen and air as the combustion gases. These gases burn in the small jet placed inside a cylindrical electrode. A potential of a few hundred volts is applied between the sample jet and the electrode. The FID works by directing the gas phase output from the column into a hydrogen flame. A voltage of 100-200 V is applied between the flame and an electrode located away from the flame. The increased current due to electrons emitted by burning carbon particles is then measured. In our experiments, the flow rate of hydrogen was maintained at 40 ml/min. The flow rate of helium was maintained at 24 ml/min. The methaniser is used in GC equipped with a FID to distinguish and identify very low levels of CO and CO₂. The methaniser functions using hydrogen gas and nickel catalyst. For analysing any sample, usually methaniser is heated to a temperature ranging from 350 °C to 400 °C. The carrier gas mixed with hydrogen and then goes through the methaniser to convert CO_x and hydrocarbons to methane. Methaniser converts each compound leaving the GC-column to methane. This allows quantitative detection of all the volatile compounds as methane, which simplifies the quantitative analysis. The retention times of hydrocarbons are unaltered as methaniser is placed after the column.

Table 2. Retention time of various components in the reaction: GC analysis

Component	Retention time (min)
Carbon monoxide	5.4
Methane	5.8
carbon dioxide	6.5
Acetic acid	12.75
Toluene	14.84
Benzaldehyde	17.75
Benzyl acetate	21.45

Gas chromatographic analysis was performed on a Shimadzu GC–2010, equipped with WCOT fused silica capillary column and FID detector: initial and final temperatures of 35 and 250 °C respectively

2.3.1 Calculations

The reactor output stream was analysed using a gas chromatograph. The amount of Tol, AcOH, BA, benzaldehyde, carbon oxides and methane was calculated by the area counts. The area counts were multiplied by the response factor to obtain the molar values of the compounds. Response factor was calculated by analysing different mixtures made with known concentration of toluene, acetic acid, benzyl acetate and benzaldehyde for liquid components. The known amount of gases like carbon oxides and methane were injected from gas mouse.

Conversion of Tol, selectivity and yield of BA were calculated by the following formulae:

$$X(\text{Tol})[\%] = \frac{n(\text{Tol})_{\text{in}} - n(\text{Tol})_{\text{out}}}{n(\text{Tol})_{\text{in}}} \times 100 \quad (23)$$

$$Y(\text{BA})[\%] = \frac{n(\text{BA})_{\text{out}}}{n(\text{Tol})_{\text{in}}} \times 100 \quad (24)$$

$$S(\text{BA})[\%] = \frac{n(\text{BA})_{\text{out}}}{n(\text{Tol})_{\text{in}} - n(\text{Tol})_{\text{out}}} \times 100 \quad (25)$$

2.4 Density Functional Theory studies

The energies of the acetoxylation reactions were determined using density functional theory (DFT). DFT studies were undertaken to evaluate the relative energies and the stabilities of toluene and various derivatives of toluene. The hybrid B3LYP functional for exchange and correlation was used throughout [113, 114]. For the description of palladium an 18-electron effective core potential [115] together with the appropriate polarized valence triplezeta basis set (TZVPP)[116] was used, which was also employed for the light atoms. All stationary points were characterized by vibrational frequency analysis to ensure to be minimal or transition states.

For the calculations with respect to the extended systems in this study the PWscf code of the Quantum ESPRESSO software package was used. All the calculations were performed on the three layer slab using a (5x5) supercell with 40 Ry kinetic energy cut off. Throughout, ultrasoft pseudo potentials were used, either of the RRKJ3 type (C,H,O atoms) or of the Vanderbilt type (Halogen atoms). The slab geometry was fully optimized with respect to cell vectors and atomic coordinates, while for adsorbed molecules the cell vectors were kept fixed. Adsorption energies (E_{ads}) were calculated using following equation:

$$E_{ads} = E_{slab+X} - (E_{slab} + E_{X,isol}) \quad (26)$$

In this equation E_{slab+X} , E_{slab} and $E_{X,isol}$ denote the total energy of the slab with the adsorbed molecule, total energy of the clean slab and total energy of isolated molecule X respectively.

3 Effect of varying thermal pre-treatment on the activity and stability of 10Pd16Sb/TiO₂ catalysts

This chapter is dedicated on the influence of thermal pre-treatment temperature and atmosphere on the catalytic performance of 10Pd16Sb/TiO₂ catalysts. The comparison of the catalytic activity with and without external pre-treatment is discussed in detail. Additionally, the effect of air, helium and 10%H₂/He pre-treatment atmosphere on the stability of the catalyst is examined. The characterisation results of fresh and spent samples obtained from ICP, BET-SA, XRD, TEM, XPS etc. are also presented.

3.1 Studies on 10Pd16Sb/TiO₂ catalyst pre-treated at 300 °C in air without external pre-treatment

0.8 g (1 ml) of 10Pd16Sb/TiO₂ catalyst particles, after oven drying were loaded in the reactor. It should be noted here that the solids loaded into the reactor were without any external pre-treatment but were Pre-treated in air flow of 27 ml/min at 300 °C for 2 h inside the reactor before starting the feed. After pre-treatment of the catalyst, the reactor was cooled down to the reaction temperature of 210 °C in the inert medium. Reaction feed of oxygen, inert gas and the mixture of toluene and acetic acid was dosed into the system and the performance of the catalyst was evaluated using gas chromatography.

3.1.1 Time-on-stream behaviour of 10Pd16Sb/TiO₂ catalyst pre-treated in the reactor (in situ) without any external pre-treatment

Fig. 2 depicts the catalytic performance of the 10Pd16Sb/TiO₂ catalyst with time-on-stream. The catalyst showed activity of X-Tol = 23 % in first hour, which increased considerably with time and reached maximum conversion of X-Tol = 65 % after nearly 7 h on-stream. After reaching the maximum performance of the catalyst (X-Tol = 65 %) it underwent deactivation with further time (X-Tol = 20 % after 32 h on-stream). In a similar way, the tendency of change in the yield of BA was also found to follow the same path as that of conversion of toluene. Yield of BA started with less than 1 % in the 1st hour, reached up to 54 % and then started to declined to Y-BA = 12 %. S-BA started with less than 1 % in the 1st hour, reached up to 84 % and then started to declined to Y-BA = 62 %.

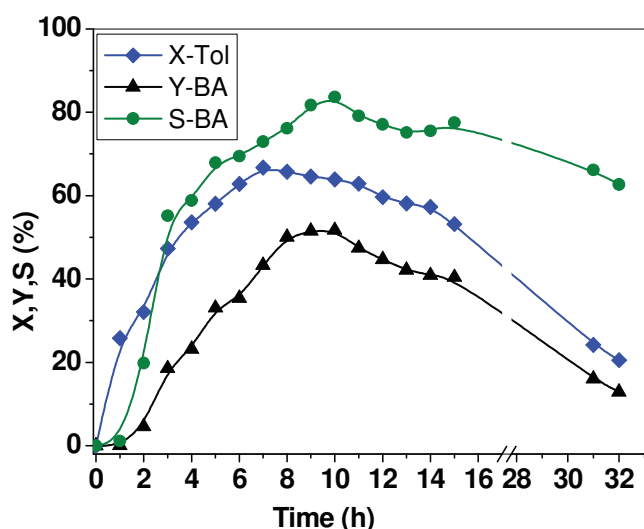


Fig. 2. Time-on-stream behaviour of the 10Pd16Sb/TiO₂ catalyst pre-treted in situ at 300 °C/air

To find out the reasons for this activity behaviour, catalysts after different time have been characterized, which is described in the next section.

3.1.2 Characterization of the 10Pd16Sb/TiO₂ catalysts pre-treated at 300 °C in air at different stages of the reaction

To understand the changes being occurred during the course of reaction, samples subjected to reaction for different time such as fresh (after pre-treatment in air), after 5 h, 11 h, 15 h and 32 h on-stream were collected and analysed. These samples were then characterized by different techniques such as BET surface area, ICP, C.H.N.S, FT-IR, XRD, TEM, XPS etc

3.1.2.1 BET surface areas and Elemental analysis

Table 3 presents BET surface area and pore volume data of fresh and spent solids collected at different stages of the reaction. A marked decrease (171 m²/g to 81.5 m²/g) of the surface area and pore volume of the pure titania support upon loading with the metal components was observed. This decrease in surface area and pore volumes is probably due to the blocking of the pores in support with the metal components. In addition, during the catalyst preparation the intermediate calcination steps (400 °C/air) after the impregnation of Sb₂O₃ on titania might have also affected the BET surface area.

Table 3. BET surface areas and pore volumes of 10Pd16Sb/TiO₂ catalysts after pre-treatment at 300°C/air/2h and at different stages of reaction

Catalyst	BET surface area (m ² /g)	Pore-volume (cm ³ /g)
Pure TiO ₂	171.0	0.27
PdSb-f	81.5	0.15
PdSb-u5	105.5	0.17
PdSb-u11	105.8	0.18
PdSb-u15	92.4	0.15
PdSb-u20	85.9	0.14
PdSb-u32	64.6	0.11

Increase in surface area (81.5 m²/g to 106 m²/g) from the fresh catalyst to the used catalyst in initial hours can be explained by the greater lattice expansion of Pd(111) during the reaction in presence of oxygen [117]. A decrease in surface area with decrease in activity in further runs was also observed i.e. decrease from 105 m²/g

(PdSb-u11) to 64 m²/g (PdSb-u32) till the deactivation. This decrease in surface area is due to the blocking of pores with coke during the reaction and fall of surface area can also be due to the agglomeration / sintering of the solids during the reaction. These finding were proved by TEM micrographs, which will be discussed in the coming sections. Pore volumes in the catalysts followed the same trend as observed in the case of surface areas.

Table 4 shows that the Pd and Sb contents of fresh and used catalysts up to 32 h on-stream are almost the same. No considerable change in the Pd and Sb contents is observed during use in the reaction. This suggests that there is no leaching of the active component in the course of reaction. From these findings, it can also be claimed that deactivation of the catalyst is not due to the leaching of catalyst. In addition, small amount of sulphur (1.1 to 1.6 %) was also found in the samples, which is due to the presence of residual sulphur from the titania support because it is originally prepared from sulphate precursor. This sulphur content is found to remain more or less constant throughout the reaction. Similarly, Na was also found in all stages of reaction, which comes from Na₂CO₃ that is used in the preparation of catalyst to maintain desired pH.

Table 4. Elemental analysis of the fresh and spent 10Pd16Sb/TiO₂ catalysts at different stages of the reaction

Catalyst	Pd	Sb	S	Na	C
PdSb-f	7.7	10.5	1.3	4.6	–
PdSb-u5	7.8	10.3	1.2	5.3	1.9
PdSb-u11	8.0	10.3	1.1	4.8	2.5
PdSb-u15	7.8	10.4	1.5	5.2	3.6
PdSb-u20	7.6	10	1.3	5.0	4.4
PdSb-u32	8.1	9.7	1.6	5.3	4.2

In the earlier studies [92], it was reported that carbon deposits are the main reason for deactivation of Pd catalyst in the gas phase acetoxylation of toluene, therefore carbon analyses were done at all stages of the reaction to examine the role of carbon formed during the course of reaction. Carbon was found to increase gradually from 1.9 % at 5 hours (X-Tol = 51 %) to 2.5 % after 11 hours (X-Tol = 62 %). This observation implies that an increase in carbon content up to almost 3 wt% has no negative effect on the performance. Probably some other changes for instance increase in particle size;

changes in surface properties etc taking place on the catalyst that are much more important than increasing carbon in the initial hours of reaction. From Table 4 and Fig. 2, it is clear that with increase in the carbon content after 11 h on-stream there is a fall in the catalytic performance and it leads to deactivation. At this point, it might be reasonable to say that in the later hours of reaction i.e. after 15 h on-stream, carbon plays a dominating role and seems to be one of the important factors causing deactivation of the catalyst.

3.1.2.2 FT-IR studies

The IR analysis (absorbance mode) in $1200\text{--}1800\text{ cm}^{-1}$ region of $10\text{Pd}16\text{Sb}/\text{TiO}_2$ catalysts was performed and is shown in Fig. 3. It depicts that in all spent catalysts, two regions of IR bands were seen, one from $1550\text{--}1600\text{ cm}^{-1}$ and other from $1380\text{--}1440\text{ cm}^{-1}$. These regions contain asymmetric and symmetric stretching vibration bands of acetate groups formed during the reaction [118]. For better comparison, IR bands of the fresh catalyst are also shown in the figure below. It displays only one band at around 1620 cm^{-1} . This band corresponds to adsorbed water from the moisture in air [119], since all of these catalysts were exposed to air before the measurements. A careful observation shows that, this band can be seen in spectra of all the catalysts in form of a shoulder at 1620 cm^{-1} . IR band at 1600 and 1628 cm^{-1} overlap; therefore just a slight hump in the spent catalysts for the stretching frequency of water could be seen. This observations hint that coke formed during the reaction is mostly from the acetate group, which is from acetic acid of the feed or the combustion of the product benzyl acetate.

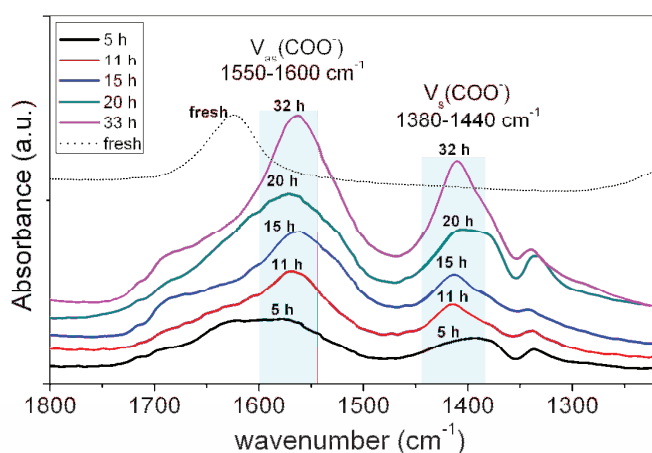


Fig. 3. FT-IR spectra of $10\text{Pd}16\text{Sb}/\text{TiO}_2$ catalysts at different stages of the reaction

3.1.2.3 X-ray diffraction

The XRD pattern of the catalysts before pre-treatment (only after drying for 16 h) and after pre-treatment ($300\text{ }^{\circ}\text{C}/\text{air}$) in the reactor is shown in Fig. 4a. The XRD pattern of

the catalyst before pre-treatment revealed reflections of TiO_2 , NaCl (which might have formed from Na_2CO_3 and PdCl_2 added during the preparation) and also significant sharp reflections of Na_2PdCl_4 . This phase is assumed to form after the addition of Na_2CO_3 to acidified PdCl_2 solution in the 2nd step of the preparation. Sb is probably present in the amorphous form which cannot be seen from XRD. However, the reflections of the pre-treated solids (PdSb-f) displays the formation of $\text{Sb}_7\text{Pd}_{20}$ alloy along with a Pd^0 phase, this phase is known to be formed in this system in the temperature range between 225-300 °C [112] while, reflections corresponding to Na_2PdCl_4 phase and PdO were not observed. This suggests that Na_2PdCl_4 decomposed during the pre-treatment treatment and formed an intermixed species ($\text{Sb}_7\text{Pd}_{20}$) with Sb. It seems that Na_2PdCl_4 phase is an intermediate phase in the process of formation of metallic Pd species from PdCl_2 precursor. Additionally some reflections corresponding to crystalline Pd are also seen. But still the possibility of existence of remains of amorphous form of Na_2PdCl_4 cannot be ruled out. A Slight shift in the position of pure Pd reflection was also observed in the PdSb-f catalyst. This shift in the Pd reflection is probably due to the expansion of Pd lattice and the incorporation of the other elements like Sb into the Pd. That means that the Sb can form some inter-metallic species and also get incorporated into the Pd lattice.

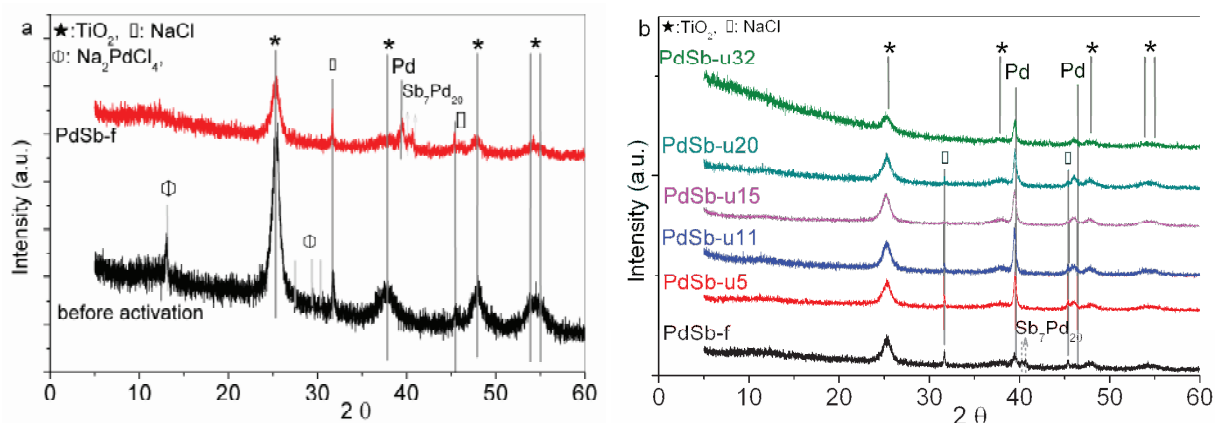


Fig. 4. XRD patterns of 10Pd16Sb/TiO₂ samples a) before and after pre-treatment at 300 °C/air/2h, b) catalyst at different stages of reaction

Fig. 4b displays the XRD pattern of the 10Pd16Sb/TiO₂ catalyst at different time i.e. fresh (after pre-treatment), after 5 h, 11 h, 15 h, 20 h and 32 h on-stream studies. In the case of spent catalysts, prominent reflections corresponding to the metallic Pd phase were observed. The intensity of Pd reflections was also noted to increase from 5 h on-stream onwards at the expense of the alloy formed in the case of PdSb-f (pre-treated catalyst). This suggests that during the reaction feed at 210 °C the alloy $\text{Sb}_7\text{Pd}_{20}$ formed in the fresh catalyst dissociated into the metallic Pd, whereas Sb phases could not be detected by XRD. Nevertheless, a slight shift in the position of Pd reflection compared to

the pure metallic Pd form was still observed during the course of reaction. This suggests that catalyst needs some amount of free metallic Pd for it to take part in the reaction, and this takes place during the course of the reaction where an intense Pd reflection in the all spent samples was observed. The catalyst obtained after 32 h on-stream was more amorphous compared to the catalysts up to 20 h on-stream due to formation of carbon layer around the catalyst observed from TEM analysis.

3.1.2.4 Morphological studies: TEM, STEM-EDX

10Pd16Sb/TiO₂ catalyst pre-treated in 300 °C/air/2h was studied by TEM, STEM together with EDX at different stages of reaction and is depicted in following figures. Fig. 5 shows the electron micrographs of fresh 10Pd16Sb/TiO₂ catalyst.

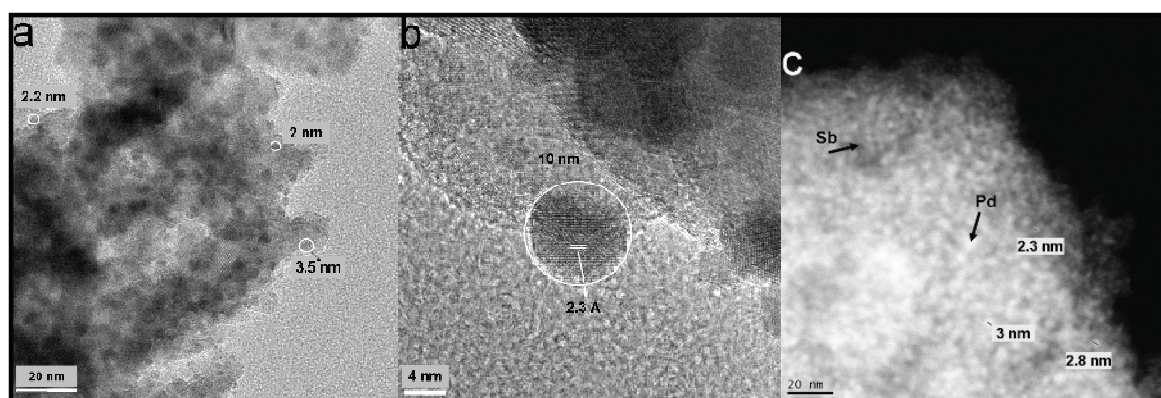


Fig. 5. Transmission electron micrographs of the fresh 10Pd16Sb/TiO₂ catalyst, a) shows small Pd particles, b) shows lattice fringes, c) HAADF image

Particle size of the fresh catalyst showed narrow size distribution from the range of 2 to 10 nm. Fig. 5a) shows that the small Pd containing particles (2-3.5 nm) are most frequently observed throughout the catalyst. Additionally little bigger Pd containing particles of around 10 nm was also seen in some parts of the catalyst. Fig. 5b) showed fringes particles of ca. 2.3 Å, which corresponds to Pd(111) lattice planes. Morphology of the particles was found to be spherically symmetric all over the catalyst. High Angular Annular Dark-Field (HAADF) analyses were performed in order to map the distribution of the heaviest chemical element. HAADF image in Fig. 5c) showed that the brighter dots of Pd particles and lighter ones i.e. gray are corresponding to Sb particles. This figure revealed that the Pd and Sb are distributed uniformly throughout the catalyst.

Fig. 6 displays the morphology and size of the particles at different time of reaction. In 11 hours of reaction, catalyst showed (X-Tol = 62 %, Y-BA = 54 %), but catalyst performance had already started to deactivate within subsequent catalytic runs. TEM showed that the particle size increased drastically compared to the fresh ones, i.e. from 2-10 nm in fresh to 50-100 nm at the 11th hour on-stream. Fig. 6a, depicts a large

spherical Pd particle of size 120 nm which is formed during the reaction. It is important to point out here that at this stage of catalytic reaction, particles had already started to agglomerate and are no more spherical in shape (Fig. 6(b)). Sintering of the particles already at this stage of reaction, hints to the quick deactivation and instability of the system at 11th hour. Fig. 6c showed the uniform lattice spacing of 2.0 and 3.0 Å, which is almost same like in the case of fresh ones but the careful observation from the Fig. 5c and Fig. 6c displayed that during the reaction uniformity of the fringes was disrupted. This is probably due to the poly crystalline nature or due to the merging of crystallites because of sintering effect.

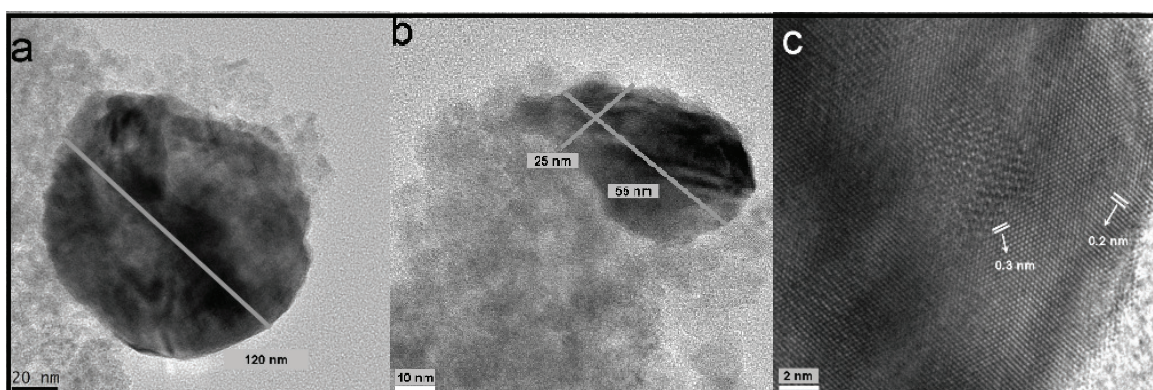


Fig. 6 Transmission electron micrographs of 10Pd16Sb/TiO₂ catalyst at 11 h on-stream a) shows spherical Pd particles, b) shows sintering of the particles, c) lattice fringes

To study the composition of the particle seen from TEM, STEM-EDX mapping of a representative particle from Fig. 6a (around 100 nm) was studied. Angle for measuring the STEM was changed for a better measurement.

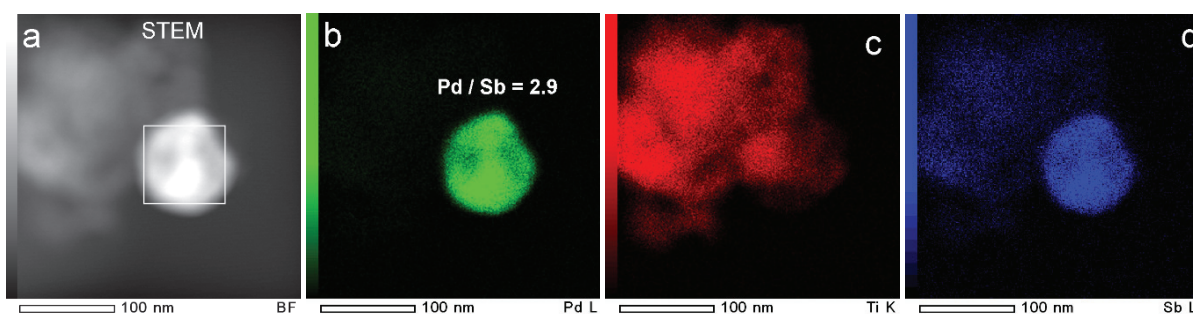


Fig. 7. a) HAADF-STEM image, b) Pd-L, c) Ti-K, d) Sb-L XEDS elemental maps of 10Pd16Sb/TiO₂ catalyst at 11 h on-stream (For mapping Fig. 6a was selected)

Mapping of the TiO₂ support, Sb and the Pd particles were performed on the particle of our interest. The results from the mapping showed that on the spherical particle there are no traces of titania, it is an intermixed particle of Pd and Sb, both homogeneous in elemental distribution the whole area. At the background, particle mainly contains titania

and some Sb distributed over it. The EDX spectrum of only the particle marked in Fig. 7a shows Pd enriched particles with a Pd/Sb ratio of 3 (Appendix Fig. A2).

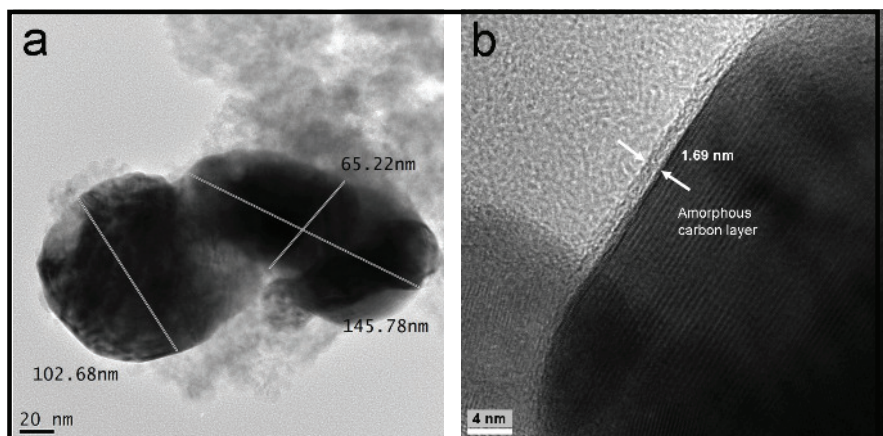


Fig. 8. Transmission electron micrographs of 10Pd16Sb/TiO₂ catalyst at 32 h on-stream a) high degree of Pd agglomeration, b) formation of amorphous carbon layer

Composition and size aspects of the catalyst after/during deactivation were also studied using TEM/STEM-EDX mapping after 32 hours of reaction. At 32nd hour the catalyst showed X-Tol = 20 %, Y-BA = 12 % reflecting marked deactivation. The carbon analysis in the previous section clearly showed that at 32 h on-stream there is significant amount of carbon (4.3 wt%) present on the catalyst. Fig. 8a-b displays the TEM images of the catalyst subjected to acetoxylation runs for 33 h on-stream. It is noteworthy that the particle size increased drastically in these catalysts (after 32 hours) compared with the corresponding fresh samples. The Pd particles in this sample revealed very high degree of agglomeration with a size of ca. 150 nm. The image in Fig. 8a is one example for higher degree of agglomeration. Besides agglomeration, migration of the Pd particles close to each other can also be noticed. Such high degree of agglomeration and migration of Pd to next nearest Pd is also seemed to be partly responsible for the observed deactivation. Additionally, a thick prominent C layer was observed around the particles of Pd (Fig. 8b), this layer accounts for the carbon deposits during the course of reaction. Loss of crystallinity at this stage was also observed from XRD due to this amorphous carbon coverage. Details can be seen in [109].

Therefore such coverage makes the catalyst more amorphous in nature, and this observation is in line with the results obtained from the XRD pattern. STEM-EDX mapping was performed for one of the particles shown in Fig. 9a, Pd was distributed inhomogeneously (Fig. 9b) over the whole particle at some distinct points, unlike in the previous case (see Fig. 7b) where Pd was found to be distributed throughout. Sb mapping showed homogeneous distribution of Sb over the catalyst (Fig. 9c) which does not change much during the course of reaction. EDX spectrum of only the part of particle

marked in box showed the Pd/Sb ratio of 4 (Appendix Fig. A3), whereas analysis for some other parts showed Pd/Sb ratios even as low as 0.75 and high over 10 (not shown here). This random or uneven distribution of Pd and Sb over the catalyst probably relates to the deactivation of the catalyst.

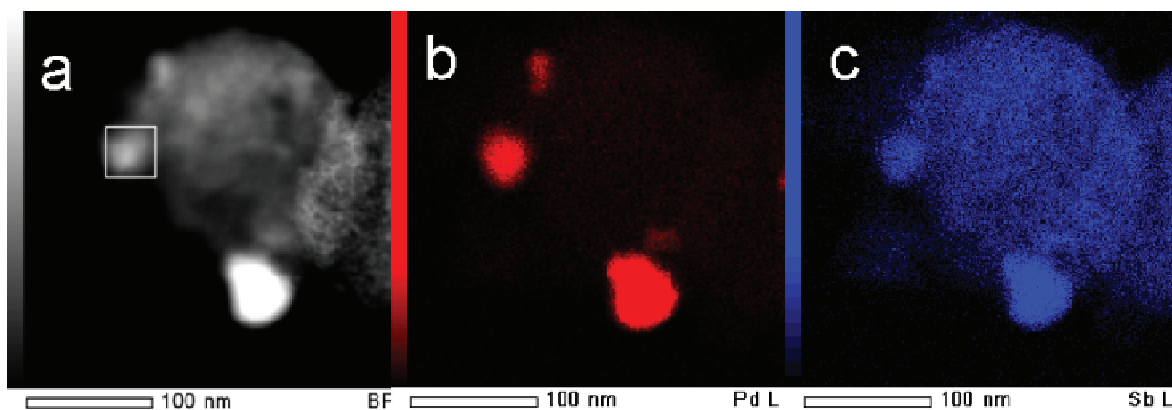


Fig. 9. a) HAADF-STEM image, b) Pd-L, c) Sb-L elemental maps of 10Pd16Sb/TiO₂ catalyst at 32 h on-stream

3.1.2.5 X-ray photoelectron spectroscopy

The XP spectra of the fresh (after pre-treatment) solids as well as of the samples after 11 h on-stream (PdSb-u11) and after 32 h on-stream (PdSb-u32) is shown in Fig. 10a.

At the near surface region of the fresh catalyst showed the peaks corresponding to oxidised Pd (grey coloured in Fig. 10, PdOx) were seen. Oxidised palladium formation on the surface is reasonable due to the air pre-treatment given to the catalyst at the start. Additionally some peak corresponding to higher binding energy than the oxidised palladium were also identified on the surface of the catalyst, which correspond to the Pd attached to chlorine (green coloured in Fig. 10, Pd²⁺(Cl)). This peak on the surface may be Na₂PdCl₄ formed on the catalyst during the preparation. However this phase was not seen in XRD, probably due to its amorphous nature.

During the reaction, after 11 h on-stream, oxidised Pd species on the surface undergo reduction in the reaction feed, therefore reduced Pd species were seen on the surface after the reaction. Along with PdOx and Pd-Cl species, metallic Pd (marked in red) and the further reduced species (namely Pd^{δ-}, marked in orange) were formed during the course of reaction, in which the electron binding energy of the Pd electron is lower than that of metallic Pd (335.1 eV). As reported earlier [120] the formation of a Pd^{δ-} state was due to the strong interaction between the surface Pd and deposited carbon. A correlation of the activity at 11 h on-stream, where catalyst showed maximum activity, and the surface composition suggests the necessity of the presence of oxidised and reduced species especially PdOx and metallic Pd together on the surface. The formation

of $\text{Pd}^{\delta-}$ is typical for a deactivated catalyst as reported by [120], and is caused by a strong interaction between Pd and carbon. The spectra of deactivated catalyst (after 32 h on-stream), showed that all oxidised and Pd-Cl species are reduced to metallic Pd^0 and $\text{Pd}^{\delta-}$ state, which together leads to loss of catalytic activity.

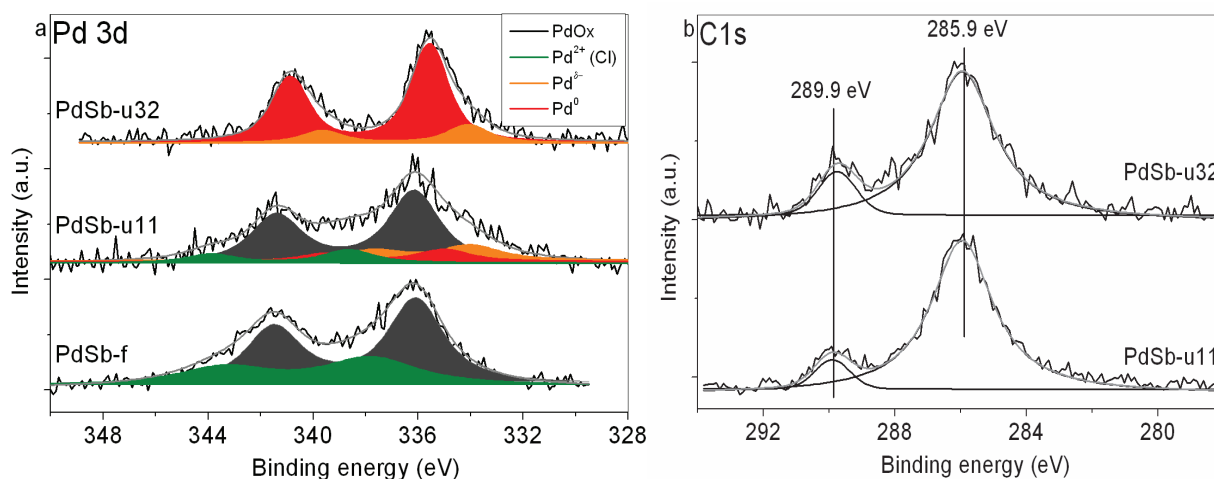


Fig. 10. XP - spectra of 10Pd16Sb/TiO₂ catalysts a) Pd3d spectra for the fresh, 11 h on-stream and 32 h on-stream samples, b) C1s of the 11 h on-stream and 32 h on-stream samples

XP spectra of C1 shown in Fig. 10b illustrates the occurrence of two types of carbon on the surface of the catalyst, which is generated during the course of reaction. C1s signal at 285 eV is evident, which is typical for C and H bound C atoms and C1s signal at 289.5 eV is formed, which is characteristic for C in carboxyl groups [118-121]. Hence, the presence of significant amount of carbon on the surface hints to the probable interaction between Pd and C, which facilitates the deactivation of the catalyst. This coke observed at 289.5 eV seems to facilitate the deactivation process. An increased intensity of this carbon peak (289.5 eV) at 32 h on-stream further proves the strong interaction of the surface Pd with carbon species which leads to unstable catalyst performance. For much clear trend of change in state of Pd on the surface is shown in Fig. 11a where it can be clearly seen the reduction of oxidised Pd and Pd-Cl species in the course of reaction. It is evident that for the catalyst to show its good performance, it must contain the Pd^0 and PdOx species on the surface as in the case of the 11 h on-stream sample. Nevertheless, the amount of these two species presents needs to maintain an optimum ratio to sustain good long-term stability. It seems that the reduction of Pd (PdOx and Pd-Cl) is much faster and stronger which even leads to reduced state of palladium that is denoted as $\text{Pd}^{\delta-}$. From the content of Pd species in the figure, it seems that Pd-Cl gets much easily reduced than PdOx up to 11 h on-stream. With further increase in reaction time, both these Pd-Cl and PdOx species get completely

reduced. This result suggests that to maintain the stability of the catalyst, extent of reduction should be balanced. Higher reduction leads to faster formation of $\text{Pd}^{\delta-}$ state, which in turn causes easy deactivation. It can be said that the presence of both Pd^0 and oxidised Pd species together in an optimum ratio is vital for the catalyst to show good performance and to maintain its long-term stability. Fig. 11b, displays the Pd/Ti and Sb/Ti ratio on the surface obtained from XPS in catalysts at different stages. It shows that Pd/Ti decreased with time compared to the fresh ones. Such a decrease in the Pd/Ti ratio can be possible due to the coverage of Pd by carbon generated during the reaction or the particle agglomeration as seen from TEM also migration of Pd into deeper layers of the surface cannot be neglected [92]. The amount of the Sb/Ti ratio in the near-surface region also changed during the course of the reaction. Slight enrichment of Sb on the surface was observed after the reaction. These opposite trends of the Pd and Sb on the surface suggests a separation of Sb and Pd. Probably spreading of Sb over the whole surface as seen from TEM, can explain such opposite phenomenon in elemental composition.

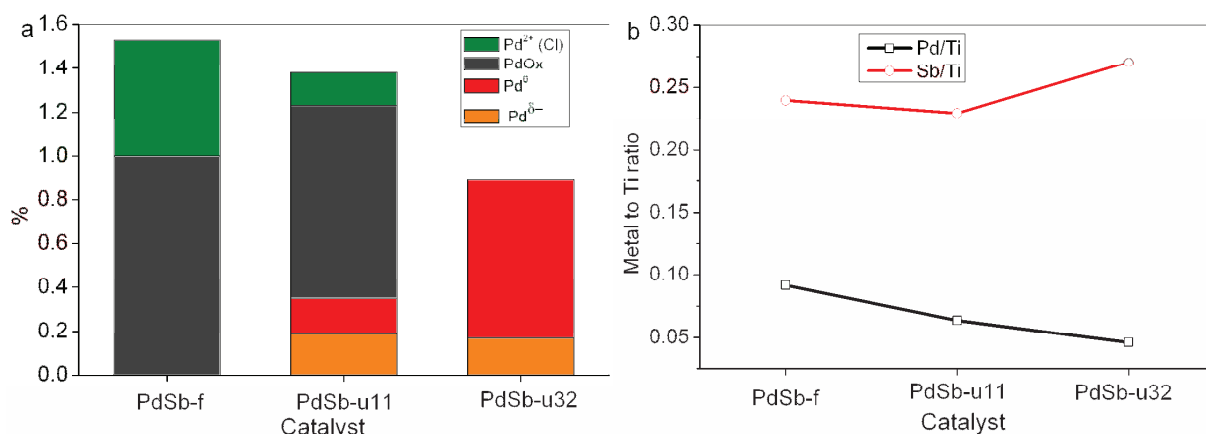


Fig. 11. a) Atomic % of different Pd species on the surface, b) Metal (Pd, Sb) to Ti surface atomic ratios, for the fresh and spent (11 h and 32 h on-stream) 10Pd16Sb/TiO₂ samples. Surface atomic ratios were calculated from the areas of the XPS Pd3d, Sb3d, Ti2p peaks

3.2 Effect of external pre-treatment (600 °C/4 h) and atmosphere (air, He and 10% H_2 /He) on the stability of 10Pd16Sb/TiO₂ solids

As described above, deactivation and instability of the 10Pd16Sb/TiO₂ catalysts pre-treated in the reactor at 300 °C (i.e. without any high temperature pre-treatment) is one of the major issues of concern. Such deactivation of the catalyst is attributed to various reasons such as i) Increase in coke content on the catalyst during the course of reaction ii) complete and fast reduction of PdO to Pd^0 species on the surface and iii) high degree of sintering of the Pd particles (e.g. particles of >150 nm size, see Fig 8a). For improving the quality of such catalysts, the stability must be increased while maintaining high

activity. As mentioned earlier, this reaction requires bigger Pd particles (50-100 nm) and hence one of the aims is to produce bigger Pd particles in the fresh sample itself. The objective is also to modify the reduction extent of oxidised Pd species so that the catalyst is able to show the long-term stability. With such objectives, the selected PdSb catalyst is subjected to external pre-treatment at 600 °C for 4 hours in three different atmospheres such as inert (He), oxidising (air) and reducing (10% H_2 /He) [122]. The structural changes of the catalysts caused by different pre-treatments are discussed in more detail in [109]. The solid treated in 10% H_2 /He atmosphere is found to be completely inactive due to formation of alloys. Therefore, both catalytic and characterisation results obtained on this particular catalyst are not shown here. However, the time-on-stream behaviour and other results of the air and He calcined solids are shown in the following sections.

3.2.1 Time-on-stream behaviour of 10Pd16Sb/ TiO_2 catalysts subjected to pre calcination in air and He at 600 °C/4 h

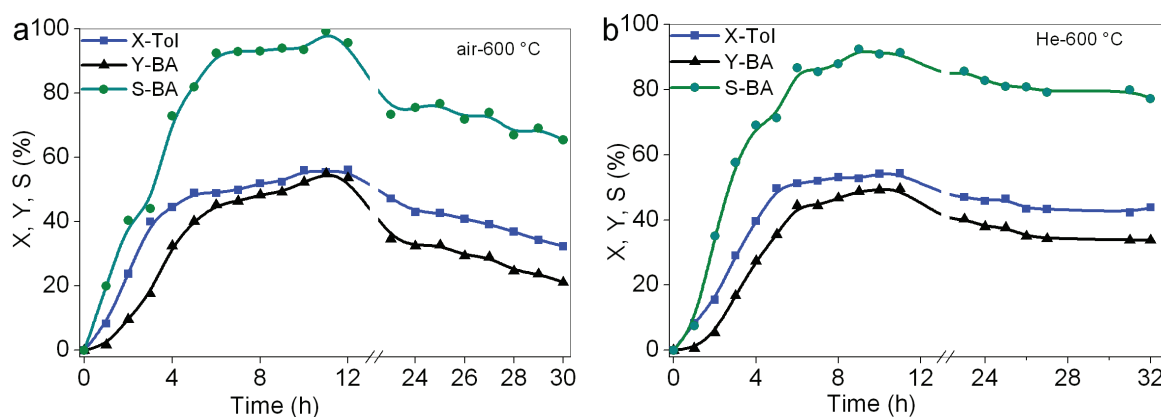


Fig. 12. Toluene conversion (X-Tol), selectivity (S-BA) and yield (Y-BA) of benzyl acetate during time-on-stream over the 10Pd16Sb/ TiO_2 catalyst pre-treated a) at 600 °C in air for 4 h and b) at 600 °C in helium for 4 h

In previous section, the performance of air treated catalysts at 300 °C/2 h in the reactor itself was discussed. In this section, the performance of the catalysts pre-treated in air and He outside the reactor at 600 °C for 4 h is depicted (Figs. 12a and b). Despite such high temperature treatment, there is no difference in the initial activity of the catalysts. After 600 °C air pre-treatment, also the catalyst showed similar low conversion of toluene (< 10 %), which is again increased with time (X-Tol = 54 %) and stayed there till 25 h on-stream and then got deactivated in further runs. However, some changes could be noticed: i) S-BA increased from 85 to 92 %, ii) X-Tol is slightly reduced from 65 % to 54 %, iii) long-term stability improved 10 h in the case of sample calcined at 600 °C in air compared to unstable catalyst treated at 300 °C (Fig. 2). Comparing the

results of air treated catalysts at 300 °C and 600 °C, it can be said that high temperature treatment in air showed more beneficial effects and hence it is preferred. Fig. 12b illustrates the catalytic performance of the solids calcined in He at 600 °C/4 h externally. This catalyst also showed improved performance in terms long-term stability, which is enhanced remarkably from 10 h in 600 °C air treated catalysts to ca. 30 h in the case of He treated. In view of this, it is obvious that the calcination in He at 600 °C is more preferred for improved performance compared to others.

3.2.2 Catalyst characterization of 10Pd16Sb/TiO₂ catalyst treated in 600 °C air and helium

It is clearly evident from previous discussions that the thermal pre-treatment has a significant impact on the catalytic performance. Therefore, to understand the changes occurring during the course of reaction, samples were characterized by different techniques such as BET surface area, carbon analysis, XRD, TEM, XPS etc.

3.2.2.1 Elemental analysis and BET surface areas

The elemental analysis displayed no leaching of the components during the reaction. The surface areas and pore volume values showed that in the case of air calcined solids there is significant decrease with time, i.e. values decreased from 115 to 52.8 m²/g in 30 h on-stream. In contrast, catalyst calcined in He atmosphere, which was stable for longer time of reaction, did not show much difference in the surface area as well as pore volume (Table 5). This suggests that high-temperature treatment in oxidizing atmosphere may have an impact on the support structure, most probably on the TiO₂ crystallite size which is smaller for the solids after air pre-treatment. This may be the main reason for the difference in surface areas.

Table 5. Elemental composition, BET surface areas and pore volume of 10Pd16Sb/TiO₂ catalysts after different thermal pre-treatments and after 30 h on-stream

Catalyst	Pd	Sb	S	Na	C	BET surface area (m ² /g)	Pore volume (cm ³ /g)
PdSb-f(A)	8.5	12.2	1.4	5.1	–	115.3	0.38
PdSb-u30(A)	8.8	12.5	1.4	5.2	2.2	52.8	0.12
PdSb-f(He)	9.3	9.3	1.5	5.7	–	28.6	0.10
PdSb-u33(He)	9.1	8.8	1.6	5.35	2.4	35.5	0.11

The amount of carbon formed during the reaction seems to be independent on the atmosphere of thermal treatment given to the catalyst. Nevertheless, the catalyst calcined in He at 600 °C is more stable than the one calcined in air at the same temperature. This suggested that coke formation is not the only reason for faster deactivation in the case of the air calcined sample. Stability of the sample treated in helium is not completely dependent on the amount of carbon over the catalyst generated during the reaction. Probably some other factors are playing crucial role in shaping the He catalyst to maintain its stability.

3.2.2.2 X-ray diffraction studies

In general, the XRD patterns of all samples commonly exhibited the reflections of the anatase support and some small traces of NaCl (Fig.13). However, some differences still exist in the phase composition between the samples calcined in air and He. For instance, XRD patterns of the fresh and spent helium calcined sample revealed the presence of a metallic Pd phase.

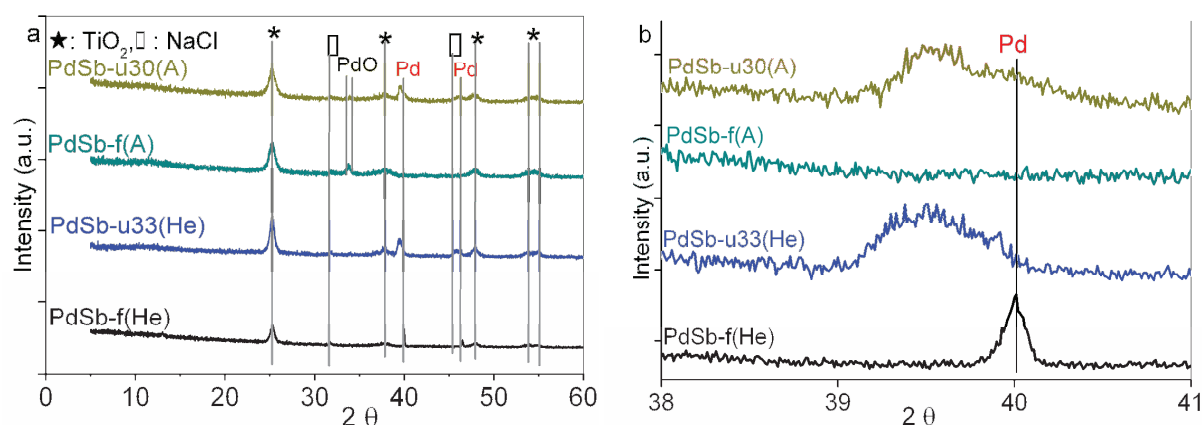


Fig. 13. a) XRD patterns of fresh and used samples calcined at 600 °C in the He (PdSb-f(He) and PdSb-u33(He)) and in air ((PdSb-f(A) samples and PdSb-u30(A)), b) XRD patterns in the 2θ range of the Pd(111) reflection (38-41 °)

On the other hand, the air pre-treated fresh catalyst showed the reflections corresponding to PdO phase as expected. It was also found that during the course of the reaction, metallic Pd species were generated due to the gradual reduction of PdO species, which is evidenced by increased intensity of the reflection, belongs to Pd at the expense of PdO intensity. To have deeper insights for the metallic Pd, only the Pd reflections were enlarged and observed carefully (see Fig. 13b). In all the cases except for the fresh one, a shift in the metallic Pd reflections to a lower theta value was observed. This behaviour points to a change of the Pd lattice during time-on-stream, which is most probably caused by the incorporation of other components such as Sb, C and/or H into the lattice of Pd.

3.2.2.3 Transmission electron microscopy

TEM-EDX results of the catalysts after pre-treatment in air at 600 °C and after 30 hours used in the acetoxylation reaction are depicted in Fig. 14. In the fresh samples, Pd-containing particles with a size of 5-10 nm were formed and are well dispersed over the support. In the XRD pattern (Fig. 13) reflections corresponding to PdO were observed. Therefore it is most probable that these particles consist of PdO. The radiation emitted from oxygen in PdO and TiO₂ cannot be distinguished. TEM of fresh solids show the formation of Pd-Sb mixed particles with inhomogeneous distribution, i.e. sometimes Pd rich (with Pd/Sb = 5.4) and sometimes Sb rich (Pd/Sb = 0.4) intermixed particles could be found (see Fig. 14a and b). Besides, there are also only Sb-containing support areas without any Pd or with only traces of Pd (Fig. 14b). This suggests that in contrast to Pd which forms a crystalline PdO phase, Sb seems to be dispersed on the support.

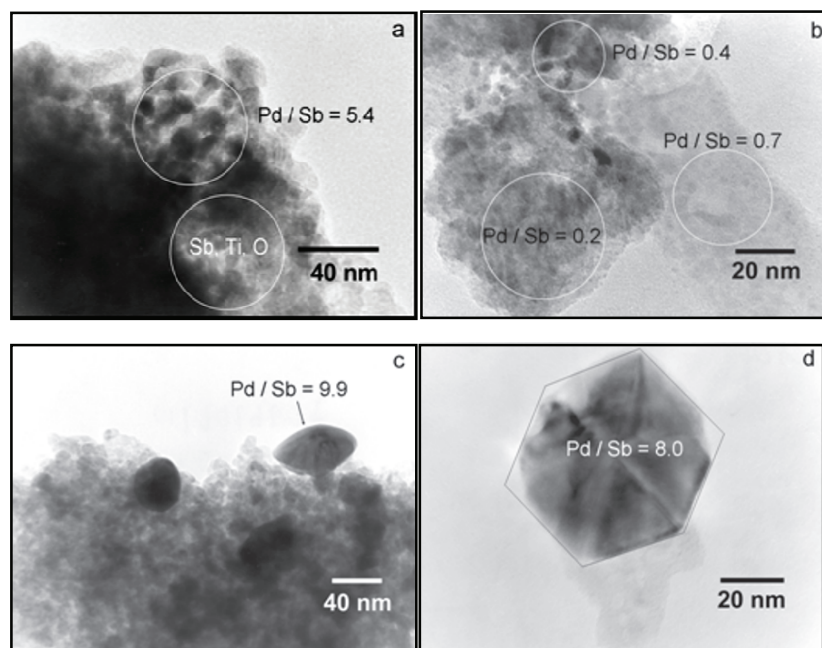


Fig. 14. Transmission electron micrographs of 10Pd16Sb/TiO₂ samples after 4 h calcination in air at 600 °C (a, b) and after 30 h use in the catalytic reaction (c, d)

After 30 h on-stream in the catalytic reaction, Pd particles of about 40-100 nm were formed, with well faceted crystallized structure (Fig. 14c, d). These particles contain only some traces of Sb. On the other hand, nearly Pd-free Sb particles were also observed. This clearly shows that the Pd and Sb remain widely separated in the catalyst.

Very different TEM-EDX results were obtained from the catalyst pre-treated in He at 600 °C. Large Pd particles of up to 2 µm diameters were formed leaving a considerable part of the support free of Pd (Fig. 15a-b) which contained Sb. After 32 h on-stream in

the catalytic reaction, surprisingly, a marked decrease of the particle size down to 40-100 nm was observed, which is equal to the size of the Pd particles formed during the course of reaction in the air-calcined catalyst (compare Fig. 15c-d and Fig. 14c-d). However, in contrast, the He catalyst, which contains only Pd particles with only traces of Sb or Sb particles with traces of Pd (Fig. 14c-d), the particles in the He pre-treated catalyst showed Pd/Sb ratios around 5 (Fig. 15c-d), while the rest of the Sb is spread over the TiO_2 support without forming a separate phase.

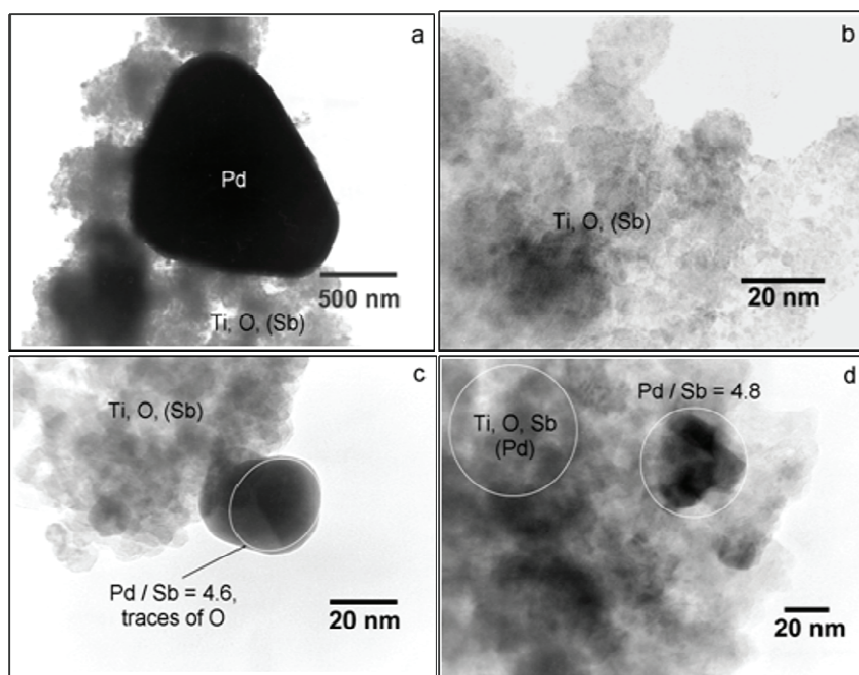


Fig. 15. Transmission electron micrographs of $10\text{Pd}16\text{Sb}/\text{TiO}_2$ - He/4 h fresh (a, b) and after 32 h use in the catalytic reaction (c, d)

3.2.2.4 X-ray photoelectron spectroscopy

In Fig. 16a XP spectra of the Pd 3d region are shown for the fresh samples after thermal pre-treatment at 600 °C in air or He and after 30-32 h on-stream. The Pd $3d_{5/2}$ peak of the catalyst after air treatment falls at 335.8 eV. These values are in the range of oxidic Pd. However, this value is considerably lower than the binding energy of 336.5 eV measured for pure PdO [122]. Surprisingly, the spectra of the catalysts after pre-treatment in He are almost identical to the one after air treatment (Fig. 16). Although metallic Pd was detected by XRD in this case, this PdOx might be due to the formation of surface oxide species on the large Pd particles obtained after the pre-treatment in helium. No $\text{Pd}^{2+}(\text{Cl})$ species were seen on the catalyst surface as observed in the solids pre-treated in air at 300 °C inside the reactor. It seems that all $\text{Pd}^{2+}(\text{Cl})$ decomposed to PdOx at higher temperature leaving just oxidised phases on the surface. After ca. 30 h

on-stream, the PdOx species disappeared completely in the sample pre-treated in air at 600 °C (Fig. 16). Only pure Pd⁰ was observed on the surface of the used air-calcined catalyst, whereas a shift of the Pd 3d peak to higher binding energy in the used He calcined catalysts indicates the presence of some oxidised Pd on the surface, while the catalyst remained still partially oxidized after 30 h on-stream.

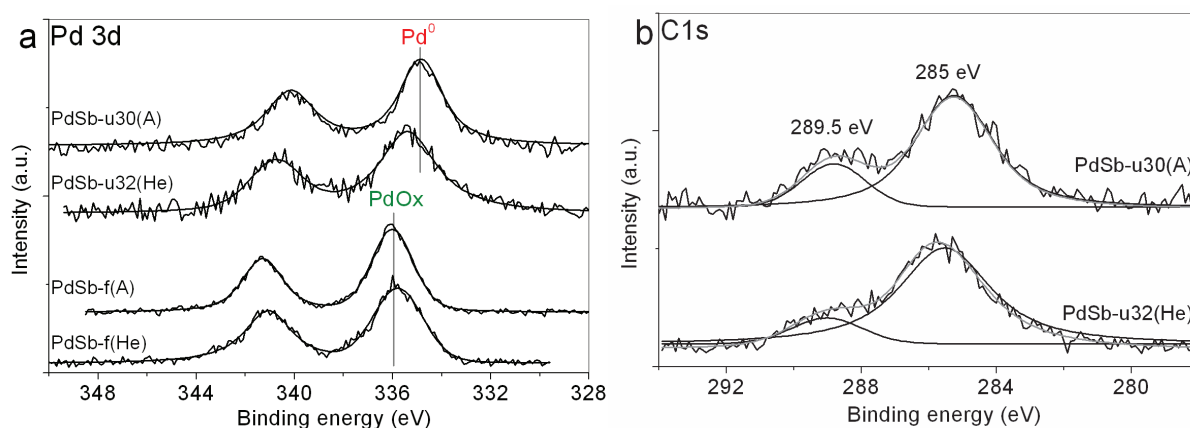


Fig. 16. a) XP spectra of the Pd 3d peak of 10Pd16Sb/TiO₂ samples, fresh He pre-treated catalyst, fresh air pre-treated catalyst, He pre-treated sample after 32 h on-stream, air-pre-treated sample after 30 h on-stream, b) XP spectra of the C 1s state at the surface of spent 10Pd16Sb/TiO₂ samples pre-treated in air or He

This has also been proposed for supported Pd catalysts in other oxidation reactions, e.g. the total oxidation of methane [123-125]. It seems that the presence of Pd⁰ alone (i.e. complete loss of PdO) is responsible for the faster deactivation in air treated sample compared to the helium one. Nevertheless, no Pd^{δ-} species were found on surface of the catalysts treated in air and helium compared to the one pre-treated in reactor at 300 °C. These Pd^{δ-} species were quite prominent on the catalyst treated in situ in air at 300 °C (see Fig. 11) and were believed to cause or facilitate deactivation in the system. Pre-treatment of the catalysts at higher temperature has undoubtedly improved the performance of the catalyst compared to the 300 °C treated ones, in terms of stability and reducibility of Pd species during the reaction. Therefore both helium and air calcined catalysts at 600 °C showed higher stability than 300 °C air treated catalysts. These observations also suggested that the extent of reduction of oxidized Pd on the surface is dependent on the pre-treatment atmosphere and temperature given to the catalyst. In all used catalysts, Sb is present in oxidized form, evidenced by a Sb 3d_{3/2} peak with a binding energy of 540 eV, being characteristic for Sb₂O₃ [126].

Coke deposition is a possible reason for the catalysts deactivation which occurs during time-on-stream, the C1s region has been analyzed in detail (Fig. 16 b). In all the samples, a C1s signal at 285 eV is evident. After long time of reaction both the samples

showed an extra C1s signal at 289.5 eV (Fig. 16). In the air pre-treated catalyst, this peak was already present after 9 h on-stream [109], while in case of He calcined sample this carbon signal was observed only after long time of reaction. A comparison of a relative surface percentage of the types of C on spent solids after pre-treated in air or He is shown Fig. 16b. It is clear that amount of the coke at 289.5 eV is higher in the case of air sample at 32 h on-stream compared to the one at after 33 h on-stream, treated in He. Interestingly, the total bulk carbon content for the two samples pre-treated at 600 °C (Table. 5) does not differ much. However, rate of deactivation in case of He is lower compared to the air pre-treated catalyst. It seems that the carbon at 289.5 eV which are formed in the air treated catalysts are stronger deactivating in comparison to carbon at 285 eV deposits in the He pre-treated catalyst.

3.3 Summary and Conclusions

10Pd16Sb/TiO₂ catalysts tested after activating it in the reactor at 300 °C/2h/air showed a gradual increase in the performance and reached maximum of X-Tol = 65 %, Y-BA = 54 %. The increase in activity is correlated with a marked increase of the Pd particle size. However, the catalyst displayed quick deactivation after reaching the maximum activity. XRD showed that metallic Pd species are generated during the course of the reaction. The shift in Pd reflection corresponding to lattice expansion and the incorporation of probably of Sb into the lattice of the Pd was seen. XRD pattern after 32 h on-stream showed the decreased intensities of XRD reflections. Elemental analysis displayed no leaching or loss of active components during the reaction. Carbon content increased progressively with increase in time of the reaction and sometimes amorphous carbon was also found. This amorphous nature of the carbon was further proved by the TEM-EDX analysis, which showed the presence of thick amorphous carbon layer surrounding the Pd particle. TEM/STEM-EDX analysis presented very useful insights on the size and composition changes occurring during the course of reaction. Size of the Pd particle increased from 5-10 nm in the fresh (after pre-treatment) to ca. 100 nm at the 11th hour. Pd and Sb species were found to be present together with a Pd/Sb ratio of ~ 3. The deactivated catalysts showed very high degree of agglomeration of the Pd particles with a prominent layer of carbon over the surface. Ratio of Pd/Sb varied dramatically over the whole catalyst from 0.75 to over 10. Moreover, XPS studies revealed the reduction of Pd²⁺ states to Pd⁰ and Pd^{δ-} during the reaction, which are detrimental for maintaining the stability of the catalysts.

The thermal pre-treatment atmosphere (10%H₂/He, Air and He) showed a clear influence on the stability of 10Pd16Sb/TiO₂ catalysts in acetoxylation runs. The catalysts pre-treated in 10%H₂/He were found to be completely inactive due to formation of alloys. The catalysts pre-treated in air and He showed similar activity, the air treated samples

showed stability of around 10 h and the He treated catalysts showed much better stability up to 25 h in the catalytic runs. The bulk analysis (XRD and TEM) of the catalysts showed that very large Pd particles were present after pre-treatment in helium, up to 2 μm . These huge particles underwent some restructuring during time-on-stream into smaller ones of size 40-100 nm by incorporation of Sb up to a ratio of Pd/Sb \approx 5. On the other hand, in the air calcined catalysts, the Pd particles obtained were much smaller and consisted essentially of PdO. These particles were reduced to metallic Pd and agglomerated during the reaction and without considerable changes in Pd/Sb ratios. The surface studies done by XPS revealed significant changes on the surface during the course of reaction of two different thermally treated catalysts (air and He 600 $^{\circ}\text{C}$ /air) compared to the one heated in the reactor (in situ) at 300 $^{\circ}\text{C}$ in air. In the case of maximum stable He treated catalyst, after 33 h on-stream, both pure metallic Pd⁰ and oxidized PdO species coexisted, while the surface of the air pre-treated catalyst lost its oxidized PdO_x with time, which goes along with a loss of activity. This suggested that the co-existence of both Pd and PdO species is beneficial for the long term catalytic performance. Another probable reason for the pronounced stability of He calcined sample was the nature of surface carbon over the catalysts. Although the total amount of coke was almost the same in both the samples, air pre-treated catalyst showed faster deactivation. XPS revealed that the nature of the carbon deposits after the pre-treatments in air and He at 600 $^{\circ}\text{C}$ was different. In the air pre-treated catalyst, the relative percentage of coke appeared at 289.5 eV was higher than that of He treated sample. Finally, it can be stated that the pre-treatment atmosphere and temperature has a clear influence on the performance and especially on the stability of catalysts. 10Pd16Sb/TiO₂ - He showed the best performance giving X-Tol = 54 % and Y-BA = 48 % with a formation period of 6 hours and was most suitable in terms of stability. In view of such superior performance, the He treated 10Pd16Sb/TiO₂ was used for further investigations in following chapters.

4 Optimization of acetoxylation reaction conditions for 10Pd16Sb/TiO₂ - He calcined catalyst

This chapter is focussed on finding the suitable parameters for the best performance of the catalyst. Various investigations were carried out to optimise the reaction variables such as the effect of the reaction temperature, acetic acid/toluene mole ratio, O₂/toluene mole ratio, contact time etc. to obtain better performance of the catalysts. All catalytic testing data presented in this chapter are obtained on He-calcined 10Pd16Sb/TiO₂ catalyst.

4.1 Influence of reaction temperature

The influence of reaction temperature on the catalytic performance is illustrated in Fig. 17. When the reaction temperature is raised from 170 to 230 °C, the conversion of toluene increased from almost 40 to 70 % and the yields of BA also increased from 20 to 54 %. Nevertheless the yield of CO₂ was quite low (<2 % at the lowest temperature), but increased continuously with increase in temperature. Therefore, it can be said that higher temperature to some extent favours total oxidation, which in turn reduces the selectivity of desired product. From these results, it can be concluded that the reaction temperature of 210 °C seems to be the optimum for high performance.

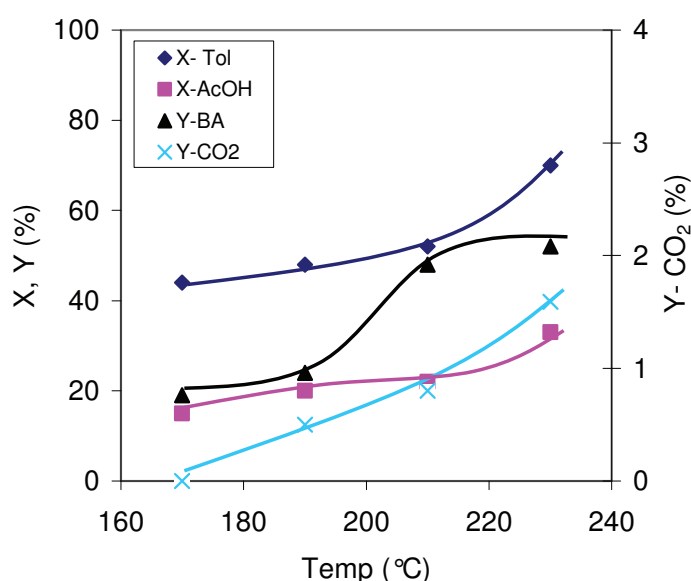


Fig. 17. Influence of temperature on the catalytic performance of 10Pd16Sb/TiO₂ - He catalyst

4.2 Influence of toluene feed rate and acetic acid : toluene feed

The influence of toluene feed rate and AcOH : toluene ratio on the catalytic performance is given in Fig. 18a-b. The toluene feed rate was changed in the range from ca. 4 to >8 mmol/h. Fig. 18a demonstrates that an increase in the toluene feed rate beyond certain level has an adverse effect on the performance, i.e. more than 5 mmoles of toluene in the reactant feed mixture has shown detrimental effect on catalytic performance. The results obtained revealed that the increase of toluene concentration in the reaction mixture leads to lowering of toluene conversion from 55 to 36 % and the yields of BA also decreased drastically from 48 to 25 %, respectively. Interestingly, the change in the feed rate of toluene in reactant feed mixture has no considerable effect on the conversion of acetic acid (X-AcOH), which is varied over a small range from 21 to

25 %. In a similar way, formation of CO_2 is also not very much affected. No effect in acetic conversion and yields of CO_2 is probably due to the lack of oxygen in the stream. Therefore toluene concentration of 5 mmol was taken as an optimum for further reactions.

In addition, the effect of AcOH : toluene mole ratio on the performance of the catalyst was studied (Fig. 18b). AcOH : Tol mole ratio was varied from 1 to 5. The Y-BA was observed to increase from 25 to 45 % with increase in AcOH : toluene ratio up to 4 and then remained more or less constant with further increase in AcOH concentration.

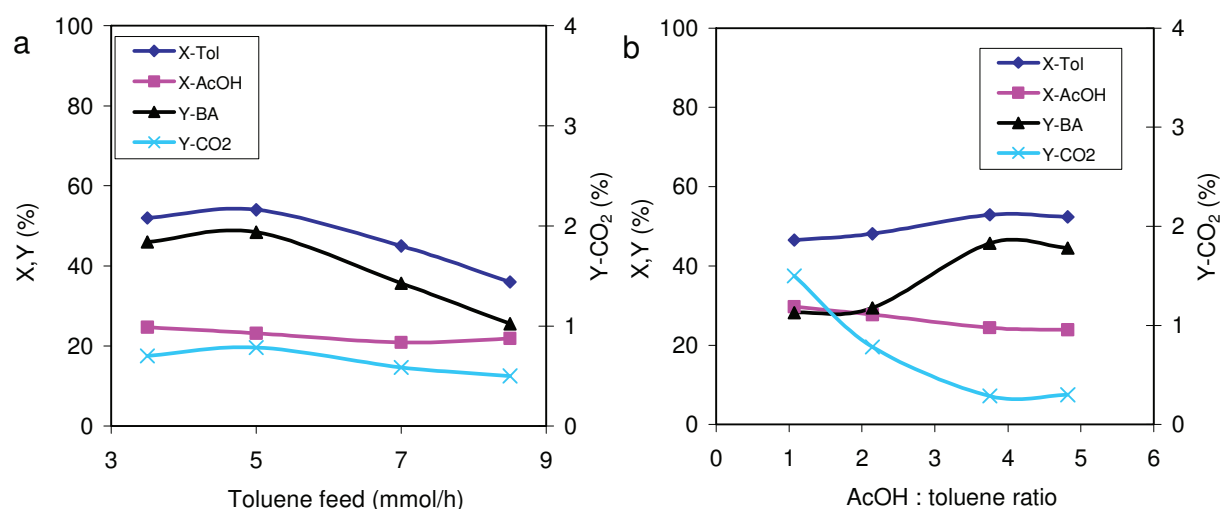


Fig. 18 a). Influence of toluene feed rate on the catalytic performance of 10Pd16Sb/TiO₂ - He catalyst; mole ratio of AcOH : O₂ : IG (inert gases) = 3 : 4 : 14-18, b). Influence of AcOH : toluene ratio on the catalytic performance of 10Pd16Sb/TiO₂ - He catalyst, GHSV = 2688 h⁻¹; mole ratio of Tol : O₂ : IG (inert gases) = 1 : 3 : 14-18, at p = 2 bar, T = 210 °C

It is quite interesting to note that the yields of carbon oxides were appreciably lowered with increase in acetic acid proportion. This result suggests that the optimum concentration of acetic acid directs the reaction in a desired way of producing more BA. In other words, increase in AcOH content in the reaction feed suppresses the formation of CO_x. These results are in good agreement with the earlier work reported [120].

4.3 Influence of oxygen : toluene ratio and feed space velocity

Fig. 19a depicts the influence of varying oxygen concentration on the performance of the catalyst in the acetoxylation of toluene. The plot displays that the conversion of toluene and yield of BA increased with increase in O₂ : toluene ratio up to 3, beyond which the total oxidation becomes dominant. X-Tol increased from almost 35 to 54 % and Y-BA rose from 28 to 50 % with increase in O₂ : toluene ratio to 3; afterwards it has no considerable effect on Y-BA.

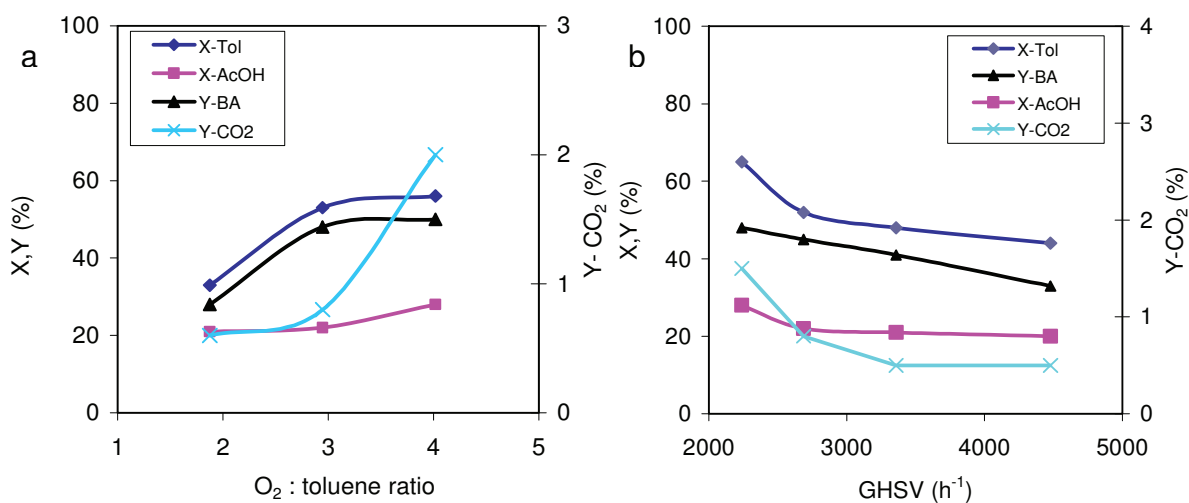


Fig. 19 a) Influence of oxygen : toluene ratio on the catalytic performance 10Pd16Sb/TiO₂ - He catalyst, GHSV = 2688 h⁻¹; mole ratio of Tol : AcOH : IG (inert gases) = 1 : 4 : 14-18; p = 2 bar, T = 210 °C, b) Influence of Gas hourly space velocity on the catalytic performance 10Pd16Sb/TiO₂ - He catalyst, mole ratio of Tol : AcOH : O₂ : IG (inert gases)=1 : 4 : 3 : 16; p = 2 bar, T = 210 °C

On the other hand, the yield of CO₂ and the conversion of acetic acid were increased with increase in O₂ : toluene ratio in the reactant feed mixture. This result clearly indicates that higher O₂ content in the feed mixture has negative effect on the performance, which in turn guides the reaction in undesired direction with higher decomposition of mainly acetic acid to CO₂. Consequently, the selectivity of BA is decreased. From this, it can be said that the O₂ : toluene ratio of 3 seems to be optimum.

The influence of space velocity on the performance of 10Pd16Sb/TiO₂ - He catalyst tested at 210 °C and at 2 bar is shown in Fig. 19b. Increasing the space velocity causes an increase in the gas velocity which promotes mass transfer but leads to a decrease in the contact time of reactant species. There is a decrease in toluene conversion from ca. 65 to ≈ 50 % with increase in gas hourly space velocity from 2240 to 4480 h⁻¹. Such increase in velocity not only affected the X-Tol but also the X-AcOH and product distribution. At the lowest space velocity (the highest contact time), the yield of CO₂ was found to be higher and hence lower selectivity of the desired product (BA). Based on these results, the best optimum space velocity in terms of performance is 2688 h⁻¹, where the higher conversion of toluene and higher yield of BA were obtained.

4.4 Study of diffusion limitations in the system

Some experiments were performed to check the mass transfer limitations in the system. The external mass transfer limitation is observed when the reactant molecules

diffuse slowly across the boundary layer of the catalyst compared to the speed with which the molecules react. The external mass transfer limitation can be checked by changing the reactant flow across the catalyst bed which will change the thickness of the boundary layer. The space velocity of the catalyst should be kept same in order to keep same reaction conditions. If no mass transfer limitations takes place then the rate of reaction is independent of flow for a given space velocity.

The internal mass transfer limitations takes place when the reactant react faster at the active sites faster than the reactant diffuses into the micro pores of the catalyst to check the internal mass transfer particle size of the catalyst were changed and the reaction was performed.

The mass transfer limitations on the fixed-bed for acetoxylation of toluene were investigated using 10Pd16Sb/TiO₂ - He catalyst by changing gas flow, catalyst pellet size, and catalyst amount.

The external mass transfer limitations on fixed-bed for acetoxylation of toluene were investigated. The catalyst was subjected to three different flows across the catalyst bed with changing the catalyst amount. Three different conditions were selected to check if there are any diffusion limits and shown in Table 6.

Table 6. External mass transfer limitations experiments

S. No.	catalyst mass (g)	pressure (bar)	Temp (°C)	total flow (ml/min)
Condition 1	0.4	2	210	22.4
Condition 2	0.8	2	210	44.8
Condition 3	1.6	2	210	89.6

The acetoxylation runs were carried out with these conditions and no change was observed in the performance of the catalyst. This result displays (Fig. 20a) that changing flow has no effect on the system. Therefore mass transfer limitations can be ruled out from this system.

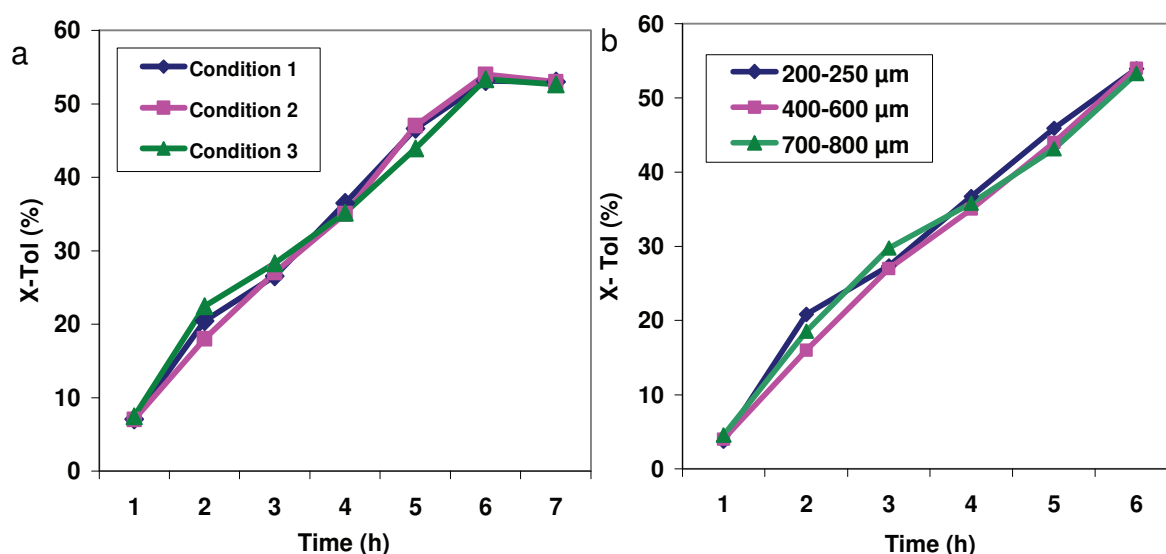


Fig. 20. Displays performance of the 10Pd16Sb/TiO₂ - He catalyst a) to check external mass transfer limitation with conditions described in table 6, b) to check internal mass transfer limitation with three different catalyst size from 200-800 μm range

To check the internal mass transfer limitation, the catalyst was deliberately sieved to three different fractions shown in Table 7 and tested.

Table 7. Internal mass transfer limitations experiments

S.No.	catalyst (g)	mass (g)	pressure (bar)	Temp (°C)	total (ml/min)	flow	catalyst (μm)	size
1	0.8		2	210	44.8		200-250	
2	0.8		2	210	44.8		400-600	
3	0.8		2	210	44.8		700-800	

The results show that the size of catalyst particles (sieved fractions) has no appreciable influence on the activity and selectivity behaviour of the catalyst. In other words, all catalyst fractions exhibit almost similar conversions of toluene and yields of benzyl acetate. This result Fig. 20b revealed that there are no internal limitations as all the catalyst fractions exhibited more or less similar activity and selectivity.

4.5 Summary and Conclusions

The optimization of the reaction parameters were carried out over 10Pd16Sb/TiO₂ - He catalysts in order to identify optimum reaction conditions required for improved

performance. The various reaction variables that can have significant influence on the catalytic performance of the catalysts, like reaction temperature, AcOH/toluene mole ratio, O₂/toluene mole ratio, diffusion limitations and contact time were checked. The catalytic runs on the catalyst showed that the reaction temperature of 210°C was optimum for better yields of BA with minimum by products and hence this temperature was selected for further catalytic tests. The AcOH/toluene mole ratio also showed strong influence on the catalytic performance of the catalysts. A significant increase in the Y-BA was observed with increase in AcOH/toluene mole ratio up to 4 and then remained unaltered beyond this ratio. From these results, the acetic acid to toluene mole ratio of 4 was taken to be optimum. Varying O₂/toluene mole ratio revealed that the X-Tol and Y-BA increased continuously up to molar ratio of 3 and then decreased with further increase in oxygen concentration. Also the yields of CO_x increased remarkably with rise in O₂ concentration. O₂/toluene mole ratio of 3 was found to be the best and hence this parameter has been selected and used in further catalytic tests. Furthermore, the effect of space velocity on the catalytic performance was also investigated. The toluene conversion decreased with increase in GHSV from 2240 to 4480 h⁻¹. The best optimum space velocity in terms of performance was found to be 2688 h⁻¹, where the higher conversion of toluene and higher yield of BA were obtained. Moreover, some additional catalytic tests were carried out to understand the diffusion limitations, under optimum reaction conditions obtained from the above tests. These acetoxylation runs were performed by sieving the catalyst to three different fractions in the range from 200 to 800 µm and by changing the total reaction flow from 22 ml/min to 90 ml/min. The catalytic results showed that the size of sieved fractions and feed flow in this range has no appreciable influence on the activity and selectivity behaviour of the catalyst. These results revealed that there are no diffusion limitations as all the catalyst fractions exhibited similar activity.

Based on these results, all further catalytic tests were carried out under optimized conditions, i.e. using the molar ratio of toluene : AcOH : O₂ : IG (inert gas) = 1 : 4 : 3 : 16 with a space velocity of 2688 h⁻¹, catalyst amount of 0.8 g and total flow of 44.8 ml/min.

5 Deactivation and Regeneration studies on using the 10Pd16Sb/TiO₂ - He calcined catalyst

The results on the long-term performance of 10Pd16Sb/TiO₂ (He calcined) catalyst are discussed in this chapter. The factors responsible for the deactivation during long-term catalytic runs are presented. The regeneration of the deactivated catalyst is carried out and the results are shown in detail. Optimization of the regeneration conditions is also described in this chapter. Furthermore, characterizations of the catalysts using various techniques (XRD, Carbon analysis, TEM, XPS) at different stages of the reaction are also given.

5.1 Time-on-stream behaviour of the 10Pd16Sb/TiO₂ - He catalyst

In chapter 3, the performance of the 10Pd16Sb/TiO₂ - He calcined catalyst up to 30 h on-stream was already discussed. However, the long term stability of this catalyst after 30 h on-stream tested under identical and optimized conditions is discussed in this chapter (Fig. 21). It is observed that the tested catalysts showed low initial activity and attained steady state conditions after six hours on-stream.

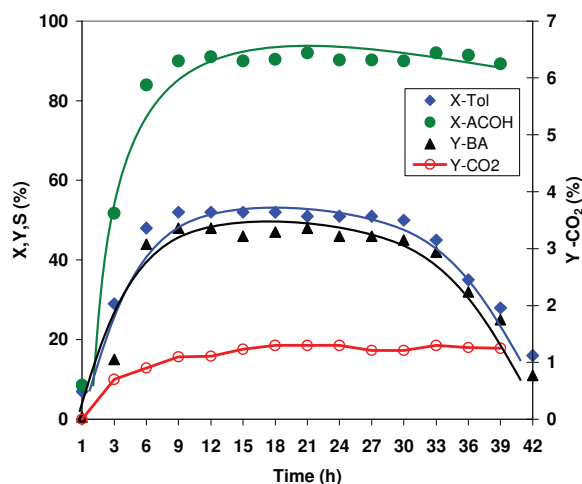


Fig. 21. Time-on-stream of 10Pd16Sb/TiO₂ - He catalyst in acetoxylation of toluene to benzyl acetate

The catalysts displayed low toluene conversion (ca. 2 %), which is observed to increase up to ca. 6 hours (> 50 %), remained stable for almost further 26 hours and then decreased with further increase in reaction time (ca. 18 % after 42 h). The Y-BA also followed the same trend like the conversion of toluene, which means the yield of BA is increased with time up to 6 hours, remained stable for next 26 hours and then decreased due to deactivation of the catalyst. It appears that the deactivation of catalyst is unavoidable process, and hence attempts were made to understand the deactivation phenomenon by characterising the samples by various techniques. In order to get deeper insights, the catalysts at different stages of reaction are characterised. The results of such approach are described below one after the other.

5.2 Characterization of the 10Pd16Sb/TiO₂ - He catalyst at different stages of reaction

In this chapter, the reasons for the deactivation of 10Pd16Sb/TiO₂ - He calcined catalyst was investigated. Various characterization studies were applied to find out the reasons for the deactivation of the catalyst. For instance, ICP, BET-SA, C H N S, XRD, TEM and XPS were used to explore the contents of metals, changes in surface area,

coke deposition, structural and composition changes, morphological changes, surface modifications, changes in valence states etc.

5.2.1 Elemental analysis and BET surface area

Table 8 displays that the Pd and Sb contents at different stages reaction are found to be more or less same. This means there is no leaching and hence no loss of active components during the course of the reaction up to 42 h on-stream.

Table 8. Elemental composition, BET surface areas and pore volume of 10Pd16Sb/TiO₂ - He catalysts after different time of reaction

Catalyst	Pd	Sb	C	BET surface area (m ² /g)	Pore volume (cm ³ /g)
Pure TiO ₂	–	–	–	171	0.27
PdSb-f(He)	9.3	9.3	–	28.6	0.10
PdSb-u32(He)	9.1	8.8	2.4	35.5	0.11
PdSb-u42(He)	9.0	8.3	3.0	34.5	0.16

BET surface areas and pore volume of pure titania, fresh and used catalyst at different stages of reaction are shown in Table 8. A significant decrease of the surface area and pore volume of the pure support was observed after loading Pd and Sb on it. This decrease is probably due to blocking of pores on the support with the metal components. However, there is no much difference in the surface areas and the pore volumes of the used solids. Even the deactivated catalyst after 42 h on-stream, did not show considerable change in the pore volume and surface area of the solids. Therefore it can be said that the changes in the catalyst surface areas and pore volumes are not the possible reason for the observed deactivation of the catalyst.

5.2.2 Carbon analysis

After the acetoxylation runs on the catalyst PdSb-f(He), it was observed that the catalyst changed the colour to black after reaction from original brown colour, indicating that the catalyst was covered by coke. Carbon contents measurements were carried out, and the relationship between catalyst activity and the amount of coke present at different stages of the reaction is shown in Fig. 22. The carbon content is progressively increased to about 2 wt% after 32 h on-stream, but still the activity of the catalyst is maintained.

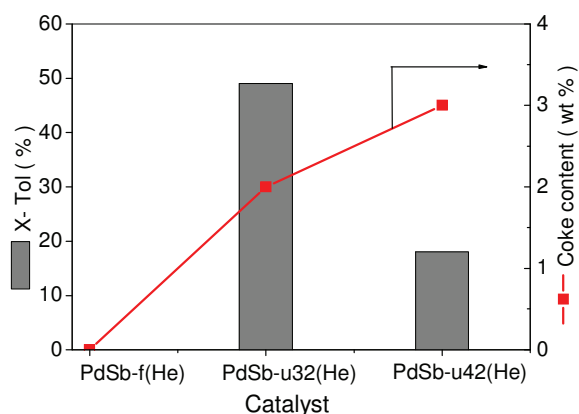


Fig. 22. Correlation between the catalyst performance and the coke formation at different time of reaction

Interesting thing here is that about 2 wt% coke has only a marginal influence on the performance. This fact suggests that the catalyst is able to sustain its performance up to a coke content of 2 wt%. However, when coke amounts raises beyond 2 wt%, the solid undergoes deactivation. Consequently, a sharp decrease in the conversion of toluene was observed. In other words, the loss of the activity is accompanied by the gain in the coke content during the reaction. Hence, coke deposits undoubtedly cause the catalyst.

5.2.3 Transmission electron micrographs

Fig. 23 shows the electron micrographs for the fresh 10Pd16Sb/TiO₂ - He calcined sample (PdSb-f(He)), after 32 h on-stream (PdSb-u32(He)) and deactivated (PdSb-u42(He)). As mentioned in the previous section 3.2.2.3, huge Pd particles (1-2 μm) were obtained after calcination in He/600 °C and during the reaction, which are however reduced to an appropriate size (50-100 nm) during the reaction to exhibit better performance. The catalyst after 42 h on-stream did not show any considerable difference in Pd size compared to the sample after 32 h on-stream (Fig. 23c). This result indicates that the deactivation of the solid is not caused by change in the size of the Pd particles.

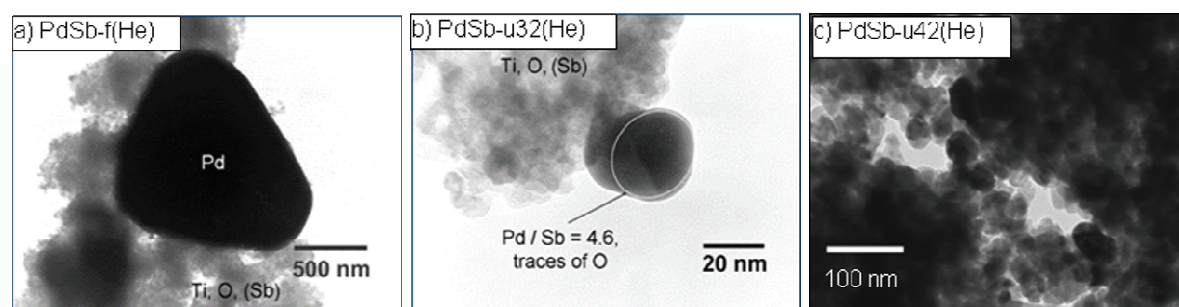


Fig. 23. Transmission electron micrographs of 10Pd16Sb/TiO₂ - He samples a) fresh, b) after 32 h on-stream and c) after 42 h on-stream

5.2.4 X-ray photoelectron spectroscopy

The XP spectra of the fresh catalyst, after 32 h on-stream and the deactivated catalyst are shown in the Fig. 24a. The spectra of the fresh sample exhibited mainly oxidised Pd species (335.8 eV) in the near surface-region. After 32 h on-stream, where the catalyst was still active, a gradual reduction of the oxidized Pd species to metallic Pd species was observed. At this stage, the catalyst contains substantial amount of metallic Pd and certain amount of oxidized Pd species. However, in the deactivated sample (i.e. after 42 h on-stream), all PdO species from the surface were reduced to metallic Pd, and the catalyst showed significantly decreased conversion of toluene. This implies that in addition to an increase in C content, change in the surface composition / change in the valence state of Pd is another cause for the catalyst deactivation.

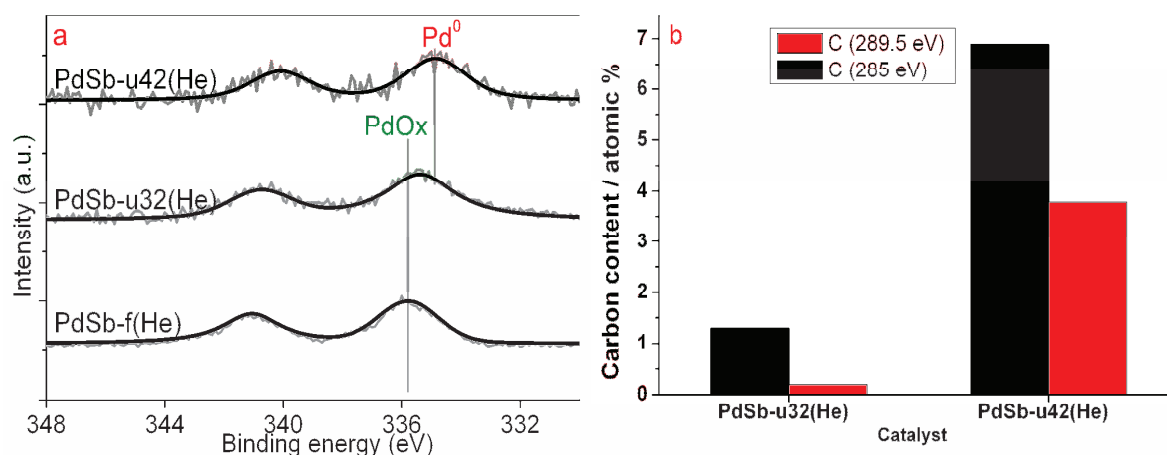


Fig. 24.a) XP-spectra of the Pd 3d peak of 10Pd16Sb/TiO₂ - He calcined fresh, 32 h on-stream and deactivated samples, b) Surface carbon concentration of 10Pd16Sb/TiO₂ - He calcined samples at 32 h on-stream and deactivated samples, analyzed from XPS. Surface atomic ratios were calculated from the areas of the XPS C1s peaks

Interesting thing is that fresh PdSb/TiO₂ (PdSb-f(He)) sample contains 100 % oxidised Pd species, where the activity is very low. During the reaction, these oxidised Pd species undergo reduction, which is accompanied by an increase in the activity. At a particular stage where the catalyst exhibited the maximum activity, it contains both oxidised and metallic Pd species more or less in equal amounts. The catalytic performance is maintained as long as both oxidised Pd and metallic Pd species are present together. However, the reduction process of oxidised Pd seems to be inevitable and hence continued further and after certain point of time, it reached a stage where only metallic Pd species are present (i.e. after 42 h on-stream). Amazingly, at this stage where no oxidised Pd species are present, the catalyst loses its performance to a large extent. This result implies that neither oxidised Pd nor metallic Pd alone is suitable for improved activity/stability of the catalyst. To maintain the better catalytic activity and to

avoid the deactivation process, both PdOx and metallic Pd in desirable amounts should be maintained. It seems that there is a good synergy between these two species. It is believed that the metallic Pd is necessary for higher activity while the oxidised Pd is crucial for improved long-term stability.

As mentioned in the previous chapter in section 2.2.6, two types of carbon peaks were observed during different stages of reaction, the first one (easily removable) at 285 eV and the second one (difficult to remove) at 289.5 eV (Fig. 24b). In general, it is expected that the coke deposition on the surface hinders the reaction and thereby causes deactivation of the catalyst due to blocking of active components. In the present study, the second type of coke seems to show more pronounced effect on the catalyst deactivation compared to the first one. Nevertheless, both the types of coke are found to increase considerably during the course of reaction. This seems to be the reason for the rapid deactivation of the catalyst that is taking place between 32 h to 42 h on-stream.

As discussed earlier, better understanding of deactivation and regeneration process is essential for improving and optimising the process conditions to considerably reduce financial burden. Deactivation of palladium catalysts can be caused by mainly particle growth/sintering, coke deposition, effect of the mechanical stability of support on long term stability and changes on Pd surface itself [93]. Major reasons for the deactivation in the present case can be concluded as follows:

- i) Increase in carbon content with time as evidenced from carbon analysis.
- ii) Changes in the valence states of Pd during the course of reaction
- iii) Complete loss of PdO species from the surface of the catalyst.
- iv) Decreased concentration of Pd in the near-surface-region.

In order to regenerate the deactivated catalyst by burning of coke and to regain the lost oxidized species, deactivated catalysts were treated in air.

5.3 Regeneration of 10Pd16Sb/TiO₂ - He calcined catalyst

At first, to find out the temperature region for the effective removal of the carbonaceous species, TG-DTA analysis was done until 700 °C in presence of air. Fig. 25 showed the corresponding TG-DTA plots of the deactivated sample. Endothermic broad peak at low temperature (70-100 °C) corresponds to desorption of physically absorbed water. Maximum weight loss due to decomposition of carbon is occurred in the temperature range of 250-400 °C. A weight loss of around 4 wt% was observed in this temperature range. Hence, four different temperatures such as 250, 300, 350 and 400 °C were chosen for regeneration of the deactivated PdSb/TiO₂ catalyst. Then the deactivated catalyst was treated in oxidising atmosphere to burn-off carbon deposits at

four different temperatures. The purpose of this study is to find out the optimum temperature for effective removal of coke and thereby efficient regeneration.

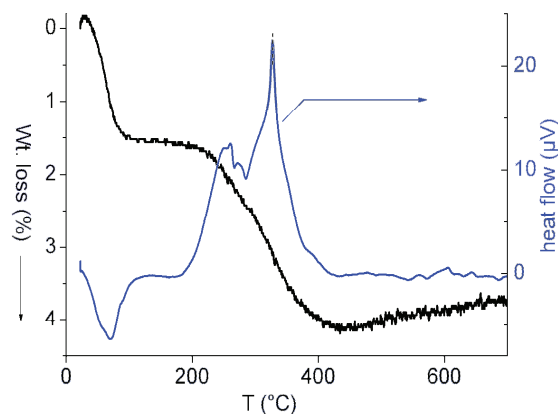


Fig. 25. TG-DTA curves of the deactivated 10Pd16Sb/TiO₂ catalyst

The catalytic performance of the solids after these regenerations is shown in Fig. 26. For example, deactivated PdSb-u42(He) catalyst was regenerated in air at 250 °C for 2 h and then the reaction was continued under identical reaction conditions as before regeneration in order to compare its performance with the fresh catalyst. It is clear from the Fig. 26 a, that the catalyst regenerated at 250 °C immediately restored its maximum activity that has been lost due to coke deposits. It is quite amazing that the conversion of toluene and the yield of BA observed on the fresh and regenerated catalysts are more or less similar. Nevertheless this regenerated catalyst undergoes much more rapid deactivation than the fresh one during time-on-stream. Considering this result, it was thought that probably, the regeneration temperature was not sufficient to effectively remove the coke to restore the activity. Therefore, another catalyst deactivated sample was taken and again regenerated in a similar way but at higher temperature of 300 °C in air for 2 h. In this case also activity and selectivity of the catalyst were completely restored (Fig. 26b). The regenerated sample showed the performance of the first run (X-Tol = 54 %, Y-BA = 48 %), which is comparable with the fresh catalyst. It was found that the carbon deposits on the surface of the catalyst were more or less completely burned-off by air flow at 300 °C and thereby restored its activity. In addition, the performance of the sample regenerated at 300 °C was much more stable than the one regenerated at 250 °C. Such result also prompted us to go for higher regeneration temperatures of more than 300 °C. Thus in the next step, the deactivated catalyst samples were treated at 350 and 400 °C for 2 h in air, with an intention to further improve the efficiency of regeneration process. Surprisingly, it was found that this regeneration at 350 totally failed to restore activity. The sample showed more or less similar performance as that of deactivated catalyst (i.e. X-Tol ~ 18 %, Y-BA ~ 12 %) as

5. Deactivation and Regeneration Studies

depicted in Fig. 26c. To confirm this result further, again the deactivated catalyst was treated at higher temperature of 400 °C. Unfortunately, it was not possible to regenerate this catalyst and hence the activity could not be restored even with 400 °C regeneration temperature (Fig. 26d). Interesting thing here is that at 350 and 400 °C, instead of removal of coke from the surface of deactivated catalyst, the amount of coke in the near-surface-region is considerably enhanced, which is probably due to migration of carbon from deeper layers to the surface at such higher regeneration temperatures. As a result the catalyst was not able to restore its activity that is lost during deactivation. From the above observations, it can be said that the catalyst deactivation is widely reversible only if the catalyst is treated at the temperatures of 250 °C and 300 °C for 2 h in air. Obviously, higher temperatures of 350 °C and above are not suitable to recover the catalyst performance. The regeneration temperature of 250 °C was able to restore the activity but not for a prolonged period of time. Among all the four temperatures investigated it is clear that 300 °C regeneration temperature is effective in restoring activity and also giving stable performance.

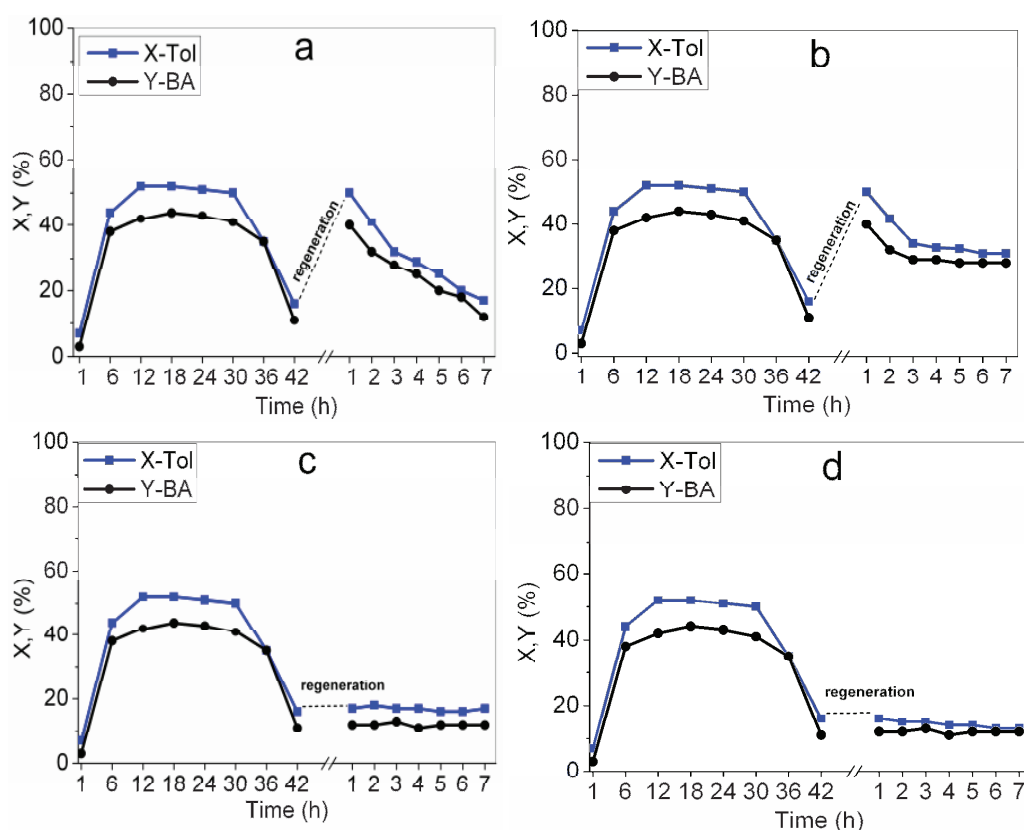


Fig. 26. Performance and regeneration of the 10Pd16Sb/TiO₂ - He catalyst at different temperatures a) 250 °C/2h/air, b) 300 °C/2h/air, c) 350 °C/2h/air, d) 400 °C/2h/air

5.3.1 Carbon analysis

Carbon content measurements were carried out for the four samples collected after regeneration at 250, 300, 350 and 400 °C for 2 h in air. Table 9 only gives the data of the samples regenerated at 300 and 350 °C because carbon contents of the other samples are quite similar (0.2-0.3 wt%). Obviously, carbon deposits can be removed from the catalyst by more than 80-90 %. Then acetoxylation runs were carried out on the regenerated samples and carbon content was analysed again. As expected, the carbon content again increased considerably in 6-7 h on-stream. Carbon deposition and the poor performance of the catalyst treated at 350 °C and higher suggest that not just the presence of coke is influencing the activity but probably also some structural changes occurred during higher temperature treatment.

Table 9. Carbon contents and BET surface areas of the 10Pd16Sb/TiO₂ catalyst at different stages of the reaction

Catalyst at different stages	C	BET surface area (m ² /g)
PdSb-u42(He)	3.0	34.5
PdSb-u42-r300(He)	0.38	31.3
PdSb-u42-r350(He)	0.26	32.2
PdSb-u42-r300-u7(He)	1.78	16.2
PdSb-u42-r350-u7(He)	1.63	18.1

5.3.2 BET surface area and pore size distribution

The BET surface area values of the deactivated (PdSb-u42(He)), regenerated at 300 °C (PdSb-u42-r300(He)) and 350 °C (PdSb-u42-r350(He)) and used (second reaction run) samples (PdSb-u-r300-u7(He) and PdSb-u-r350-u7(He)) are presented in Table 9. A significant increase in surface area of the catalyst was observed from fresh to maximum active catalyst. i.e. from 28.6 to 40.6 m²/g, respectively. However, no such significant difference was observed in the surface area during the course of reaction and even after regeneration, it remained in the range of 40-32 m²/g. However, a dramatic decrease in surface area, from nearly 32 m²/g to ~16 m²/g, was observed in the solids after regeneration and second reaction run. This suggests that the nature of catalyst has been changed after regeneration.

The pore size distribution of the deactivated, regenerated and used samples in a second reaction run after regeneration is quite similar to that of the fresh catalyst (Fig. 27). However, sample regenerated at 350 °C shows a significant increase in pore volume; it is nearly doubled for larger pores compared to the sample regenerated at 300 °C. Nevertheless, catalysts retain the same pore structure as that of fresh ones during all the stages of the reaction.

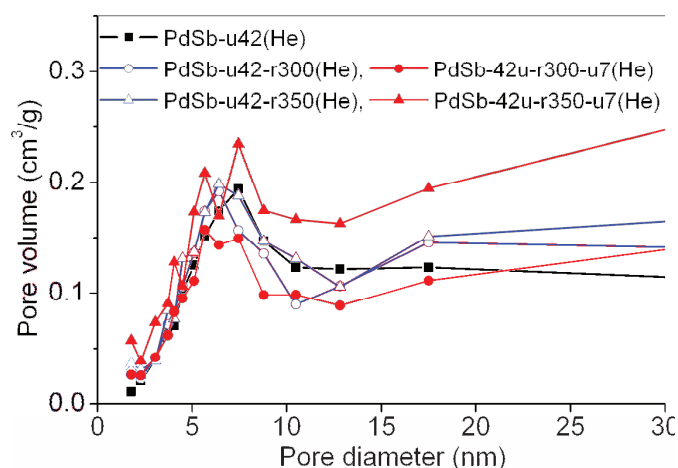


Fig. 27. Pore size distribution of 10Pd16Sb/TiO₂ - He samples at different stages of reaction

5.3.3 X-ray diffraction

XRD patterns of the fresh, deactivated catalyst along with the solids regenerated at 300 °C and 350 °C are shown in Fig. 28a. The XRD patterns of all samples show reflections of the anatase support, NaCl (which is formed by Na₂CO₃ and PdCl₂ used during the preparation). In addition, a shift in metallic Pd reflections was observed compared to the fresh one during the course of reaction. Shift in peak position can be explained due to the Pd lattice expansion during time-on-stream, which is most probably caused by the incorporation of other components such as Sb and/or C into the Pd lattice. In contrast, the completely deactivated catalyst PdSb-u42(He) did not show any clear splitting of the peak. In [127], such shift of the reflection was also observed and was explained earlier by the incorporation of Sb and C in the Pd lattice. It is known that such incorporated carbon can be removed by heating in air below 300 °C [128]. The most active catalyst (PdSb-u6(He)) has negligible amount of carbon (0.65 wt%) and the regenerated samples showed lattice expansion with two separate reflections at $2\theta = 39.8$ and 39.5 . This is due to the incorporation of Sb in the Pd lattice. It must be noted that the diffractograms of the most active and the regenerated samples are very similar. In contrast, the completely deactivated PdSb-u42(He) showed a broad asymmetric reflection below 40° consisting of various Pd species. A deconvolution of

this peak is not possible due to the presence of various Pd species. The differences between the Pd reflections in the spent sample (PdSb-u42(He)) and the both regenerated samples are caused by the removal of carbon during the regeneration. However, XRD provides no hint for the poor performance of the samples regenerated at higher temperature (350 and 400 °C) in the subsequent catalytic run. This surprising result is clearly explained by other techniques as described in the coming sections

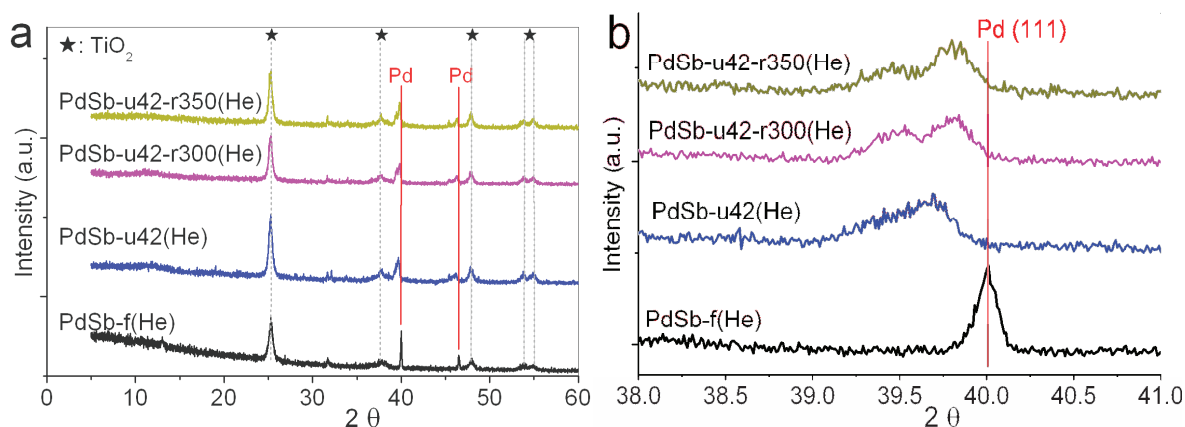


Fig. 28. a) XRD patterns of samples of fresh (PdSb-f(He)), deactivated (PdSb-u42(He)), and regenerated 10Pd16Sb/TiO₂ catalysts (PdSb-u42-r300(He) and PdSb-u42-r350(He)), b) XRD patterns in the 2θ range of the Pd(111) reflection (38-41 °)

Fig. 29a-b display the diffractograms of the catalysts used in a second acetoxylation run after regeneration at 300 and 350 °C (PdSb-u42-r300-u7(He)) and PdSb-u42-r350-u7(He). From these reflections, it can be seen that the shifted splitting of the Pd peak at 40.01° is significantly observed only in the sample treated at 300 °C for 2 h in air, whereas in case of 350 °C, no such reflections were observed after second run.

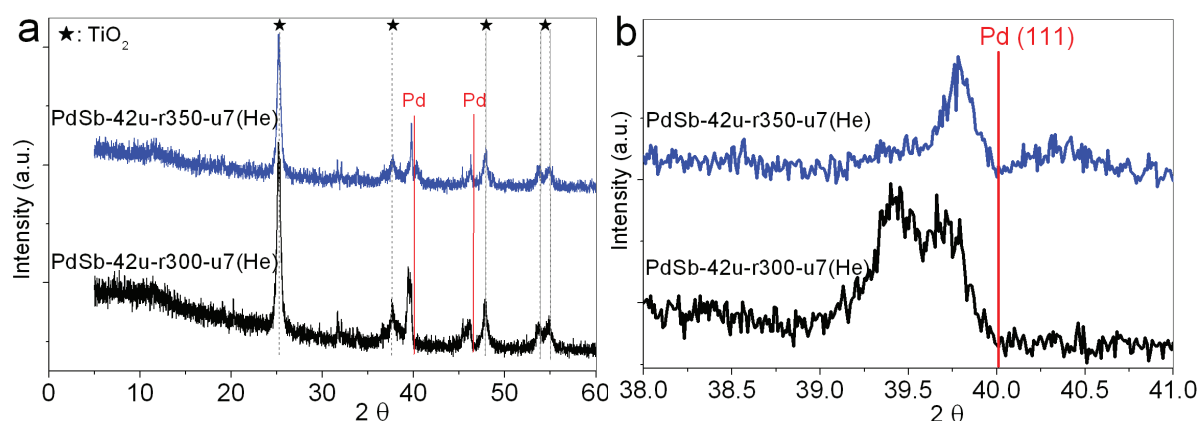


Fig. 29. a) XRD patterns of 10Pd16Sb/TiO₂ samples used in a second reaction run after regeneration at 300 and 350 °C (PdSb-u-r300-u7(He) and PdSb-u-r350-u7(He) resp.), b) XRD patterns in the 2θ-range of the Pd(111) reflection (38-41 °)

5.3.4 Transmission electron microscopy

Fig. 30 a-c shows electron micrographs of regenerated catalysts. (Deactivated (PdSb-u42(He) is shown in Fig. 23c). These samples display spherical shape particles with size varying in the range of 50-100 nm. TEM images of the samples regenerated at different temperatures displayed that most of the particles are spherical and their size remain unchanged through out, irrespective of thermal pre-treatment given. That means regeneration treatment had no effect on the size and morphology of the catalyst. However, restructuring of particle with tri or hexagonal array was observed only in the sample after regeneration at 400 °C. From previous studies [120, 129] it is known that the catalytic activity is strongly dependent on Pd particle size. It is also known that the sizes of Pd particles need to attain some critical size (50-100 nm) to show the best performance. But in this series, all regenerated catalysts exhibit almost the same size (50-100 nm) as that of the maximum active catalyst. These observations suggest that the size of Pd particles play a key role mainly during the initial stages of the reaction (i.e. during induction period), where the fresh catalyst contains Pd size in the range from 1-2 μm (He calcined catalyst). However, during time-on-stream these bigger Pd particles undergo restructuring and adjust the size of the Pd to 50-100 nm. Interestingly, after reaching its critical size and showing the best performance, the particle size does not change much with time. Even regeneration treatments of 300 °C to 400 °C for two hours in air have showed no influence on the Pd particle size. Based on these results, it can be said that the poor performance of the regenerated catalysts at higher temperatures of 350 and above has nothing to do with the Pd particle size of the catalyst. Surface properties probably play more important role in the determining the performance of the regenerated catalysts in the acetoxylation reaction.

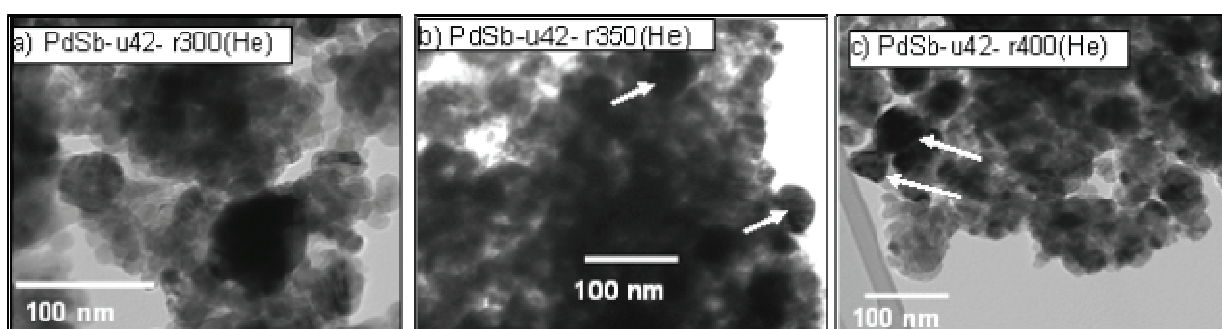


Fig. 30. Transmission electron micrographs of 10Pd16Sb/TiO₂ - He samples after regeneration at a) 300 (PdSb-u42-r300(He)), b) 350 (PdSb-u42-r350(He)) and c) 400 °C (PdSb-u42-r400(He)) for 2 h in air

As such, from the above observations it can be stated that bulk compositions are not determining the performance of the catalyst. The distribution and valence state of active

surface components probably plays an important role and are may be related to the activity of the catalysts

5.3.5 X-ray photoelectron spectroscopy

Fig. 31 displays the XP spectra of the maximum active sample, deactivated sample (PdSb-u42(He)), two regenerated samples one at 300 °C (PdSb-u42-r300(He)) and the other at 350 °C (PdSb-u42-r350(He)) For better comparison, the catalysts used in a second reaction run for additional 7 h after regeneration at 300 and 350 °C, i.e. PdSb-u42-r300-u7(He)) and (PdSb-u42-r350-u7(He)) are also shown in this figure. The Pd 3d_{5/2} binding energies are found to vary in the range of 334.8-335.2 eV, which indicates that the palladium is in a metallic state [130]. The surface composition of the fresh sample exhibits mainly oxidised Pd species (335.8 eV) in the near surface-region. After 6 h on-stream reaction, where the catalyst reaches its maximum performance, XPS peaks corresponding to both the metallic Pd⁰ and PdO were observed. This means that during the first hours of reaction, a gradual reduction of oxidised Pd species is occurring to a certain extent, therefore the formation of metallic Pd species along with PdO species was observed. As the reaction proceeds, a progressive reduction of PdO species was continued further. As a result, all the oxidised Pd species are completely reduced to metallic Pd after 42 h on-stream and then the catalyst is deactivated. From these observations, it can be concluded that the presence of both Pd⁰ and PdO species on the surface is vital for the best performance of the catalyst with good long-term stability. After regeneration at 300 °C in air for 2 h, PdO species, which were lost in the deactivated sample, could be restored back to a larger extent. In contrast, the spectra of the catalyst treated at 350 °C for 2 h reveals that this treatment could not restore the required concentration of PdO on the surface and hence such treatment is not able to regenerate the catalyst. The absence of enough PdO species on 350 °C regenerated catalyst strongly indicates the necessity of PdO on the surface for better performance of the catalyst. Therefore, the catalyst treated at 350 °C did not restore the performance compared to the one treated at 300 °C. Additionally, surface concentration of Pd⁰ and PdO species in these samples were also estimated and presented in Fig. 31b. These results once again gave clear hints that PdO presence in addition to coke removal was essential to obtain good performance. It is clear from this estimation that the sample regenerated at 350 °C could only show a Pd⁰ : PdO surface ratio of 9 : 1, while the sample regenerated at 300 °C reveals such ratio of 6 : 4. Interestingly, this ratio is comparable with that of maximum active sample, which shows a Pd⁰ : PdO surface ratio of 4.5 : 5.5.

5. Deactivation and Regeneration Studies

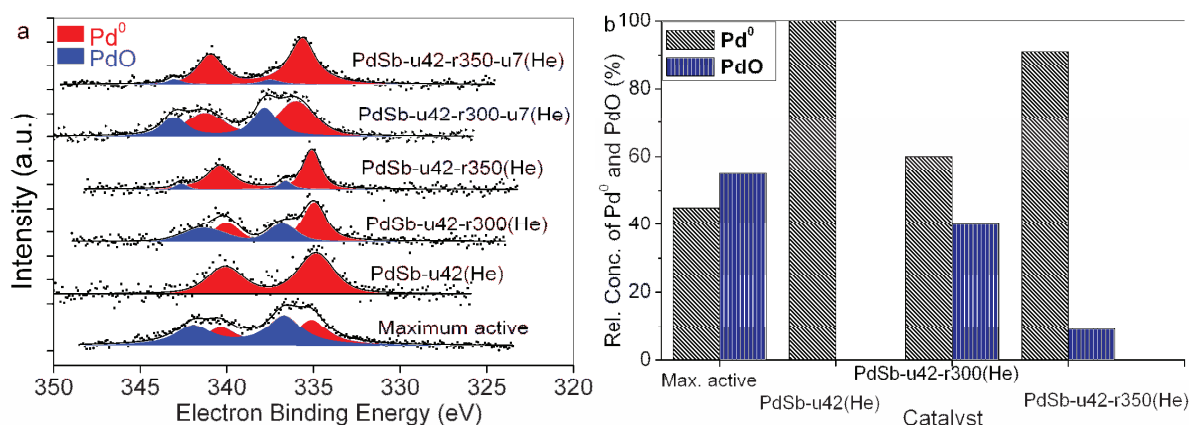


Fig. 31. a) XP spectra of the Pd 3d peak of 10Pd16Sb/TiO₂ - He samples at different stages of the reaction, b) Relative surface concentration of Pd⁰ and PdO in 10Pd16Sb/TiO₂ - He samples at different stages of reaction

It is very interesting to note that even though very small amounts of PdO species were found on the surface of the catalyst treated at 350 °C, but the surface ratio of the Pd⁰ : PdO is much far from the required optimum ratio. In conclusion, it must be stated that not just the existence of PdO and Pd⁰ species but their optimum ratio is essential to exhibit the better performance of the catalyst. Additionally, Sb concentration on the surface of fresh (PdSb-f(He)), maximum active, deactivated (PdSb-u42(He)) and regenerated solids (PdSb-u42-r300(He)) and PdSb-u42-r350(He)) were also studied using XPS. The spectra shown in Fig. 32a revealed that Sb is present in oxidized form, evidenced by a Sb 3d_{3/2} peak with a binding energy of 540 eV, being characteristic for Sb₂O₃ [126]. The surface Sb : Ti atomic ratios (Fig. 32a) showed that maximum active sample contains the highest Sb portion at the surface compared to deactivated and regenerated samples. Interestingly the sample treated at 350 °C could not restore the Sb concentration in the near surface region and hence no effective regeneration with regard to the parent Sb : Ti surface ratio was possible. A similar trend was also observed in the case of total Pd : Ti ratio on the surface during the reaction (Fig. 32b). The total Pd concentration was also found to be reduced on the surface of the deactivated catalyst (PdSb-u42(He)) compared to the one at maximum activity (PdSb-u6(He)). This loss of total Pd on the surface couldn't be restored adequately even after regeneration. This loss of total Pd from the surface can be accounted for the quick deactivation of the catalysts in subsequent runs after regeneration. Here one should note that elemental analysis by ICP-OES of the spent catalyst at different stages, deactivated and fresh regenerated catalyst did not show any loss of Pd or Sb from the catalyst. So the possibility of leaching of the Pd or Sb from the catalyst can be ruled out.

In summary, the catalytic performance is related to the surface concentration of Pd and Sb and the amount of deposited coke. If the optimum combination is altered, the

performance will be lowered. The amount of carbon at the surface plays a crucial role in the catalytic performance of the regenerated sample.

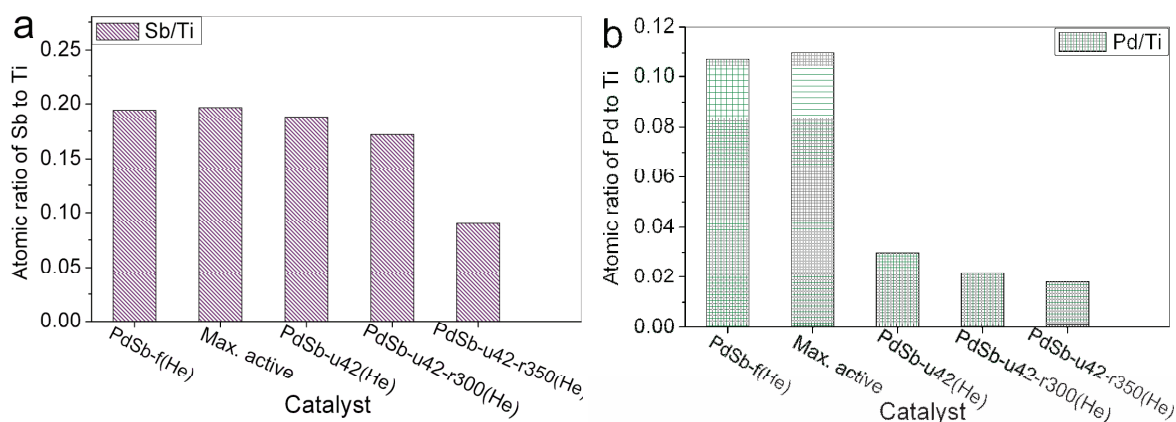


Fig. 32. Surface atomic ratio in 10Pd16Sb/TiO₂ - He samples at different stages of the reaction analyzed from XPS. a) Sb : Ti, b) Surface Pd : Ti. Surface atomic ratios were calculated from the areas of the XPS Sb3d, Pd3d, and Ti2p peaks

As discussed earlier, the coke deposits accumulated during the reaction are an important factor in the deactivation and regeneration of the catalyst. Fig. 33 shows some additional results from XP spectroscopy. Results reveal that there are two types of carbon species, one at 285.1 eV related to C–H, coke, and other at 289.8 eV, which is related to O–C=O, [118] [121]. From the trend of occurrence of such peaks on the surface, it again hints that coke species at 289.5 eV accounts for deactivation; it does not allow the catalyst to maintain its stability for a longer time. In the maximum active catalyst, only small amount of first type of coke (285.1 eV) was noticed, but, this coke has no considerable effect on the performance. However, the deactivated sample contained both types of cokes where the coke corresponds to 289.8 eV peak is in higher amount. When this deactivated catalyst was regenerated at 300 °C/2 h in air both types of cokes were removed from the surface to a certain extent. But such removal was not possible if the deactivated samples were treated at higher temperatures. Therefore, the catalyst could not be regenerated effectively and showed poor performance. Additionally, such high temperature treatment also appears to promote the migration of C species from the deeper layers to the surface. As a result, the amount of C on the surface is considerably increasing while the surface Sb content is simultaneously decreasing. Both these effects together have negative influence on the performance and hence the catalyst treated at such temperatures can not be effectively regenerated. Amount of the carbon present, especially the second type of coke on the surface of the solids regenerated at 300 °C is still higher as compared to the carbon content on the catalyst on maximum active. Probably, this is one of the reasons for the significant deactivation of the catalyst during first hours in second catalytic tests (see Fig. 26b).

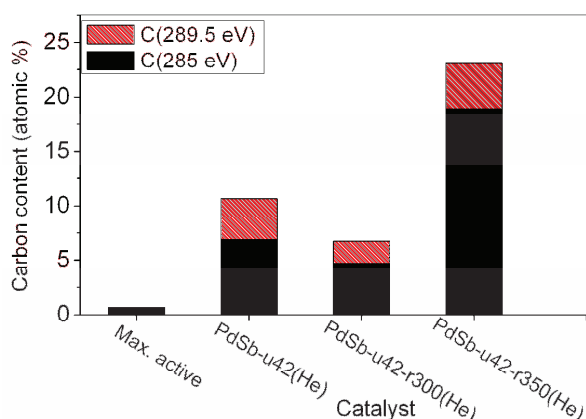


Fig. 33. Surface carbon concentration of 10Pd16Sb/TiO₂ samples at different stages of the reaction, analyzed from XPS. Surface atomic ratios were calculated from the areas of the XPS C1s peaks

However, more or less similar features could be seen from XRD and XPS (Pd^0 : PdO ratio) for the maximum active and sample regenerated at 300 °C (PdSb-u42-r300(He)) (Fig.28a and Fig.31a). In addition, formation of carbon species on the surface seems to accelerate the deactivation process of the catalyst. Therefore, it can be said that the regenerated sample at 300 °C could show immediately similar performance to the catalyst at its maximum activity due to the accumulation of optimum Pd^0/PdO ratio, while easy deactivation such solid in subsequent runs can be correlated to the presence of excess of C content on the surface of the regenerated catalyst. In the case of 350 °C treated catalyst, insufficient amount of PdO , less Sb and excess of carbon (both types) on the surface together accounts for the poor performance of this solid.

5.3.6 Effect of regeneration time (2, 4 and 6 hours) at 300 °C in air

In the studies shown in the previous sections, the 10Pd16Sb/TiO₂ deactivated catalyst (after 42 h on-stream catalyst) was regenerated in air for two hours at four different temperatures. The regeneration at 250 and 300 °C for 2 h in air was found to be suitable to regain its catalyst performance. In contrast, treatment at (350 and 400 °C) was not suitable for regeneration. The treatment at 300 °C for 2 h in air was found to be the best procedure tested to regenerate the catalyst reaching again X-Tol = 54 % and Y-BA = 48 %. Therefore to further optimize the regeneration parameters temperature of 300 °C in air was selected and duration for regeneration was varied. 10Pd16Sb/TiO₂ - He calcined catalyst was subjected to acetoxylation runs till it gets deactivated and then the reaction feed was stopped. The deactivated catalyst was heated in air at 300 °C for 2, 4 and 6 hours individually (in total 3 experiments). Fig. 34(a-c) shows the effect of the duration of regeneration on the performance of catalyst.

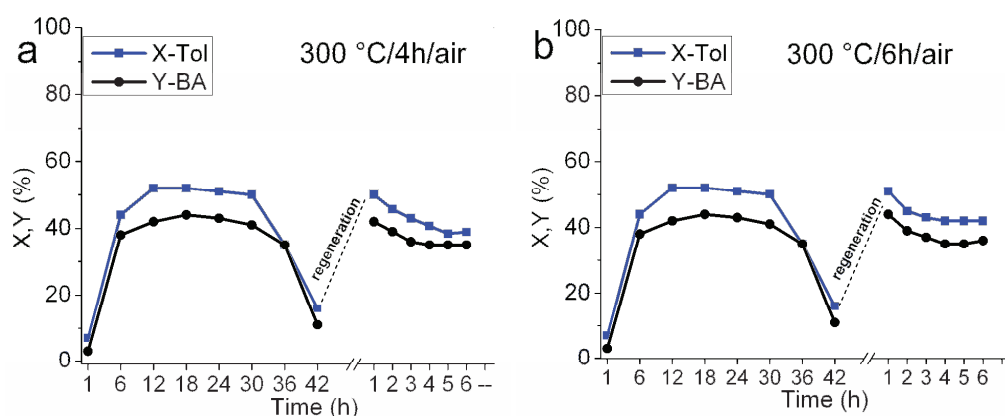


Fig. 34. Influence of regeneration time on the performance of the 10Pd16Sb/TiO₂ (He-calcined one) a) 300 °C/4h/air, b) 300 °C/6h/air

The catalyst activity clearly shows that regeneration duration has an influence on the stability of the regenerated catalyst activity. It was found that the catalyst regenerated after 300 °C for 2 hours immediately restored its maximum activity (X-Tol = 54 %, Y-BA = 48 %), but again undergoes deactivation much more rapidly than the fresh one in the following runs i.e. in 2nd hour of the reaction (Fig. 26b). If the deactivated catalyst was subjected for 4 hours regeneration in air, such catalyst not only restore its maximum performance (X-Tol = 54 %, Y-BA = 48 %) but also improves the stability compared to the one regenerated for 2 hours. Catalyst activity after regeneration for 4 hours did not show sharp fall in its performance compared to the earlier one which was regenerated only for 2 hours (Compare fig. 26b and Fig 34a). Although in the case of 4 hours regeneration also, activity did not remain same throughout for next 33 h on-stream like in the case of fresh, but the fall in activity was much gradual compared to 2 hours treated one. In view of such beneficial effect of regeneration time, further efforts were focussed to regenerate the deactivated catalyst for much longer durations, e.g. for a duration of 6 hours. The catalyst showed stable performance after regeneration, which was somewhat comparable with that of the one regenerated for 4 hours. In other words, the regeneration duration of either 4 or 6 hours has no significant effect on the performance and hence 4 h seems to be optimum for the regeneration of catalyst at 300 °C in air.

5.4 Summary and Conclusions

The 10Pd16Sb/TiO₂ - He catalyst showed the best performance of X-Tol = 54 % and Y-BA = 48 %. However, this catalyst undergoes deactivation nearly after 33 h on-stream (X-Tol = 18 % and Y-BA = 12 %). The deactivation is due to accumulation of carbon deposits and a change in the valence state of Pd during the reaction. The regeneration of the deactivated catalysts was carried out in air for 2 h at four different temperatures (250-400 °C). The treatment at 250 and 300 °C was found to be suitable to regain

catalyst performance. Higher temperature treatment (350 and 400 °C) was not suitable for regeneration and hence the catalyst did not regain the activity that is lost during the deactivation. Carbon analysis by C H N S reveals an effective removal of coke deposits during the regeneration irrespective of the temperature applied. However, the samples regenerated at higher temperatures remained inactive. TEM studies revealed that there is no change in Pd particle size between deactivated and regenerated one. Detailed XPS characterizations showed that an optimum amount of PdO and Pd⁰ on the surface is necessary for the better performance of the catalyst. The PdO deficit in the sample regenerated at 350 °C seems to be mainly responsible for the ineffectiveness of regeneration beyond 350 °C. Carbon deposits in turn caused a decrease in the surface concentration of both Pd and Sb as discovered by XPS. Thus, the existence of Pd⁰, PdO and Sb synergy on the catalyst surface is needed to maintain a stable and high performance of the catalyst.

6 Effect of reaction pressure on the performance of 10Pd16Sb/TiO₂ - He catalyst

This chapter contains the descriptions and evaluations of the catalytic data obtained by varying the reaction pressure. The changes in the performance of the catalyst with varying reaction pressure in the range of 1 to 10 bar are shown. The nature of the catalysts is analyzed at each pressure and discussed with the help of various characterization methods.

6.1 Calculation of the dew point for the reaction mixture

To study the effects of varying the reaction pressure on the catalyst performance, the pressure was chosen in a range in which the reaction components remain in gaseous phase at the reaction temperature of 210 °C. In order to ensure that the phase behaviour of the components (preferred gaseous phase) under the reaction conditions applied, it is necessary to conduct a dew point calculation.

According to Raoult's law, the partial pressure in the gas phase can be calculated from the vapour pressure of each component. This is defined as:

$$p_i = x_i \cdot p_i^0(T) \quad (27)$$

p_i is the partial pressure of the component i in the mixture

$p_i^0(T)$ is the vapour pressure of the pure component i

x_i is the mole fraction of the component i in a liquid droplet at the dew point (in mixture)

and according to Dalton's law

$$y_i \cdot P_{\text{total}} = p_i \quad (28)$$

y_i is mole fraction of the i^{th} component in the total mixture in the gas phase

p_i is the partial pressure of the component i in the mixture

P_{total} is the total pressure of the mixture

$$\sum x_i = 1 \text{ and } \sum y_i = 1 \quad (29)$$

To elucidate the dew point of our system, the above equations have been combined:

$$x_i \cdot p_i(T) = y_i \cdot P_{\text{total}} \quad (30)$$

Additionally, the vapour pressure can be calculated from the Antoine equation:

$$p_i(T) = e^{A/(B+CT)} \quad (31)$$

A, B, C are the Antoine constants, defined for every component.

Substituting eq. 30 in eq 29, we get

$$x_i \cdot e^{A/(B+CT)} = y_i \cdot P_{\text{total}} \quad (32)$$

Solve the system of equations (given by eq. 32) and the summation equation (given by eq. 29). After solving these two equations one can obtain the composition of the first droplet of dew (as x_i) as well as the temperature of the dew point (T). Calculations were done using Aspen plus software.

Fig. 35 shows the dew point curve of the system, where the mixtures of gases (Tol, AcOH, BA, benzaldehyde, carbon dioxide, methane, nitrogen and oxygen) start to condense below the curve (i.e. < 180 °C) and they are in gaseous state above the curve

(i.e. $> 180\text{ }^{\circ}\text{C}$). Thus, it is quite clear from the curve that up to a reaction pressure of 12 bar and under the desired reaction temperature of $210\text{ }^{\circ}\text{C}$, the reactant feed mixture of toluene acetoxylation remains in gaseous state.

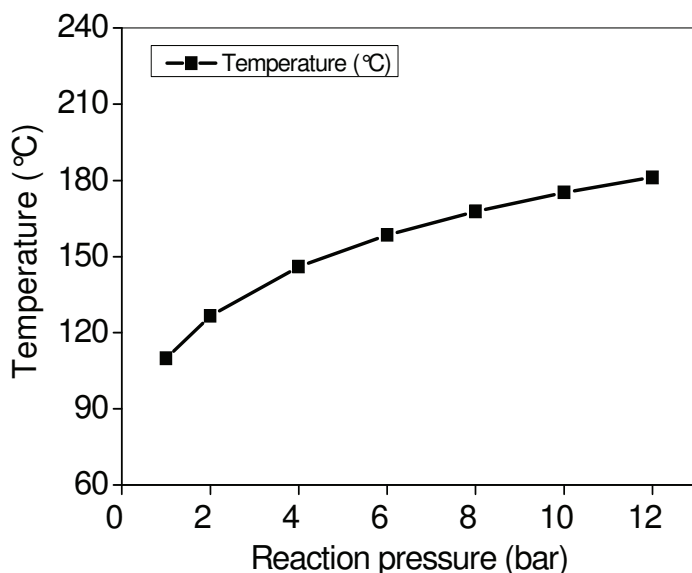


Fig. 35. Dew point temperature curve for the present reaction with varying pressures

6.2 Time-on-stream performance of the 10Pd16Sb/TiO₂ - He catalyst with varying pressure

10Pd16Sb/TiO₂ - He calcined catalyst was subjected to acetoxylation runs with conditions of molar ratio of toluene : AcOH : O₂ : N₂ = 1 : 4 : 3 : 16 with space velocity of 2688 h^{-1} , a catalyst amount of 0.8 g and total flow of 44.8 ml/min, $p = 1$ to 10 bar.

Fig. 36 displays the performance of the catalysts tested with varying pressure in the range from 1 bar to 10 bar. It is evident from the figure that the pressure has a pronounced effect on the performance of the catalyst. 1 bar reaction pressure displayed low initial activity (X-Tol $\sim 1.8\%$, Y-BA $\sim 0.1\%$), which increased with time-on-stream and reached maximum at 11th hour (X-Tol = 34 %, Y-BA = 25 %, S-BA = 74 %). To further check the effect of pressure, reactor was loaded with fresh catalyst and tested under the same reaction conditions as mentioned above but the reaction pressure was increased to 2 bar. The catalyst showed similar trend of low initial activity (X-Tol $\sim 2.9\%$, Y-BA $\sim 0.3\%$), which increases up to 6 hours where the catalyst displayed X-Tol = 54 %, Y-BA = 48 %, S-BA = 89.5 %. This means the catalyst tested at 2 bar showed an induction period of 6 hours to exhibit maximum activity. In view of this, the reaction pressure was enhanced further from 2 bar to 4 bar for new catalyst and tested. Similar behaviour was noticed with (X-Tol $\sim 4.6\%$, Y-BA $\sim 1.3\%$) at the start and attains stability with (X-Tol = 57 %, Y-BA = 52 %, S-BA = 91 %). However, the catalyst treated

at 4 bar did not show significant difference from 2 bar in terms of induction period. i.e. catalyst reached its maximum activity after 5 hours which is comparable with the induction period observed at 2 bar.

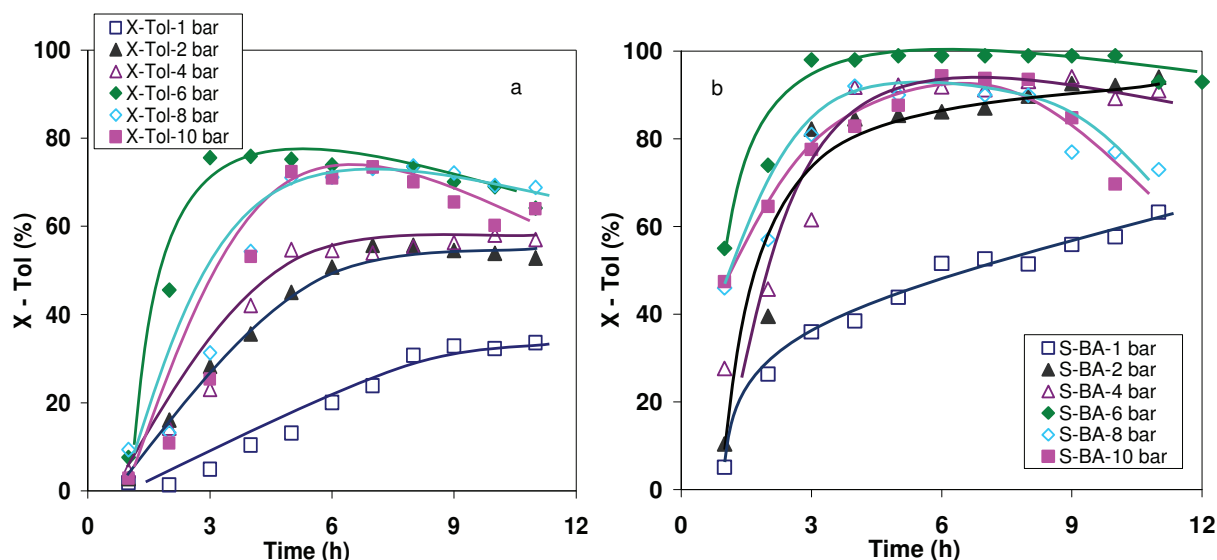


Fig. 36. Time-on-stream behavior of the 10Pd16Sb/TiO₂ - He catalyst w with varying reaction pressures ($P = 1$ to 10 bar, molar ratio of toluene : AcOH : O₂ : N₂ = 1 : 4 : 3 : 16 with space velocity 2688 h⁻¹); a) X-Tol vs. Time, b) S-BA vs. Time

The catalyst subjected to an even higher pressure of 6 bar, showed some extraordinary performance. It again started with low initial activity (X-Tol ~ 8 %, Y-BA ~ 5 %), which reached maximum within just 3 h on-stream and gave X-Tol = 75 %, Y-BA = 75 %, S-BA = 100 %. The most striking feature here is that the catalyst exhibited 100 % selectivity towards benzyl acetate, which is an outstanding outcome of this study. Another notable achievement is that the induction period is substantially decreased from 11 hours in case of 1 bar to 3 hours in case of 6 bar reaction pressure. Such increase in catalytic performance with increase in pressure further motivated us to raise the pressure even higher. Therefore, in the next step, the catalysts were also tested with reaction pressures of 8 and 10 bars. Nonetheless, the catalysts subjected with 8 and 10 bars showed same results of X-Tol = 74 %, Y-BA = 65 %, S-BA = 87 % with slight longer induction period of 6 hours compared to the catalyst tested at 6 bar. Surprisingly with further increase in pressure beyond 6 bar did not influence the conversion of toluene anymore, that means at and above 6 bar X-Tol ~ 75 % remains constant. On the other hand, the selectivity towards benzyl acetate was found to decrease considerably from 100 % to 87 %. It is clearly evident that the reaction pressure has a significant influence on the performance of the catalyst in acetoxylation of toluene.

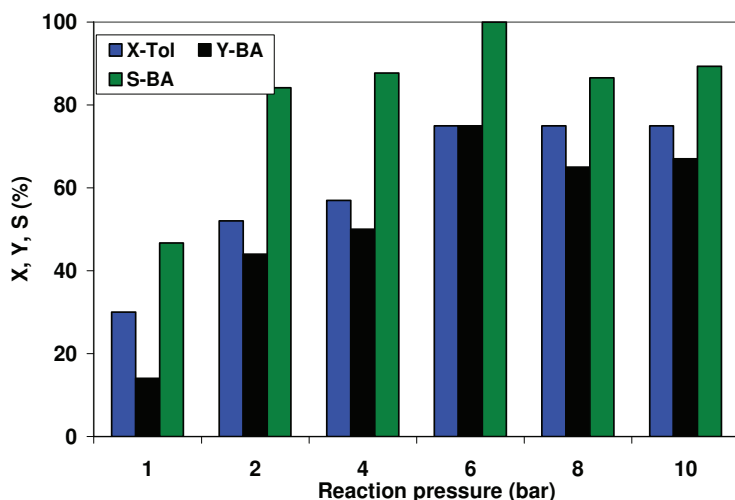


Fig. 37. Comparison of maximum activity obtained on 10Pd16Sb/TiO₂ - He catalysts at different reaction pressures

The maximum performance of the catalysts at different pressures is shown in the Fig. 37. The catalysts showed that the conversion of toluene is observed to increase from 30 % to 75 % with rise in total pressure from 1 to 6 bar and then remained more or less constant with further increase beyond 6 bar. The selectivity of BA also increased and reached almost 100 % at 6 bar, but decreased to 87 % beyond this pressure and then remained constant.

In ref. [131] it was reported that the reaction rate increases initially with increase in partial pressure of the reactants when surface reaction is the rate limiting step. It can be explained by increased adsorption of toluene with increase in pressure up to 6 bar. Given that the surface reaction is also the rate limiting step in the acetoxylation reaction, the beneficial effect of raising the pressure to 6 bar may be due to the increase of surface coverage of active centres by the reactants with increasing pressure. A further increase in pressure saturates the surface coverage with reactants and the active centres are no longer available. In this process reactant molecules can adsorb from the gas phase on surface centres. The molecules adsorbed on those centres can react as well form product molecules which desorbs immediately. With increase in pressure up to 6 bar, adsorption, surface reaction and desorption are continuously increasing. These three surface phenomena are in harmony till the reaction is taking place up to reaction pressure of 6 bar. After 6 bar, the rate of conversion of toluene becomes constant due to the saturation of the adsorption centres on the catalyst surface, which become fully covered with toluene. Therefore a further increase of toluene partial pressure (as a consequence of increase of total partial pressure) does not promote the reaction rate and hence the conversion anymore. However, it seems that at higher pressure, the conversion (and surface reactions) of acetic acid increases while that of toluene

becomes constant (Fig. 38). Higher amount of CO_2 was observed at 8 and 10 bar, leading the reaction to towards the unselective direction (Fig. 38). As reported earlier in previous contributions [92], CO_2 is mainly the product from the oxidative decomposition of acetic acid and only minor amounts of CO_2 are formed by toluene combustion. Therefore an increase of the total pressure saturates toluene adsorption sites, while acetic acid continues to adsorb, most probably on the support, and consequently undergo combustion in the presence of oxygen in reactant feed mixture.

Decrease of the selectivity at a pressure above 6 bar can also be explained by the dramatic jump in the amount coke formed. The extent of coke formation at 8 bar is much more in comparison to 6 bar (Fig. 39b). Coke can be the product from high molecular mass vapours like toluene and the product BA. All these findings suggest that this reaction occurs effectively under optimal reaction conditions, i.e. at 6 bar and 210°C , where almost 100 % selectivity of BA at significantly high conversion of toluene is achieved. Such result is remarkable among vapour phase heterogeneous catalytic reactions.

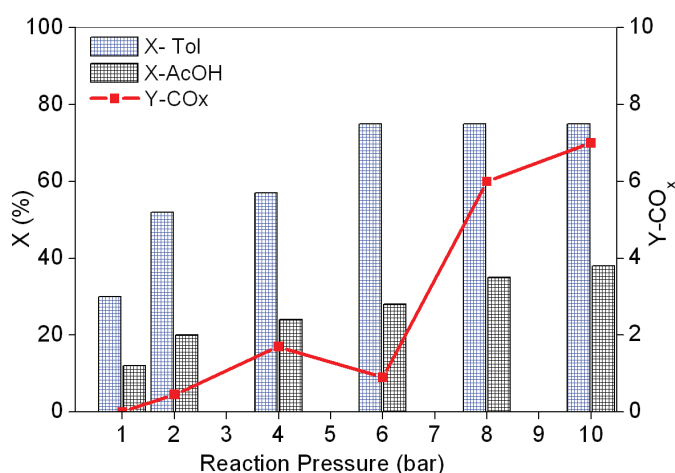


Fig. 38. Comparison of conversion of toluene and acetic acid and yields of carbon dioxide produced at varying reaction pressures

6.3 Characterization of catalysts used under different pressures

The catalysts treated under different total pressure have been characterized by C.H.N.S, XRD, XPS and TEM to understand the influence of pressure on the nature of the catalyst. The results are described in this section.

6.3.1 Extent of carbon formation on 10Pd16Sb/TiO₂ - He catalyst with varying reaction pressure

From the time-on-stream performance of the catalyst at different pressures it was observed that, apart from a difference in conversion, selectivity and induction period in each case, there is a remarkable change in the stability of the catalyst performance during the course of reaction. Fig 39a shows number of hours in which solids displayed stable performance in the acetoxylation reaction tested at varied pressures. It was found that the stability decreased with increasing pressure, which means that catalysts tested at the lowest pressure showed the longest stability and vice versa. Among all, the catalyst tested at 8 bar reaction pressure showed minimum stability for just 12 h on-stream.

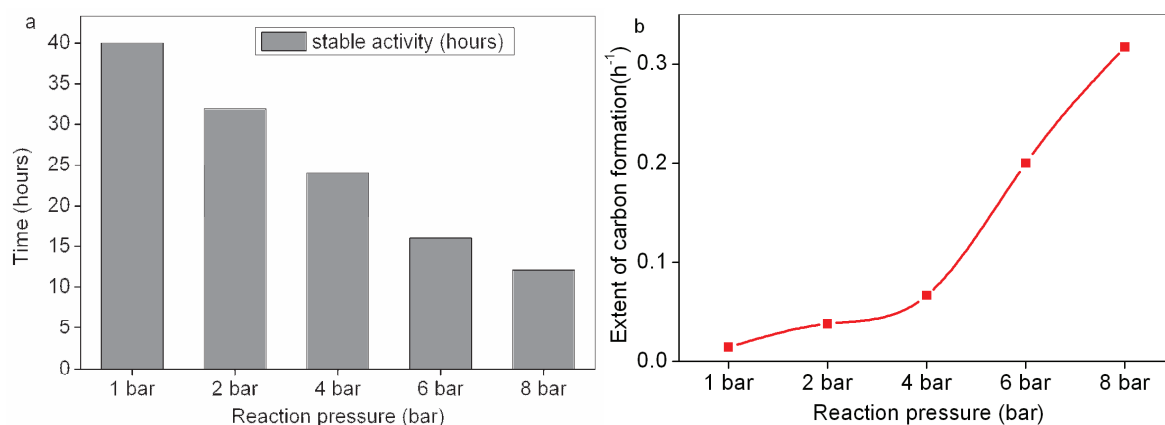


Fig. 39. a) Dependence of the stable catalytic performance on varying pressure, b) Extent of coke formation with varying pressure

It is known from our previous investigations that carbon deposits on the catalyst were one of the major reasons for the easy deactivation of the catalyst. Keeping this aspect in mind, the carbon contents were estimated in each case. The extent of formation of carbon is plotted as a function of reaction pressure and shown in Fig. 39b. It is clear that the extent of formation of carbon is increasing gradually with increasing pressure from 1 to 4 bar, beyond which there is a sharp increase in the carbon formation. From this result, it was once again confirmed that the instability of the catalyst is due to increased formation of carbon over the catalyst during the course of the reaction.

6.3.2 BET surface area and pore size distribution

The influence of reaction pressure on the BET surface areas (at their maximum activity and after long runs of reaction) is illustrated in Table 10. It is evident that the lower reaction pressures (1 and 2 bar) exhibited surface area values of $\sim 40 \text{ m}^2/\text{g}$, but some decrease in surface areas of the catalyst was observed when the pressure raised

higher (i.e. beyond 4 bar). The surface areas observed beyond 4 bar pressure are varied in the range from 25-28 m²/g.

Table 10. BET surface area values of the maximum active and deactivated catalysts subjected to varying reaction pressures

Catalyst	At max ^m activity (m ² /g)	Deactivated (m ² /g)
1 bar	39.4	28.1
2 bar	40.6	25.1
4 bar	27.7	23.8
6 bar	24.8	21.4

However, a more pronounced decrease in surface area was observed in the deactivated solids after long reaction runs. This again points to the fact some sort of changes are occurring on the catalyst during the reaction. The pore size distributions of the maximum active catalysts are shown in Fig. 40. Apart from the fact that samples treated at different pressures showed considerable difference in their performance, some of them showed similar pore diameter (in the range below 150 nm). Nevertheless, the decrease in pore volume of the catalyst treated at 6 bar was remarkable compared to other catalysts. This hints to the fact that the catalyst at 6 bar has some different nature than other catalysts.

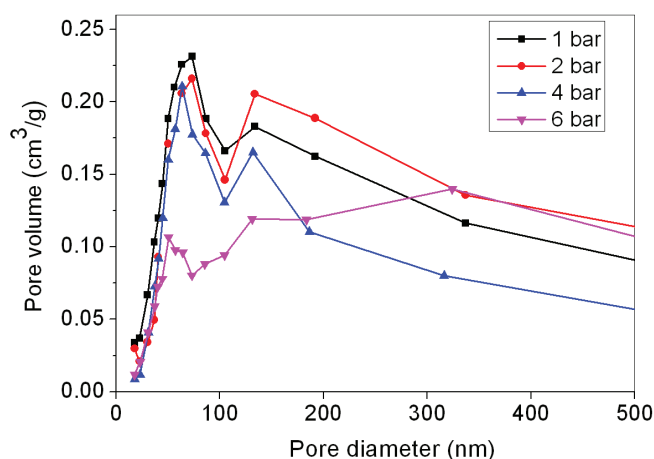


Fig. 40. Pore size distribution of 10Pd16Sb/TiO₂ - He samples subjected to different reaction pressures

6.3.3 X-ray diffraction

XRD patterns of the maximum activated catalyst at different pressure are given in Fig. 41a. Reflections regarding the different phases like metallic Pd, NaCl and TiO_2 were present in all the solids irrespective of the pressure (1, 2, 4, 6 and 8 bar). These reflections do not show any considerable differences regarding the existence of any different phase. However, some changes were observed in Pd reflections, in terms of peak intensity or shift in peak position at different pressures (Fig. 41b).

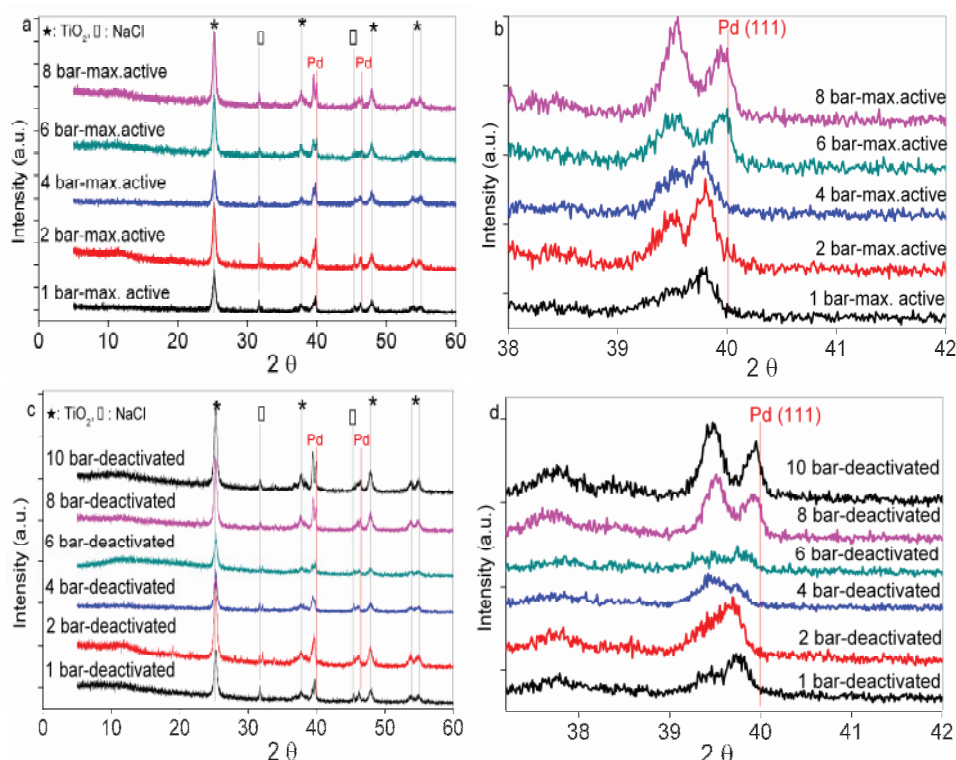


Fig. 41. XRD patterns of maximum active and deactivated 10Pd16Sb/ TiO_2 - He samples treated at different reaction pressures ($P = 1$ to 10 bar), a) maximum active catalysts, b) XRD patterns of maximum active solids in the 2θ range of the Pd(111) reflection ($38-42^\circ$), c) Deactivated catalysts, d) XRD patterns of deactivated samples in the 2θ range of the Pd(111) reflection ($38-42^\circ$)

In order to get deeper insights on the metallic Pd reflection belongs to maximum active catalysts, the 2θ range from 38 to 42° was zoomed and shown in Fig. 41b. It was found from these diffractograms that there is a shift to left in Pd reflections compared to the fresh ones (Fresh one is showed in Fig. 13a).

A careful examination of the reflections showed that with increase in pressure, a shift in the peak position is also decreased i.e. shift in Pd reflection is much more prominent in case of 1,2 and 4 bar compared to the 6 and 8 bar samples. At higher pressure, Pd seems to exist in metallic form. Additionally, this Pd peak splits into two more sub-peaks.

This splitting of peaks is probably due to the presence of different kinds of Pd species, which can be incorporated Sb, C or H. An increase in pressure seems to have a slight impact on the relative increase in the intensity of the left peak at $2\theta = 39.4^\circ$. The intensity of such peak was found to increase with increase in pressure up to 8 bar. At 6 bar reaction pressure, the intensity of both the reflections (of splitted Pd) was found to be almost same, and it increased with further increase in pressure. Probably this peak at $2\theta = 39.4^\circ$ corresponds to the some Pd–C species, because the carbon content increases with increase in pressure (Fig.39b). XRD patterns (Fig. 41c) of the catalyst tested for long runs showed as such no difference in the phase composition except for the Pd reflection (Fig. 41d). The shift of the Pd reflection was still observed in all the samples, however, there is a less shift in the samples treated at higher pressures. Furthermore, the splitting of the Pd reflections is also seemed to be influenced by the pressure and longer time of catalytic runs. In case of samples treated for 1, 2 and 4 bar reaction pressure, splitted reflections have disappeared or the peak has become quite broad. The sample treated at 6 bar for longer time reaction showed low intense broad peak, whereas further increase in pressure again shows peaks with similar split as in the case of maximum active catalyst (Fig. 41b).

6.3.4 Transmission electron microscopy

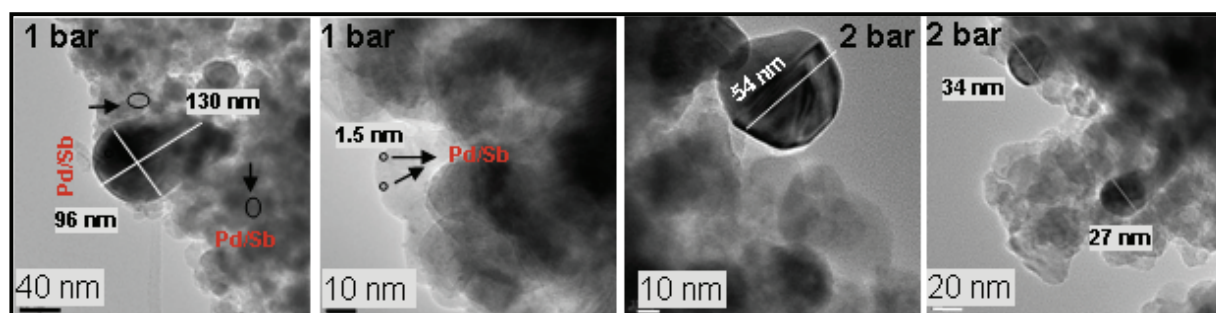


Fig. 42. Transmission electron micrographs of maximum active 10Pd16Sb/TiO₂ - He samples treated at 1 and 2 bar reaction pressure

The particle size in the catalysts subjected to lower pressure (at their maximum activity) was found to be distributed over a wide range, i.e. from 2 nm to 100 nm (Fig. 42). The fresh catalysts, after pre-treatment in helium showed huge Pd particle size of 2 μm , which restructured to give particles consisting of as small as 27 nm to 54 nm. The EDX analysis of such solids treated at lower pressure was also carried out. It was found that all the particles, irrespective of the size, comprised of Pd and Sb all over. Nevertheless, the Pd and Sb contents were widely scattered. In addition, Sb was broadly spread over the titania support, whereas no traces of Pd were observed on the support. (EDX patterns of some of the particles are shown in Fig. A6)

In the solids treated at higher pressures of 6 bar and 8 bar, similar wide range of Pd size starting from 1.5 nm to 100 nm were noticed (Fig. 43). It is clear from the particle size analysis that increase in pressure, did not influence the size of the particles at their maximum activity. Nevertheless, the EDX analysis of such particles gave some interesting hints on the distribution with respect to Pd and Sb. At lower pressures i.e., 1 and 2 bar, all the particles irrespective of the sizes (in 2 nm to 100 nm) contained Pd and Sb together in different ratios.

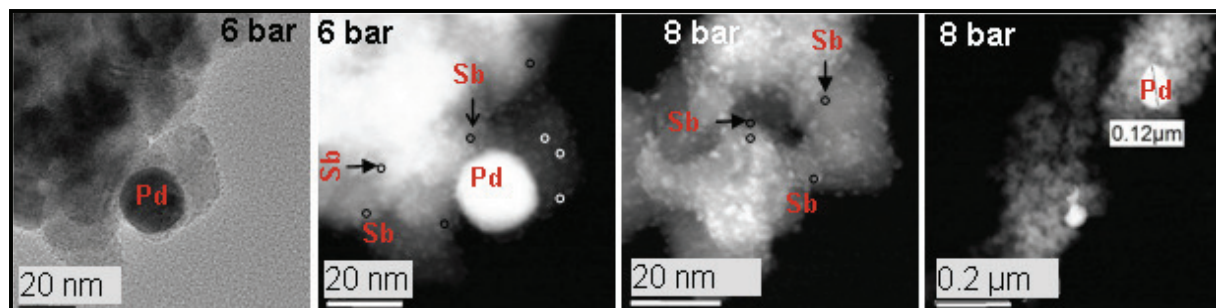


Fig. 43. Transmission electron micrographs of maximum active 10Pd16Sb/TiO₂ - He samples treated at 6 and 8 bar reaction pressure

However, at the higher pressure (6 and 8 bar) it was found that the population of Pd, over the catalyst is segregated majorly on the bigger particles, almost no Pd was seen over the smaller particles (< 5 nm). This hints to the fact that at the higher pressure Pd particles are restructuring in a way which is without any Sb migration or the incorporation into the Pd (EDX patterns of the samples treated at higher pressure are shown in Fig. A7). The XRD analysis also revealed that the solids treated at lower pressure displayed a significant shift of the Pd peak due to the incorporation, while at higher pressure this shift was reduced / shortened, and Pd peaks were found to be more or less at the position of pure Pd without any incorporation. It should be noted that solids treated at higher pressure showed much less stability with time-on-stream compared to the catalysts treated at lower pressures. Similar Pd and Sb distribution was also seen in the solids pre-treated in air for 600 °C, where either Pd rich particles or Sb rich particles were found. This outcome supports the fact that the existence of optimized intermixed Pd and Sb particles is essential for the long stability of the catalyst, whereas the pure Pd particles account for the higher activity in the system.

6.3.5 X-ray photoelectron spectroscopy

The surface analysis was carried out for all the catalysts tested under different pressures i.e. 1, 2, 4, 6, 8 and 10 bar. The catalysts tested under different reaction pressures showed quite different performance. The surfaces of the catalysts were tested in order to check if an increase in the pressure also affects the surface composition. Fig.

44a shows the spectra of 3d Pd species of the maximum active catalysts obtained after their testing at different pressures. We have seen in the previous section (3.2.2.4) that helium calcined catalyst showed broad band corresponding to oxidized palladium species in the fresh catalyst. Nevertheless, during the course of reaction these oxidized species gets reduced to metallic palladium species. The catalyst treated at different pressures shows that it undoubtedly undergoes reduction at all the pressures, but the extent of reduction depends on the reaction pressure applied, In other words, the extent of reduction is not the same in all the cases. The distribution of oxidized species over the surface of the catalysts varies with varying reaction pressure. Considerable amount of PdO species were found on the surface of the catalysts tested at 1 bar and 2 bar and hence good long-term stability. On the other hand, with increasing pressure, the amount of oxidized Pd species was scarcely spread over the surface. Peak of metallic palladium was found to increase quite sharply with increasing pressure. Probably the reduction is faster with the increase in pressure and hence decreased long-term stability.

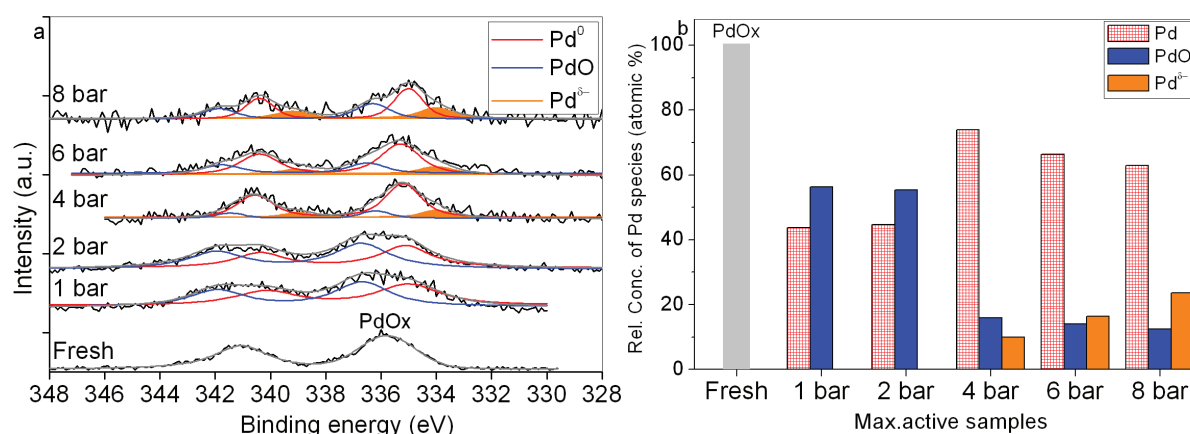


Fig. 44. a) XP-spectra of 3d Pd for the 10Pd16Sb/TiO₂-He calcined catalysts at their maximum performance of different reaction pressures as mentioned, b) Relative surface atomic ratio of Pd species. Surface Pd atomic ratios were calculated from the areas of the XPS under the peak

Interestingly, Pd^{δ-} species (highly reduced Pd) was found to generate in the catalysts when tested at higher pressures. As explained earlier, the formation of such species is expected from the stronger interaction between surface carbon species and palladium species. These species was not seen in the catalyst treated at 1 and 2 bar, but started to appear at higher reaction pressures of 4 bar and above. This Pd^{δ-} species is believed to account for faster deactivation in the system because of high and fast reduction of oxidised palladium. This is in good line with the results shown in Fig. 39a, that the catalyst was much more stable at lower pressure, but its life time starts to fall quickly at higher reaction pressure. Reaction at lower pressure in fact prevents the formation of such undesired Pd^{δ-} species and thus improves the lifetime of the catalysts. Hence it is

clear that generation of $\text{Pd}^{\delta-}$ is the one of the possible reasons for faster deactivation of the catalyst at higher pressures.

Fig. 44b displays the relative atomic content of various palladium species (PdO , Pd^0 and $\text{Pd}^{\delta-}$) on the surface of various catalysts. The fresh catalyst contained completely oxidized species, with increasing pressure PdO and metallic Pd were generated due to the reduction of the PdOx to lower oxidized species. The concentration of PdO species was found to decrease with increasing pressure due to reduction in the reaction, while the content of reduced species is constantly increasing. An increase in concentration of Pd^0 was observed, but with further increase in pressure even this Pd^0 gets reduced to $\text{Pd}^{\delta-}$, therefore decrease in concentration of Pd^0 was observed which was compensated by increase in $\text{Pd}^{\delta-}$. At high pressure, the catalyst displayed minimum stability with time-on-stream and which can be explained because of lack of synergy between oxidised and reduced species present on the surface.

6.4 Summary and Conclusions

The effect of the reaction pressure showed a clear influence on the performance of the catalysts in the acetoxylation of toluene to benzyl acetate. The catalytic activity and long-term stability were found to depend on the reaction pressure. The catalyst activity increased from $\text{X-Tol} = 20\%$ at 1 bar to $\text{X-Tol} = 75\%$ at 6 bar reaction pressure and the selectivity of the product also displayed steep increasing trend up to 6 bar ($\text{S-BA} = 100\%$) reaction pressure. However, beyond 6 bar, the selectivity of BA dropped gradually. From the time-on-stream reactions, it was found that the catalyst subjected at high pressure of 8 bar was stable for lesser time ~ 12 h on-stream, whereas the catalyst treated at 1 bar showed maximum stability ~ 40 h on-stream. The stability of the catalyst was found to be directly related to the amount of carbon accumulated on the catalyst at each pressure. The lower pressure treated catalyst showed the least amount of carbon and the amount of carbon formed increased with increasing pressure and hence led to the faster deactivation of the catalysts. The surface analysis from XPS showed that the extent of reduction of PdOx species also increased with increasing pressure. The formation of $\text{Pd}^{\delta-}$ species in the catalysts tested from 4 bar onwards is also the reason for the observed catalyst deactivation. A significant decline in the amount of PdO species was seen from 2 bar to 4 bar treated catalysts. This fall in the PdO and simultaneous generation of $\text{Pd}^{\delta-}$ showed a great impact on the stability of the catalyst during long-term tests.

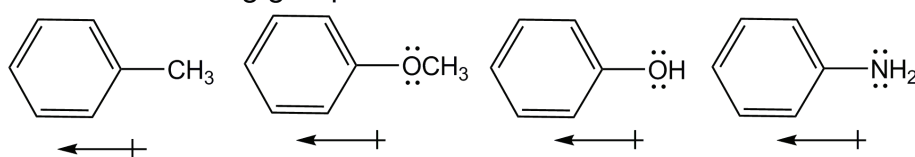
7 Acetoxylation of various substituted toluenes

In this chapter, catalytic results obtained from the acetoxylation reaction of fluoro, chloro, methoxy and methyl toluenes to corresponding esters are presented. Different substrates were tested in fixed bed reactor at 210 °C with the conditions optimized in previous chapters. DFT calculations undertaken are also shown to understand this reaction system with various derivatives of toluene.

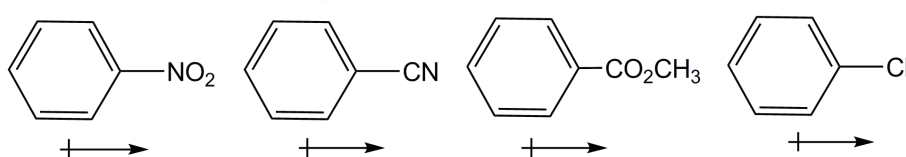
7.1 Catalytic data for various substituted toluenes in the acetoxylation reaction

The catalytic activity in the acetoxylation of toluene to benzyl acetate in the presence of acetic acid and oxygen over 10Pd16Sb/TiO₂ was explored in previous sections. It was found that the Pd-Sb/TiO₂ catalyst has shown good performance (X-Tol = 75 % and S-BA = 100 %) at a molar ratio of toluene : AcOH : O₂ : Inert gas = 1 : 4 : 3 : 16, a space velocity of 2688 h⁻¹, using a catalyst amount of 0.8 g and total flow of 44.8 ml/min. To gain deeper insights on the influence of second substituents on the aromatic ring, various substituted toluenes were tested in the acetoxylation runs. It is widely known that the nature of the substituent on benzene ring can influence the reactivity of the compound. Substituents with different electron withdrawing or electron donating nature can manipulate the fate of the product formed. For example, a hydroxy or methoxy substituent increases the rate of electrophilic substitution, whereas a nitro substituent decreases the reactivity. In the following diagram one can see that electron donating substituents activate the ring and electron withdrawing substituents deactivate the ring towards an electrophilic attack.

electron donating groups



electron withdrawing groups

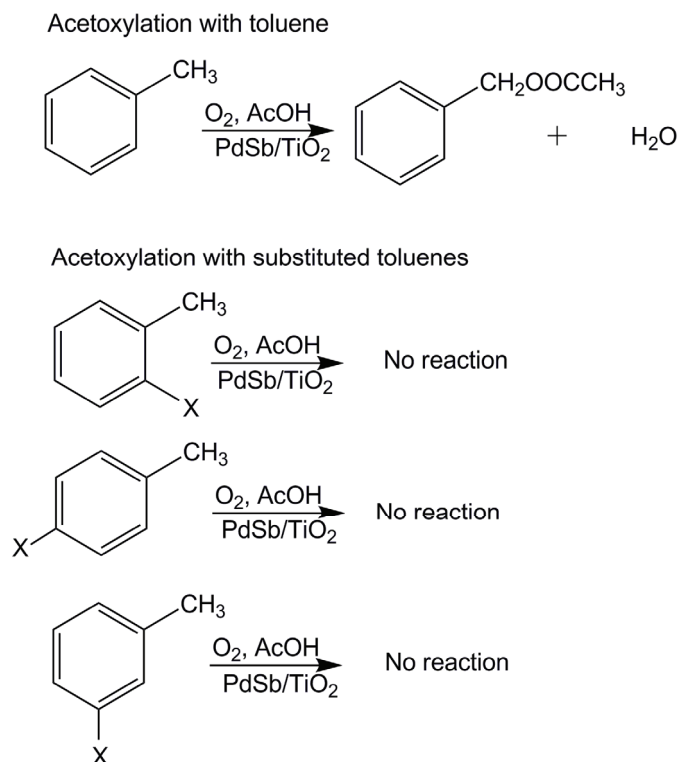


Scheme 6. Some selected the electron donating and electron withdrawing groups on the benzene ring

Acetoxylation runs were carried out over 10Pd16Sb/TiO₂ - He with a number of substituted toluenes with some electron withdrawing and electron donating properties. Due to temperature limitations of the present experimental set up, only selected substituents having boiling points lower than 220 °C were tested. The list of substituted toluenes selected is given below in Scheme 7.

Toluene substituted with various groups, for e.g. methoxy, chloro or fluoro in ortho, meta and para positions and additionally xylenes were tested under the above

mentioned conditions. Results from the catalytic runs revealed that almost all the substituted toluenes under the above mentioned reaction conditions are totally inactive in the acetoxylation reaction (Scheme 7).



where X = Cl, F, OMe, Me

Scheme 7. Acetoxylation of toluene and its derivatives in gas phase on 10Pd16Sb/TiO₂ - He catalyst

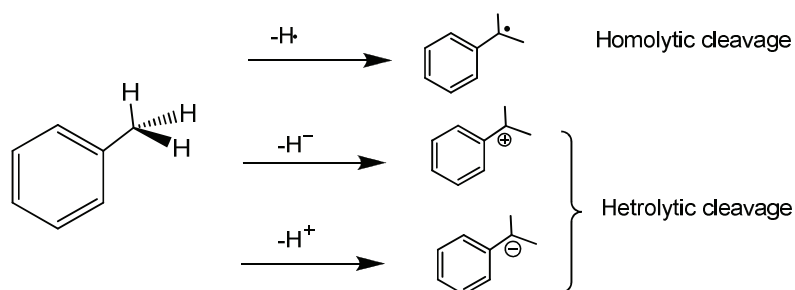
A negligible amount of carbon dioxide was observed mainly from the oxidative decomposition of acetic acid. Additionally, a few tests were also performed with changing reaction parameters such as temperature, pressure, feed ratios etc. to check the possibility of converting these substituted toluenes over 10Pd16Sb/TiO₂ catalyst. An overview of the experiments performed is listed in Appendix Table A1.

There are different reasons that are responsible for the inactive nature of toluene derivatives to produce their corresponding esters. Some of the reasons include: i) very weak adsorption of the reactants on the catalyst surface, ii) when the adsorption is too weak they may not react properly, iii) difficult desorption of the products etc. To study this problem in detail, some theoretical calculations (DFT calculations) were performed with an aim to explore the thermodynamic feasibility of formation of different reaction intermediates (both toluene and substituted toluenes), and the change in Gibbs free energy of the whole reaction. Furthermore, the relationship between the activity and the

strength of adsorption of the substrate and the energy released during bond cleavage after the adsorption, were calculated. Density functional theory (DFT) was used for such calculations. The calculation results can give more reliable information to interpret the experimental data. For this purpose, the C–H activation of the substrates and the interaction of the substrates with the Pd(111) surface are considered. Pd(111) is the most significantly exposed crystal plane from the present analytical studies.

7.2 Potential reaction steps

Seven steps leading to any catalytic reaction were discussed in chapter 1. After the transport of the reactant from the gas phase to the catalyst surface (outer diffusion) and inner diffusion through a pore, the next important step of a catalytic reaction is the adsorption of the reactant on an active site on the inner catalyst surface. Adsorption of toluene and its derivatives was studied in detail over the Pd(111) in coming sections. After adsorption, it is the chemical reaction that takes place in the next step. Chemical reactions of organic substrates usually involve breaking and making of chemical bonds usually covalent bonds. In a covalent bond, two atoms share a pair of electrons. Thus, when a bond breaks there are two possibilities either heterolytic cleavage or homolytic cleavage: In acetoxylation reaction, C–H bond cleavage from the methyl group can take place in the following way; homolytic cleavage of C–H bond leading to radical formation or heterolytic cleavage leading to either a benzyl cation or a benzyl anion.



Scheme 8. Homolytic and heterolytic cleavage of benzylic C–H bond

After the formation of a benzyl cation or anion, attack of acetic acid or acetate takes place that leads to the formation of corresponding ester.

7.3 Density Functional Theory studies

Density functional theory was undertaken to study the relative stabilities and reactivities of surface species on Pd(111) of toluenes and substituted toluenes obtained by subsequent removal of hydrogen atoms from methyl group. Thermodynamic values of bond cleavage and reactions were calculated for the most probable intermediates and also for the intermediates leading to exothermic bond cleavage reactions. DFT

calculations were done to identify the most favourable pathway for the adsorption and the cleavage of C–H bond during acetoxylation reaction.

7.3.1 Evaluation of the properties/nature of the substrates without catalyst

First of all, toluenes and substituted toluenes were studied purely on the basis of thermodynamics, without including the catalyst surface. Only the physical aspects of substrates were investigated, i.e. without considering the chemical interactions with the catalyst surface.

7.3.1.1 Homolytic and heterolytic C–H bond cleavage of toluene and its derivatives of the benzylic carbon

The energy difference between the neutral molecule and its radical species (homolytic) or its anionic/cationic species (heterolytic) was examined. Three routes (via anionic, cationic and radical mechanism) of C–H bond cleavage were speculated and studied. If the energy difference between these two states is large that means a low stabilization. Difference in Gibbs free energy (ΔG) was calculated for toluene first at the reaction temperature of 210 °C. Such ΔG values show the feasibility of the reaction, if it is more negative then the reaction is more favourable. ΔG is negative for any reaction means that it is favoured by both the enthalpy and entropy terms. Therefore it can be concluded that any reaction for which ΔG is negative should be favourable, or spontaneous.

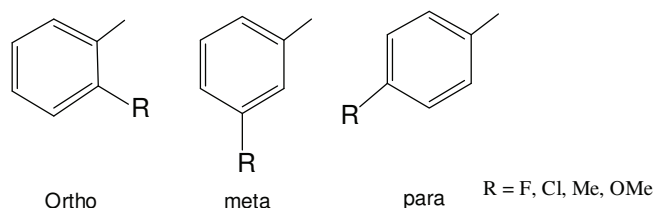
$$\Delta G = G (\text{Toluene}) - G (\text{cation, radical or anion}) \quad (33)$$

$$\Delta G (\text{Radical}) = -1868 \text{ kJ/mol}$$

$$\Delta G (\text{Cation}) = -2564 \text{ kJ/mol}$$

$$\Delta G (\text{Anion}) = -1789 \text{ kJ/mol}$$

In acetoxylation of toluene or its derivatives, the C–H bond at benzylic position must be cleaved for the AcOH to further react and form the ester. From the catalytic tests, it was observed that acetoxylation of toluene is feasible but surprisingly acetoxylation with any derivative of toluene is not at all feasible. Therefore, it would be interesting to find whether the substituted toluenes also stabilize homolytic/heterolytic bond cleavage.



Scheme 9. Illustration of ortho, para and meta positions on the ring

The stabilization of the C–H bond cleavage is analyzed on the all above substrates shown in scheme. 9. This has been done by calculating the difference in ΔG according

$$\Delta G_{\text{stab}} = \Delta G (\text{toluene}) - \Delta G (\text{substituted toluene}) \quad (34)$$

It gives the value in comparison with toluene. The more negative ΔG_{stab} , the more stable is the intermediate derived from the substituted toluene after C–H bond cleavage. For individual set of values of entropy, enthalpy in each case, see appendix Table A2-A4, which shows the comparison of stabilization from homolytic and heterolytic cleavage of C–H adsorption in various substrates including toluene.

Stabilization of the heterolytic cleavage (anionic and cationic) was studied. First the cationic, heterolytic cleavage energies were calculated and are given in Appendix Table A2. A direct elimination of a hydride is very energy consuming and is particularly stabilized by para substituents. The strongest of these effects are observed by methyl and methoxy derivatives of toluenes, i.e. the stabilization energy of the positive charge is especially favoured by the electron donating substituent and additionally at para position. From the Table A2, ΔG values can be seen that methyl (34 kJ/mol) and methoxy (75 kJ/mol) stabilises the positive charge considerably better.

The anionic cleavage, deprotonation of the methyl group of the benzene ring was also explored. It showed that cleavage via removal of H^+ in these cases has shown somewhat positive effect on the stabilization energy compared the removal of H^+ from toluene. In particular, the electron withdrawing halogen (Cl and F) atoms stabilizes markedly the negative charge on the carbon (appendix Table A3). From the ΔG values of the halogenated toluenes, it is observed that Chloro toluene at meta position stabilizes the C–H bond cleavage in comparison to toluene by -35 kJ/mol; Similarly p- and o-chloro as well as fluoro also stabilize the substrate even more than toluene. Hence the speculation of the anionic cleavage leading to unstable species can not be the reason for the inactive nature of substituted toluenes.

Therefore, stabilization of homolytic cleavage was studied. It illustrates that all the derivatives of toluene do not differ from each other substantially (appendix Table A4). Regardless of the type of substituent attached (electron withdrawing or donating), all showed more or less same energy difference among each other. This implies that the radical cleavage of the C–H bond should not affect the path of reaction for toluene or the substituted toluene. Probably reaction does not proceed via radical mechanism or C–H bond cleavage is not determining the course of the reaction.

From the above observations, it can be concluded that generally substituted toluenes should have a positive impact on the bond cleavage step, i.e. substituted toluene should facilitate the cleavage step in the reaction. A significant positive stabilizing influence was

observed on the bond cleavage by the substituents in case of ionic intermediate. Therefore, it can be said that the inactivity of toluene derivatives can not be deduced by substrate properties alone. It is clear from the above studies that the reaction of toluene or substituted toluenes in the acetoxylation reaction is independent of the substrate used and theoretically substituted toluenes favour the initiation of the reaction.

7.3.1.2 Thermodynamics of the reaction of the toluene and its derivatives to form products

After the evaluation of the bond cleavage in toluene and substrates, thermodynamics of the whole reaction was studied without catalyst. Energies of the whole network were calculated without considering the catalyst system. Only the nature of substrates at a temperature of 210 °C in the presence of acetic acid and oxygen was analysed (Appendix, Table A5). The free reaction energy of toluene derivatives at 210 °C is generally more favourable than that of toluene. Here also it was found, purely in terms of thermodynamics, the substituents should have a positive effect on the reaction. Hence, even this is not the reason for inactivity of the toluene derivatives in the acetoxylation reaction.

7.3.2 Evaluation of the interaction of the substrates with Pd(111) catalyst surface

After investigating the properties of toluene and its derivatives nature without catalyst, studies were performed on Pd(111) surface. In the following sections, adsorption energies of various substrates were examined and also the C–H bond cleavage energy was calculated to understand the catalytic performance obtained from various substrates.

7.3.2.1 Adsorption studies of toluene and its derivatives on the Pd(111) surface

As found in the above sections, the substrates itself cannot decide the fate of this reaction. Therefore to further understand the performance of the substrates in the reaction, a catalyst system is introduced. The necessary first step in a heterogeneous catalytic reaction involves activation of a reactant molecule by adsorption onto a catalyst surface. As mentioned earlier, Pd(111) phase is the preferentially exposed plane observed from the analytics. Hence all the investigations will be carried out on the Pd(111) system. To check the adsorption of the toluene derivatives on the Pd(111) surface, 5x5x3 supercell with periodic boundary conditions was chosen. The 5x5 surface is an adequate size to describe and investigate the adsorption of toluene Fig. 45. Three Pd layers is the minimal size to describe the ABC geometry of the Pd(111) surface accurately.

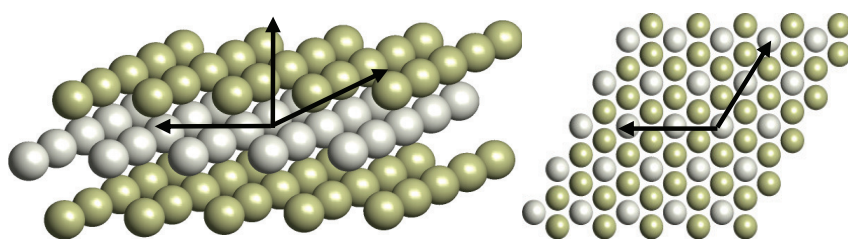


Fig. 45. Modeling of the Pd-surface

To investigate the adsorption energy a 20 Å slab model was taken. The energy difference (of total energy) between free and adsorbed substrate results in the adsorption energy. The supercell repeats itself in three dimensions. Local 5x5x3 bulk, but NxNx3layer in a distance of 20 Å. The adsorption energy for toluene was found to be -64.6 kJ/mol. The geometry of the adsorbed toluene was deduced after simulation. Adsorbed toluene is not bound planar (as assumed). It can be clearly seen in Fig. 46 that the methyl group attached to the ring in toluene points out of the plane along with the hydrogens of the ring. Each C=C bond of the benzene ring is attached to one Pd atom, that means 2 carbons are adsorbed over one Pd atom. After calculating the adsorption energy of the toluene molecule over Pd, adsorption energies of various substrates, which were failed to yield any product or react in acetoxylation reaction. Table 11 shows the adsorption energies values of various substrates on Pd(111) phase from the catalyst.

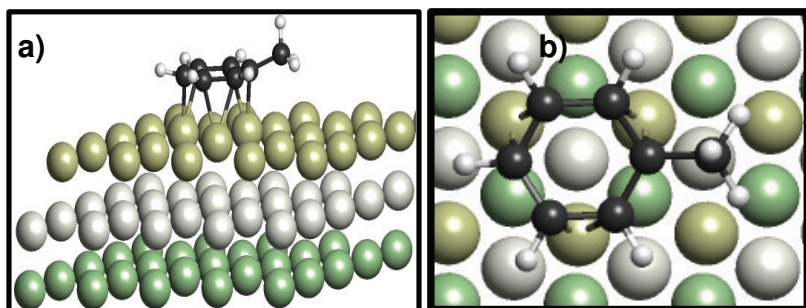


Fig. 46. Adsorbed toluene on the Pd(111) catalyst surface a) side view b) top view

A significant difference was noticed in the adsorption energy values of the toluene and the substituted toluenes at the same conditions. The comparison of the adsorptions strength of the aromatics showed that toluene binds much stronger on Pd(111) surface than its derivatives. The adsorption of the substrate is the key step before the C–H bond cleavage. Toluene showed the value of -64.6 kJ/mol, whereas its derivatives showed much higher values, fluoro, chloro (electron withdrawing) substituted toluenes were in the range -20 to -22 kJ/mol, and the methoxy substituted (electron donating) showed less negative values in the range of -13 to -16 kJ/mol. The most strongly bonding substrate apart from toluene are xylenes with a value of almost -40 kJ/mol (Table 11).

Table 11. Adsorption energy of toluene and its derivative on the Pd(111) surface

Adsorption energy on Pd(111)	ΔTE (kJ/mol)
Toluene	-64.6
o-Fluoro	-21.3
o-Chloro	-20.8
o-Methyl	-37.8
o-Methoxy	-13.7
m-Fluoro	-20.0
m-Chloro	-22.3
m-Methyl	-39.1
m-Methoxy	-14.8
p-Fluoro	-20.2
p-Chloro	-21.8
p-Methyl	-39.1
p-Methoxy	-16.1

These observations showed that electron withdrawing groups make the substrates unsuitable for strong adsorption, also highly electron donating groups, like methoxy is also not suitable for the optimum adsorption. Probably steric hindrance (bulk methoxy group) plays a major role, which does not let this substrate to get adsorbed on the surface of the catalyst. Methyl substituents seem to be much better with respect to transmission of electron density and steric hindrance. Therefore toluene and the xylenes bind to the surface much stronger than others. On the other hand, it seems that the adsorption of the xylene is not sufficient enough to get bonded on the solid, probably it is on the border line of the adsorption and desorption state. At the reaction temperature of 210 °C, it is more likely that the adsorption will even be weakening due to temperature effect. Due to the high temperatures and the entropy decrease during the adsorption process, it is most likely that the substrates even do not adsorb on the Pd(111) surface at reaction conditions and hence no reaction can take place.

7.3.2.2 Cleavage of the C–H bond on the adsorbed toluene and its derivatives on the Pd(111) surface

After adsorption, the next key step during the reaction is the C–H bond cleavage. The simulation shows (Fig. 47) that after breaking of the C–H bond, the hydrogen released is bridged over 3-Pd atoms. The bond over 2-Pd atoms (14 kJ/mol) is quite small compared to the bridge over 3-Pd atoms. C–H bond cleavage energies for the selected molecules (i.e. toluene, m-F, o-, p- xylene) were also calculated. The values obtained (Table 12) show that there is not much difference between the cleavage energies of the C–H bond of the benzylic group of toluene and in various substituted toluenes.

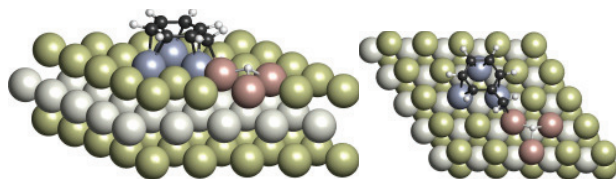


Fig. 47. Orientation of the H bridge over 3 Pd, after its cleavage from C–H bond of methyl group

Table 12. C–H bond cleavage energy of the benzylic carbon

Substrate	Toluene	m-fluoro	o-xylene	p-xylene
Cleavage	23.7	28.4	31.7	25.4

This hints to the fact that C–H bond cleavage is not determining the path of the reaction. In fact, it is the adsorption step of the substrate is the key step. However, amount of energy released during the whole process accounts for the feasibility of the reaction.

Table 13. Nett energy (i.e. energy difference) from the adsorption and cleavage process of toluene and its derivatives on Pd(111) surface

Adsorption and cleavage	Toluene	m-fluoro	o-xylene	p-xylene
adsorption	-64.4	-20.0	-37.8	-39.1
cleavage	23.7	28.4	31.7	25.4
sum	-40.7	8.4	-6.1	-13.7

Table13 gives the total energy released after adsorption of the molecule over the catalyst and cleavage of the C–H bond for the various substrates. It was found that the sum of energies from both the processes released is much higher in case of toluene in comparison to the other substrates. For m-fluoro toluene value of 8.4 kJ/mol is derived, which is quite unfavourable for this process to take place, and the energy released for the xylenes is negative (exothermic), this means that from calculation there is a probability of the reaction to take place with xylenes. One should keep in mind that the standard temperature and pressure conditions for the calculations have to be taken into the account. It is quite probable that at reaction temperature of 210 °C, the adsorption of all the substrates decreases. There is a decrease in entropy during the adsorption step over the catalyst and this decrease in entropy favours the increase in Gibbs free energy. Therefore from the calculations it can be said that it is very likely that only toluene gets adsorbed over the catalyst surface at the reaction temperature.

7.4 Summary and Conclusions

The C–H bond cleavage of the benzylic group, either homolytic cleavage or heterolytic showed no significant difference between toluene and its derivatives. The feasibility of any intermediate (radical, anionic or cationic) of the derivatives of tolunes was found to be somewhat more favourable than toluene itself. Inactivity of the substrates in the gas phase acetoxylation reaction cannot be explained by nature of substrates and its feasibility to react. Nevertheless comparison of the adsorptions strength of the aromatics showed that toluene binds much stronger on Pd(111) surface than the toluene derivatives. The adsorption of the substrate is the key step before the C–H bond cleavage. The C–H bond cleavage is endothermic. Additionally when the adsorption step was additionally considered then the process is exo-energetic. The energy released after adsorption and the cleavage step, is much more negative in case of toluene than in its derivatives. The comparison of C–H bond cleavage and adsorption of toluene and m-fluoro toluene showed a huge energy difference for this process between the two substrates. Toluene gives the energy value of -40.7 kJ/mol whereas m-fluoro showed +8.4 kJ/mol. But the next highest value was corresponding to p-xylene of -13.7 kJ/mol. However the adsorption of this substrate would decrease with increase in temperature so the only substrate with the highest probability to adsorb with enough high adsorption energy is toluene. Hence adsorption is the key step for the reaction to proceed and where the substituted tolunes were found to fail.

8 Overall summary and outlook

In this chapter, conclusions are derived based on compilation and evaluation of the results obtained from the entire study.

The palladium based catalysts showed remarkable performance in the gas phase acetoxylation reaction. The effect of thermal pre-treatment on the catalyst activity was studied in detail. The oven dried catalyst samples were subjected to different thermal treatments such as: (i) activation inside the reactor for 300 °C/2h/air, (ii) external treatment for 600 °C/4h/air, (iii) external treatment for 600 °C/4h/He, (iv) external treatment for 600 °C/4h/(10%H₂/He). These catalysts subjected to different atmospheres i.e. oxidising, inert and reducing showed contrasting behaviour during the reaction. The catalyst pre-treated in the reactor showed low initial activity, which increased with time and reached maximum activity (X-Tol = 65 %, Y-BA = 54 %), however, the catalyst performance started to decline gradually and the catalyst underwent deactivation. The TEM analysis showed that the increase in activity is accompanied by increasing Pd particle size during the course of the reaction. The deactivation in this system is accounted due to the increasing coke and subsequently loss of both Pd and Sb in the near-surface-region. Additionally, the generation of Pd^{δ-} species, which are formed due to the strong interaction between Pd and surface carbon were seen in the deactivated catalysts. These Pd^{δ-} species are also responsible for the fast deactivation of the catalyst.

Among the catalysts treated externally in the calcination oven, the one calcined in 10%H₂/He was found to be completely inactive due to the formation of Pd₇Sb₂₀ alloy. On the other hand, the catalysts treated in air and helium showed better and comparable performance (X-Tol = 54 % and Y-BA = 48 %) but very different stability. 10Pd16Sb/TiO₂ catalyst treated in helium (600 °C for 4 hours) was found more stable up to almost 25 h on-stream. While the catalyst calcined in air lost the majority of its activity already after 10 h. Reasons for the long term stability in case of the He treated sample were analysed by various characterization techniques. The TEM-EDX analysis of the air and helium treated catalyst showed wide differences in morphology, size and composition. Large sized Pd particles of up to 2 µm diameters were formed in the He calcined catalyst; whereas the tiny particles (5-10 nm) were seen in the samples calcined in air. During the reaction, the helium calcined catalysts showed a decrease in particle size to 50-100 nm and homogeneous intermixed particles with a Pd : Sb ratio of 3-5 was found throughout the catalyst. In the case of air treated catalyst, particles underwent sintering and the size increased from 5-10 nm in freshly calcined catalysts up to 50-100 nm also, but PdSb inter mixed particles formed in this case were found to be inhomogeneously spread over the catalyst with either Pd rich particles or Sb rich. The homogeneous mixed PdSb

particles with a Pd : Sb ratio of 3-5 seem to be beneficial for maintaining stable behaviour for a longer time. XPS studies also revealed that the extent of reduction of PdO_x species formed in the fresh samples was also influenced by the thermal pre-treatment given. In case of helium calcined solid, the reduction of PdO_x to metallic Pd was found to be much lower than the air treated one. The XPS studies also revealed that for good activity and stability of the catalyst, in this system, it must contain both Pd and PdO species on the surface. It appears that good synergy between Pd and PdO is essential for the high performance of the catalyst.

In view of improved performance, the He-calcined 10Pd16Sb/TiO₂ sample was used for further investigations. Various reaction conditions (Tol, AcOH, O₂ rates) were optimized with an aim to enhance the activity and selectivity of the catalyst. Along with these parameters, temperature, space velocity and mass transfer limitations of the system were checked. Reaction conditions were optimized with the aim to improve S-BA with minimum CO_x and other by products. Catalytic results related to optimization studies revealed that a molar ratio of toluene : AcOH : O₂ : IG = 1 : 4 : 3 : 16, reaction temperature of 210 °C with space velocity 2688 h⁻¹ and a catalyst amount of 0.8 g at total flow of 44.8 ml/min are optimum.

Furthermore, long-term catalytic testing of 10Pd16Sb/TiO₂ - He catalyst was performed with optimized conditions. The catalyst showed long stability (X-Tol = 54 %, Y-BA = 48 %) up to almost 25 h on-stream and then started to deactivate (X-Tol = 18 %, Y-BA = 12 %). The catalyst underwent deactivation due to the high amount of carbonaceous deposits. The surface analysis showed the loss of oxidised palladium species and excess of carbon on the surface of the catalyst during the reaction. Two types of carbon (B.E = 285 eV and 289.5 eV) were generated and one of them at value of 289.5 eV was believed to facilitate deactivation in the system. This deactivated 10Pd16Sb/TiO₂ - He catalyst was then subjected to regeneration / oxidising treatment by burning off the carbon from catalyst in presence of air. In order to obtain the best regeneration condition, the deactivated catalysts were heated in air for 2 h at four different temperatures (250-400 °C). After such treatment it was found that the deactivated catalyst could restore its lost activity at temperature of 250 °C and 300 °C, whereas higher temperature treatment of 350 °C and 400 °C did not help in restoring the lost activity. The catalyst nature was studied after such regeneration treatments to find out the reason for the inability of the catalyst treated at higher temperature to restore the activity. The XPS studies showed that treatment of the catalyst at 300 °C/2h/air could substantially regain back the oxidised Pd which was completely lost in the deactivated catalyst. In contrast, the catalyst treated at 350 °C/2h/air could not gain back oxidised

Pd on the surface of the catalyst. Additionally, migration of Sb and Pd to the deeper layers from the surface at higher temperature was also noticed.

Additionally, studies were done to check the stability and performance of the 10Pd16Sb/TiO₂ - He catalyst depending on the reaction pressure. The catalysts were tested in the pressure ranging from 1 to 10 bar at temperature of 210 °C and at a molar ratio of toluene : AcOH : O₂ : IG = 1 : 4 : 3 : 16. The activity was found to increase progressively with increasing pressure; For instance, at 1 bar reaction pressure X-Tol = 34 % which increased up to X-Tol = 75 % at 10 bar. The selectivity of the BA was also improved with increasing pressure, at 1 bar, S-BA = 74 % which increased up to S-BA = 100 % at 6 bar, but at even higher pressure, this selectivity of BA started to drop down. Even more, the stability of the catalysts in the long runs of reaction was affected by the pressure applied. The catalyst at lower pressure was found to be stable for longer time compared to the one subjected at higher pressure. The decline in stability of the catalyst with time at higher pressure was attributed due to the increase in the coke formation at higher pressure. BET surface area values showed that at lower pressure (1 and 2 bar), the catalyst exhibited surface area values of ~ 40 m²/g, but decrease in surface areas of the catalyst was observed at higher pressure with values in the range of 25-28 m²/g. A similar pore structure was observed for all of these catalysts but some decrease in pore volume of the catalyst treated at higher pressure was noted compared to other ones treated at lower pressure. The surface analysis from XPS showed that the reduction of oxidized Pd also varied with varying pressure, reduction was much faster at higher pressures and led to the formation of Pd^{δ-} species, which is considered to be a poison for the stability of the catalyst. These findings may account for the decline in stability at higher pressures.

Finally it was found in the present work that the gas phase acetoxylation of substituted toluenes with 10Pd16Sb/TiO₂ - He, under 210 °C and molar ratio toluene : AcOH : O₂ : IG = 1 : 4 : 3 : 16 is not a successful route. The various derivatives of toluene (Cl, F, OMe, Me) were tested but they were found to be inactive in this system. DFT calculations were made to understand such differences in the performance of these substrates. It was found out that all the derivatives of toluene could not be adsorbed on the Pd(111) surface of the catalyst, while toluene showed reasonably good adsorption over the catalyst and hence could generate corresponding ester.

The results presented in this work might open new perspectives for future designing of catalysts, which can further improve the stability and performance. Some investigations are necessary to understand the role of promoters, which has drastically improved the performance of the catalyst. A deeper study and attention on their behaviour can open new routes for the enhancement of the catalytic system. Further

analysis using in-situ methods are needed to confirm the defined nature of active sites, to identify the probable reaction mechanism and to derive structure-activity relationships. Some attempts are also required in the direction of gas phase acetoxylation of substituted toluene and other substrates. Design of the suitable catalysts and the optimization of the reaction parameters for the acetoxylation of substituted toluenes should be tried. Apart from varying the derivatives of toluene, some other sources of acetates (other than acetic acid, e.g. CO, acetic anhydride etc.) should be tested so that the problem of corrosion and GC analysis can be avoided. A kinetic model, based on the gas phase acetoxylation of toluene is rarely studied up to now; therefore the kinetic model and process development outcome of the system can provide valuable knowledge and hold of the system for any future investigations.

9. References

- [1] I. Chorkendorff, J.W. Niemantsverdriet, Introduction to Catalysis, pages 1-25, Wiley-VCH Verlag GmbH & Co. KGaA, 2005.
- [2] J. Hagen, Homogeneously Catalyzed Industrial Processes, pages 59-82, Wiley-VCH Verlag GmbH & Co. KGaA, 2006.
- [3] National Research Council Panel on New Directions in Catalytic Sciences and Technology, in, National Academy Press, Washington D.C 1992, pp. p. 1.
- [4] BCC, Report code CHM027D, (2011).
- [5] World Catalysts Market, 2011, <http://www.reportlinker.com/p097925/World-Catalysts-Market.html>.
- [6] J.A. Dumesic, G.W. Huber, M. Boudart, Principles of Heterogeneous Catalysis, pages 56-90, Wiley-VCH Verlag GmbH & Co. KGaA, 2008.
- [7] W.J. Biggar, North American Palladium Ltd., http://www.nap.com/Theme/NAP/files/NAP_Investor_Presentation_July_2011.pdf
- [8] World Production of Palladium, <http://www.stillwaterpalladium.com/production.html>.
- [9] International Business Times, 2011, <http://www.ibtimes.com/articles/121063/20110310/tight-supply-of-palladium-expected-for-2011.htm>.
- [10] Y. Li, D. Song, V.M. Dong, J. Am. Chem. Soc., 130 (2008) 2962.
- [11] R.J. Nielsen, W.A. Goddard, J. Am. Chem. Soc., 128 (2006) 9651.
- [12] D.C. Powers, D.Y. Xiao, M.A.L. Geibel, T. Ritter, J. Am. Chem. Soc., 132 (2010) 14530.
- [13] R. Mélenérez, G. Del Angel, V. Bertin, M.A. Valenzuela, J. Barbier, J. Mol. Catal. A: Chem., 157 (2000) 143.
- [14] C.R. Lederhos, M.J. Maccarrone, J.M. Badano, G. Torres, F. Coloma-Pascual, J.C. Yori, M.E. Quiroga, Appl. Catal. A: Gen, 396 (2011) 170.
- [15] L. Guczi, Z. Schay, G. Stefler, L.F. Liotta, G. Deganello, A.M. Venezia, J. Catal., 182 (1999) 456.
- [16] E. Gbenedio, Z. Wu, I. Hatim, B.F.K. Kingsbury, K. Li, Catal. Today, 156 (2010) 93.
- [17] V.M. Gryaznov, M.M. Ermilova, N.V. Orekhova, Catal. Today, 67 (2001) 185.
- [18] R. Maatman, W. Ribbens, B. Vonk, J. Catal., 31 (1973) 384.
- [19] L. Rodríguez, D. Romero, D. Rodríguez, J. Sánchez, F. Domínguez, G. Arteaga, Appl. Catal. A: Gen, 373 (2010) 66.
- [20] Studies in Surface Science and Catalysis, in: J.A. Moulijn, P.W.N.M.v. Leeuwen, R.A.v. Santen (Eds.) Stud. Surf. Sci. Catal., Elsevier, (1993). 461.
- [21] Y. Bi, H. Xu, W. Li, A. Goldbach, Int. J. Hydrogen Energy, 34 (2009) 2965.
- [22] Y. Sato, K. Terada, S. Hasegawa, T. Miyao, S. Naito, Appl. Catal. A: Gen, 296 (2005) 80.
- [23] I.A.C. Ramos, T. Montini, B. Lorenzuti, H. Troiani, F.C. Gennari, M. Graziani, P. Fornasiero, Catal. Today, In Press, Corrected Proof.
- [24] L.S.F. Feio, C.E. Hori, S. Damyanova, F.B. Noronha, W.H. Cassinelli, C.M.P. Marques, J.M.C. Bueno, Appl. Catal. A: Gen, 316 (2007) 107.
- [25] N. Iwasa, T. Mayanagi, W. Nomura, M. Arai, N. Takezawa, Appl. Catal. A: Gen, 248 (2003) 153.
- [26] M.A. Soria, C. Mateos-Pedrero, I. Rodríguez-Ramos, A. Guerrero-Ruiz, Catal. Today, In Press, Corrected Proof.
- [27] A. Martin, B. Lücke, Catal. Today, 57 (2000) 61.
- [28] P.M. Henry, Kuwer, Catalysis my metal complexes, pages 1-42, D. Redel publishing company, 1980.
- [29] J. Tsuji, Palladium Reagents and Catalysts, pages 35-98, Wiley, New York, 1995.
- [30] F.C. Phillips, Am. Chem. J, 16 (1894) 255.
- [31] C. van Giezen, M. Intven, M.D. Meijer, J.W. Geus, A. Mulder, G.J. Riphagen, J.P. Brouwer, Catal. Today, 47 (1999) 191.

- [32] E.H. Voogt, Palladium model catalysts, in, Proefschrift Universiteit Utrecht, utrecht, 1997.
- [33] T. Yoneyama, R.H. Crabtree, *J. Mol. Catal. A: Chem.*, 108 (1996) 35.
- [34] J. Tsuji, *Synthesis*, 9 (1990) 739.
- [35] P.M. Henry, Reidel, Dordrecht (1980) 310.
- [36] R.A. Sheldon, J.K. Kochi, Academic Press, New York (1981) 201.
- [37] H. Borchert, B. Jürgens, T. Nowitzki, P. Behrend, Y. Borchert, V. Zielasek, S. Giorgio, C.R. Henry, M. Bäumer, *J. Catal.*, 256 (2008) 24.
- [38] C. Samanta, V.R. Choudhary, *Chem. Eng. J. (Lausanne)*, 136 (2008) 126.
- [39] H. Zhu, Z. Qin, W. Shan, W. Shen, J. Wang, *J. Catal.*, 225 (2004) 267.
- [40] R.Q. Long, R.T. Yang, *Catal. Lett.*, 78 (2002) 353.
- [41] M.S. Kwon, I.S. Park, J.S. Jang, J.S. Lee, J. Park, *Org. Lett.*, 9 (2007) 3417.
- [42] E.W. Werner, M.S. Sigman, *J. Am. Chem. Soc.*, 132 (2010) 13981.
- [43] K. Pattamakomsan, E. Ehret, F. Morfin, P. Gélin, Y. Jugnet, S. Prakash, J.C. Bertolini, J. Panpranot, F.J.C.S. Aires, *Catal. Today*, 164 (2011) 28.
- [44] D. Seth, A. Sarkar, F.T.T. Ng, G.L. Rempel, *Chem. Eng. Sci.*, 62 (2007) 4544.
- [45] L. Torrente-Murciano, A.A. Lapkin, D.V. Bavykin, F.C. Walsh, K. Wilson, *J. Catal.*, 245 (2007) 272.
- [46] M. Caravati, J.-D. Grunwaldt, A. Baiker, *Catal. Today*, 92 (2004) 1.
- [47] J. Muzart, *Tetrahedron*, 59 (2003) 5789.
- [48] H. Krekel, W. Kronig, in: *Proc. 7th world Petrol. Congr*, 1968.
- [49] S.A. Miller, *Ethylene and its Industrial Derivatives*, pages 24-108, Ernest Benn limited London, 1969.
- [50] J. J. Moiseev, M.N. Vargaftic, J.K. Syrkin, *Dokl. Akad. Nauk SSSR*, 133 (1960) 377.
- [51] W. Schwerdtel, *Hydrocarbon proc*, 47 (1968) 187.
- [52] H. Fernholz, H. J. Schmidt, F. Wunderassigned, in: *Hoechst Aktiengesellschaft*, 1971.
- [53] L.M. Cirjak, M.F. Lemanski, D.R. Wagner, N.C. Benkalowycz, P.R. Blum, M.A. Pepera, C. Paparizos, US 5550281, (1996).
- [54] J.M. Davidson, P.C. Mitchell, N.S. Raghavan, *Front. Chem. React. Eng. (Proc. Int. Chem. React. Eng. Conf.)* 300 (1984).
- [55] T.C. Bissot, *Surface Impregnated Catalysts*, in: U.S 4048096, (1977).
- [56] E. Crathorne, D. MacGowan, S.R. Morris, A.P. Rawlinson, *J. Catal.*, 149 (1994) 254.
- [57] H. Lothar, F. Hans, U.S Pat. 3658888, (1967).
- [58] W. Kronig, G. Scharfe, U.S Pat. 3822308, (1974).
- [59] I. Rivalta, G. Mazzone, N. Russo, E. Sicilia, *J. Chem. Theory Comput.*, 5 (2009) 1350.
- [60] S.A. Schunk, A.L. de Oliveira, *Acetoxylation of Ethylene*, Wiley-VCH Verlag GmbH & Co. KGaA, 2008.
- [61] P. Voskanyan, *Catalysis in Industry*, 2 (2010) 167.
- [62] Y.F. Han, D. Kumar, D.W. Goodman, *J. Catal.*, 230 (2005) 353.
- [63] C.Y. Hou, L.R. Feng, F.L. Qiu, *Chin. Chem. Lett.*, 20 (2009) 865.
- [64] D. Kumar, M.S. Chen, D.W. Goodman, *Catal. Today*, 123 (2007) 77.
- [65] M.L. Luyben, B.D. Tyréus, *Comput. Chem. Eng.*, 22 (1998) 867.
- [66] N. Macleod, J.M. Keel, R.M. Lambert, *Appl. Catal. A: Gen*, 261 (2004) 37.
- [67] B. Samanos, P. Boutry, R. Montarnal, *J. Catal.*, 23 (1971) 19.
- [68] S. Nakamura, T. Yasui, *J. Catal.*, 17 (1970) 366.
- [69] BASF, in, Japan Kokai, 74-124010, 75-24204.
- [70] General Electronics, in, Japan Kokai, 75- 30809, 75-30810.
- [71] S. Uemura, A. Tabata, M. Okano, K. Ichikawa, *J. Chem. Soc., Chem. Commun.*, (1970) 1630.
- [72] H. Shinohara, *Appl. Catal.*, 10 (1984) 27.
- [73] C. Jia, P. Müller, H. Mimoun, *J. Mol. Catal. A: Chem.*, 101 (1995) 127.
- [74] P.W. Jolly, *Angew. Chem.*, 92 (1980) 975.
- [75] E. Benazzi, C.J. Cameron, H. Mimoun, *J. Mol. Catal.*, 69 (1991) 299.

- [76] D.R. Bryant, J.E. McKeon, B.C. Ream, *J. Org. Chem.*, 33 (1968) 4123.
- [77] L.M. Stock, K.-t. Tse, L.J. Vorvick, S.A. Walstrum, *J. Org. Chem.*, 46 (1981) 1757.
- [78] M.O. Unger, R.A. Fouty, *J. Org. Chem.*, 34 (1969) 18.
- [79] P.M. Henry, *J. Org. Chem.*, 36 (1971) 1886.
- [80] T. Tissue, W.J. Downs, *Chem. Commun.*, 410 (1969).
- [81] D.R. Bryant, J.E. McKeon, B.C. Ream, *Tetrahedron Lett.*, 9 (1968) 3371.
- [82] M.K. Starchevskii, M. N. Vargaftik, I.I. Moiseev, *Kinet. Katal.*, 20 (1979) 1163.
- [83] J.M. Davidson, C. Triggs, *Journal of the Chemical Society A: Inorganic, Physical, Theoretical*, (1968) 1331.
- [84] K. Bauer, D. Garbe, H. Surburg, *Ullmann's Encyclopaedia of Industrial Chemistry*, VCH, Weinheim, A 11 (1988) 141.
- [85] K. Ebitani, K.-M. Choi, T. Mizugaki, K. Kaneda, *Langmuir*, 18 (2002) 1849.
- [86] W.D. Provine, P.L. Mills, J.J. Lerou, Joe W. Hightower, W.N. Delgass, E. Iglesia, A.T. Bell, in: *Stud. Surf. Sci. Catal.*, 101, pages 191, 1996.
- [87] L. Ebersson, L.G. Gonzalez, *Acta Chem. Scand.*, 27 (1973) 1249.
- [88] S.K. Tanielyan, R.L. Augustine, *J. Mol. Catal.*, 87 (1994) 311.
- [89] L. Ebersson, E. Jonsson, *Acta Chemica Scandinavica B*, 28 (1974) 771.
- [90] T. Komatsu, K. Inaba, T. Uezono, A. Onda, T. Yashima, *Appl. Catal. A: Gen*, 251 (2003) 315.
- [91] A. Benhmid, K.V. Narayana, A. Martin, B. Lücke, M.M. Pohl, *Catal. Today*, 112 (2006) 192.
- [92] V.N. Kalevaru, A. Benhmid, J. Radnik, B. Lücke, A. Martin, *J. Catal.*, 243 (2006) 25.
- [93] A. Benhmid, K.V. Narayana, A. Martin, B. Lücke, S. Bischoff, M.M. Pohl, J. Radnik, M. Schneider, *J. Catal.*, 230 (2005) 420.
- [94] C.H. Bartholomew, *Appl. Catal. A: Gen*, 212 (2001) 17.
- [95] U. Lassi, Ph.D. Thesis : Deactivation Correlations of Pd/Rh Three-way Catalysts Designed for Euro IV Emission Limits, Department of Process and Environmental Engineering, University of Oulu, (2003).
- [96] X. Zheng, Q. Xiao, Y. Zhang, X. Zhang, Y. Zhong, W. Zhu, *Catal. Today*, In Press, Corrected Proof.
- [97] P. Albers, J. Pietsch, S.F. Parker, *J. Mol. Catal. A: Chem.*, 173 (2001) 275.
- [98] R. Pellegrini, G. Agostini, E. Groppo, A. Piovano, G. Leofanti, C. Lamberti, *J. Catal.*, In Press, Corrected Proof.
- [99] R.J. Card, J.L. Schmitt, J.M. Simpson, *J. Catal.*, 79 (1983) 13.
- [100] P. Euzen, J.-H. Le Gal, B. Rebours, G. Martin, *Catal. Today*, 47 (1999) 19.
- [101] R.J. Liu, P.A. Crozier, C.M. Smith, D.A. Hucul, J. Blackson, G. Salaita, *Appl. Catal. A: Gen*, 282 (2005) 111.
- [102] H.G. Karge, W. Nießen, H. Bludau, *Appl. Catal. A: Gen*, 146 (1996) 339.
- [103] Z. Pan, Y. Sha, *Appl. Catal. A: Gen*, 252 (2003) 347.
- [104] S.D. Jackson, I.J. Huntingdon, N.A. Hussain, S.R. Watson, *Stud. Surf. Sci. Catal.*, 126 (1999) 453.
- [105] B. Heinrichs, F. Noville, J.-P. Schoebrechts, J.-P. Pirard, *J. Catal.*, 220 (2003) 215.
- [106] S.D. Jackson, I.J. Huntingdon, N.A. Hussain, S.R. Watson, Furan hydrogenation over Palladium catalysts: Deactivation and regeneration, in: B. Delmon, G.F. Froment (Eds.) *Stud. Surf. Sci. Catal.*, Elsevier, pages 453, 1999.
- [107] P. Albers, K. Seibold, G. Prescher, H. Müller, *Appl. Catal. A: Gen*, 176 (1999) 135.
- [108] P.C. L'Argentiere, N.S. Fi'goli, *Appl. Catal.*, 61 (1990) 275.
- [109] S. Gatla, Ph.D Thesis: Impact of precursor materials and synthesis procedures on structure and performance of TiO₂- supported Pd catalysts in the gas-phase acetoxylation of toluene. Department of Catalytic in situ studies, Universität Rostock, (2011).
- [110] M. Behrens, *Angew. Chem.*, 122 (2010) 2139.
- [111] M. Campanati, G. Fornasari, A. Vaccari, *Catal. Today*, 77 (2003) 299.

-
- [112] G. Suresh, J. Radnik, V.N. Kalevaru, M.-M. Pohl, M. Schneider, B. Luecke, A. Martin, N. Madaan, A. Brueckner, *Phys. Chem. Chem. Phys.*, 12 (2010) 4833.
- [113] A.D. Becke, *J. Chem. Phys.*, 98 (1993) 1372.
- [114] C. Lee, W. Yang, R.G. Parr, *Physical Review B*, 37 (1988) 785.
- [115] C. T. Lee, W.T. Yang, R.G. Parr, *Phys. Rev. B*, 37 (1988) 785.
- [116] D. Andrae, U. Häußermann, M. Dolg, H. Stoll, H. Preuß, *Theor. Chem. Accounts Theor. Comput. Model Theor. Chim. Acta*, 77 (1990) 123.
- [117] J. Han, G. Zhu, D.Y. Zemlyanov, F.H. Ribeiro, *J. Catal.*, 225 (2004) 7.
- [118] NIST Standard Reference Database 20, V. 3.5, <http://srdata.nist.gov/xps>.
- [119] S.-Y. Lin, S.-L. Wang, Y.-S. Wei, M.-J. Li, *Surf. Sci.*, 601 (2007) 781.
- [120] J. Radnik, A. Benhmid, V.N. Kalevaru, M.-M. Pohl, A. Martin, B. Lücke, U. Dingerdissen, *Angew. Chem., Int. Ed.*, 44 (2005) 6771.
- [121] J.S. Stevens, S.L.M. Schroeder, *Surf. Interface Anal.*, 41 (2009) 453.
- [122] C.J. Powell, *Appl. Surf. Sci.*, 89 (1995) 141.
- [123] S.H. Oh, P.J. Mitchell, R.M. Siewert, *J. Catal.*, 132 (1991) 287.
- [124] J.G. McCarty, *Catal. Today*, 26 (1995) 283.
- [125] K. Okumura, T. Kobayashi, H. Tanaka, M. Niwa, *Appl. Catal., B*, 44 (2003) 325.
- [126] R. Delobel, H. Baussart, J.M. Leroy, J. Grimblot, L. Gengembre, *J. Chem. Soc., Faraday Trans.*, 179 (1983) 879.
- [127] S. Gatla, N. Madaan, J. Radnik, V.N. Kalevaru, M.M. Pohl, B. Lücke, A. Martin, A. Brückner, *Appl. Catal. A: Gen*, 398 (2011) 104.
- [128] M. Maciejewski, A. Baker, *Pure & Appl. Chem*, 67 (1995) 1879.
- [129] V.N. Kalevaru, A. Benhmid, J. Radnik, M.M. Pohl, B. Lücke, A. Martin, *Catal. Today*, 141 (2009) 317.
- [130] H. Gabasch, W. Unterberger, K. Hayek, B. Klotzer, E. Kleimenov, D. Teschner, S. Zafeiratos, M. Havecker, A. K. Gericke, R. Schlogl, J. Han, F. H. Ribeiro, B. A. Kiss, T. Curtin, D. Zemlyanov, *Surf. Sci.*, 600 (2006) 2980.
- [131] H.S. Fogler, *Elements of Chemical Reaction Engineering*, in, page 645-685, 2004.

Appendix

List of Abbreviations, Acronyms and Symbols used

Å	Angstrom
BE	Binding energy
BET	Brunauer-Emmett-Teller and their adsorption model
°C	Degree Celsius
DTA	Differential Thermal Analysis
EDX	Energy-Dispersive X-ray emission spectroscopy
e.g.	Exempli gratia
et al.	et alii
FID	Flame Ionization Detector
FTIR	Fourier Transform Infrared spectroscopy
GC	Gas Chromatography
GHSV	Gas Hourly Space Velocity
HPLC	High Performance Liquid Chromatography
HRTEM	High Resolution Transmission Electron Microscopy
i.e.	id est
ICP - OES	Inductive Coupled Plasma Optical Electron Spectroscopy
MFC	Mass Flow Controller
ml	milliliter
mm	millimeter
nm	nanometer
SEM	Scanning Electron Microscopy
TEM	Transmission Electron Microscopy
TGA	Thermogravimetric Analysis
XRD	X-ray Diffraction
XPS	X-ray Photoelectron Spectroscopy
µm	micrometer

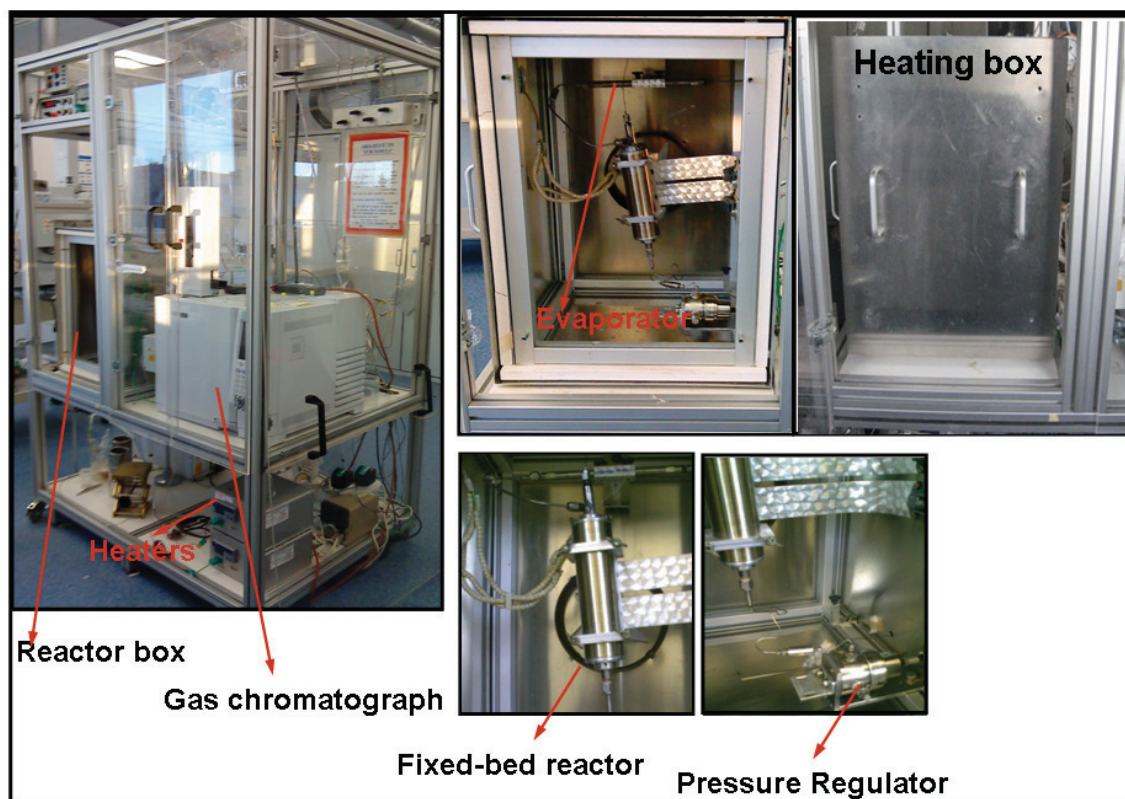


Fig. A1. Acetoxylation reaction setup consisting of gas chromatograph, mass flow controllers, heaters and the heating box containing fixed bed reactor, evaporator and the pressure regulator.

Catalyst Pressing

Calcined catalyst were pressed and sieved in the particle size range of 0.425-0.6 mm size, keeping in mind appropriate size to avoid diffusion limitations.

Empirical formula for the catalyst size depending on the reactor dimensions is

$(1/10 \text{ to } 1/15) \times \text{Internal diameter of the reactor}$

In the present case, reactor inner diameter is 6 mm; therefore the catalyst particles were sieved in the range of

$$\frac{1}{10} \cdot 6\text{mm} = 0.6\text{mm}$$

$$\frac{1}{15} \cdot 6\text{mm} = 0.4\text{mm}$$

Therefore, the catalysts were sieved in the range of 0.4-0.6 mm size

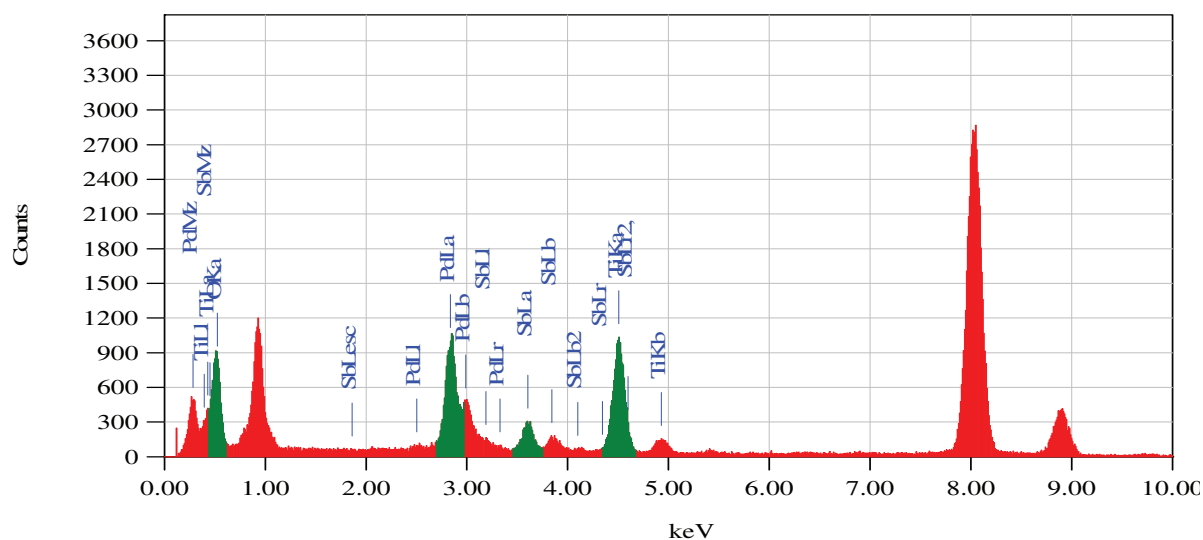


Fig. A2. EDX spectrum of the 10Pd16Sb/TiO₂, pre-treated in air for 300 °C after 11 h on-stream as indicated with the box in Fig. 7a

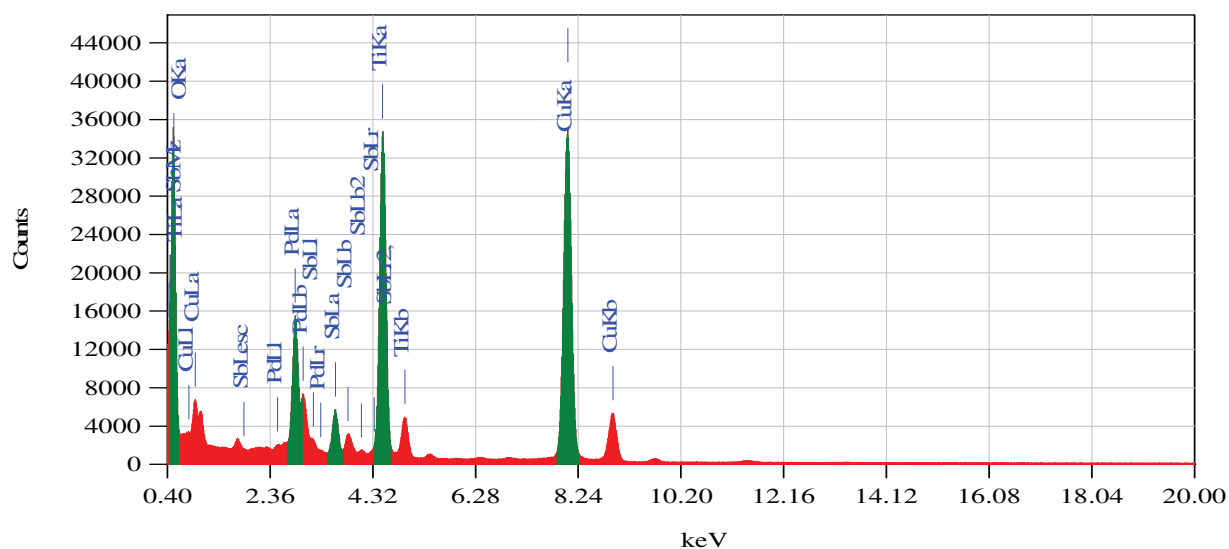


Fig. A3. EDX spectrum of the 10Pd16Sb/TiO₂, pre-treated in air for 300 °C after 32 h on-stream as indicated with the box in Fig. 9a.

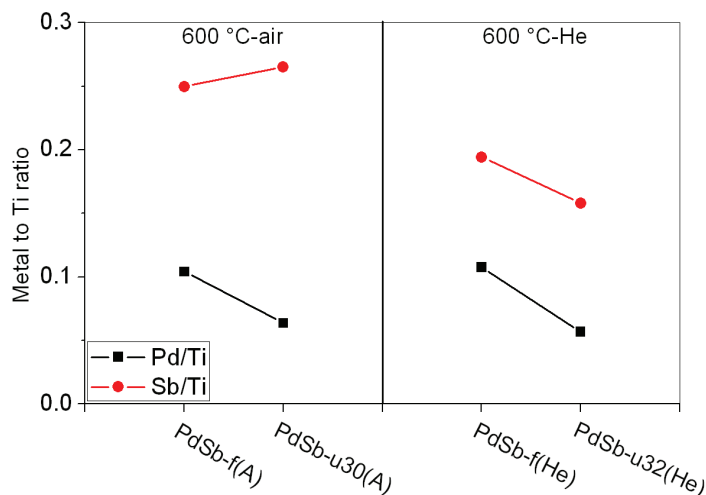


Fig. A4. Metal (Pd, Sb) to Ti surface atomic ratios for the fresh He and air pre-treated and spent of 10Pd16Sb/TiO₂ samples. Surface atomic ratios were calculated from the areas of the XPS Pd3d, Sb3d, Ti2p peaks.

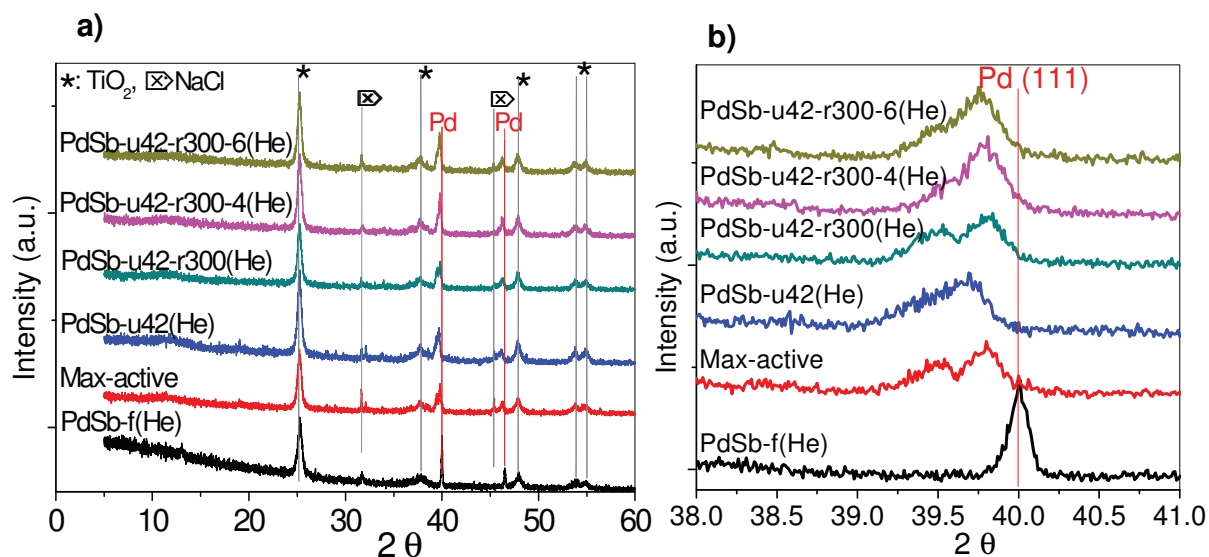


Fig.A5 a) XRD patterns of samples of fresh (PdSb-f(He)), maximum active, deactivated (PdSb-u42(He)), and regenerated 10Pd16Sb/TiO₂ - He catalysts for different duration in 300 °C air, for 2 hours (PdSb-u42-r300(He)) for 4 hours (PdSb-u42-r300-4(He) and 6 hours (PdSb-u42-r300-6(He). **b)** XRD patterns in the 2θ range of the Pd(111) reflection (38-41°).

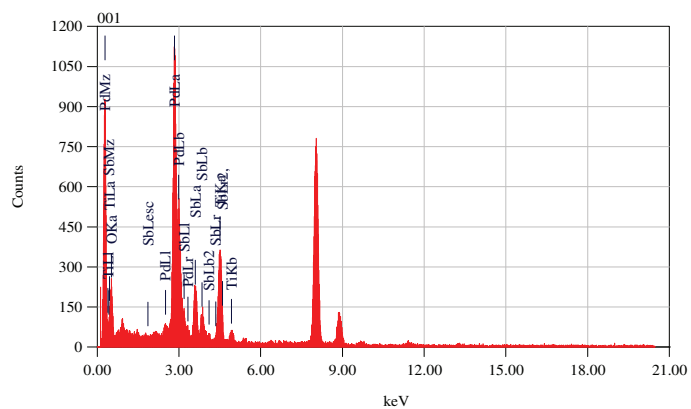
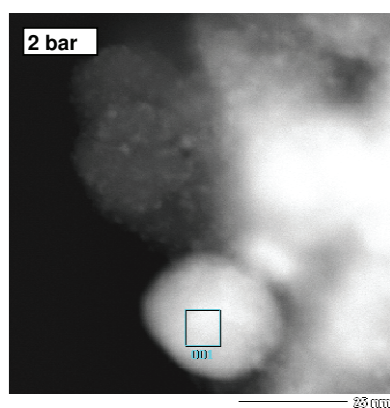
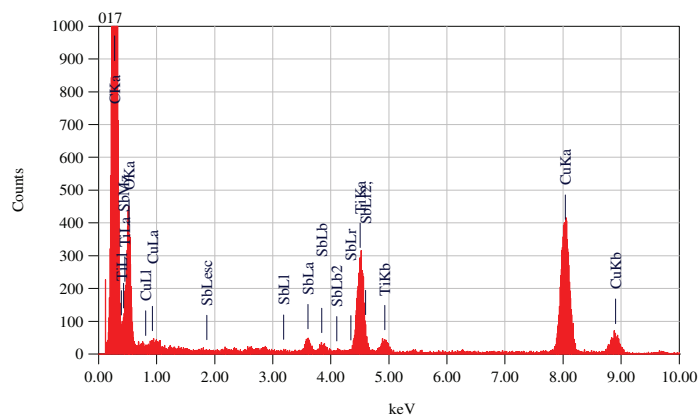
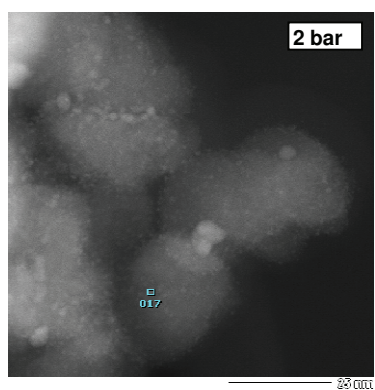
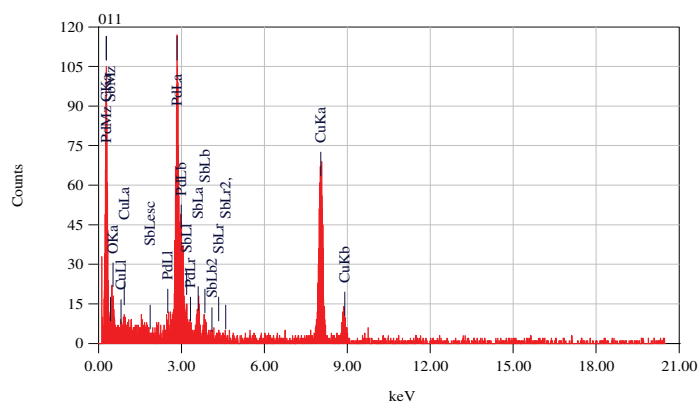
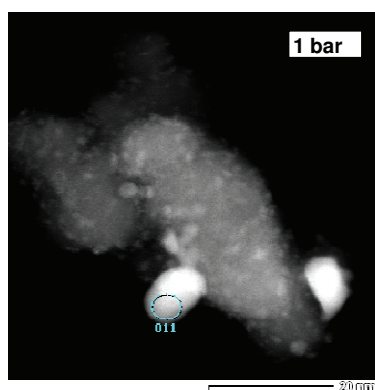


Fig. A6. EDX analysis of the samples of the maximum active $10\text{Pd}16\text{Sb}/\text{TiO}_2$ - He samples treated at 1 and 2 bar reaction pressure

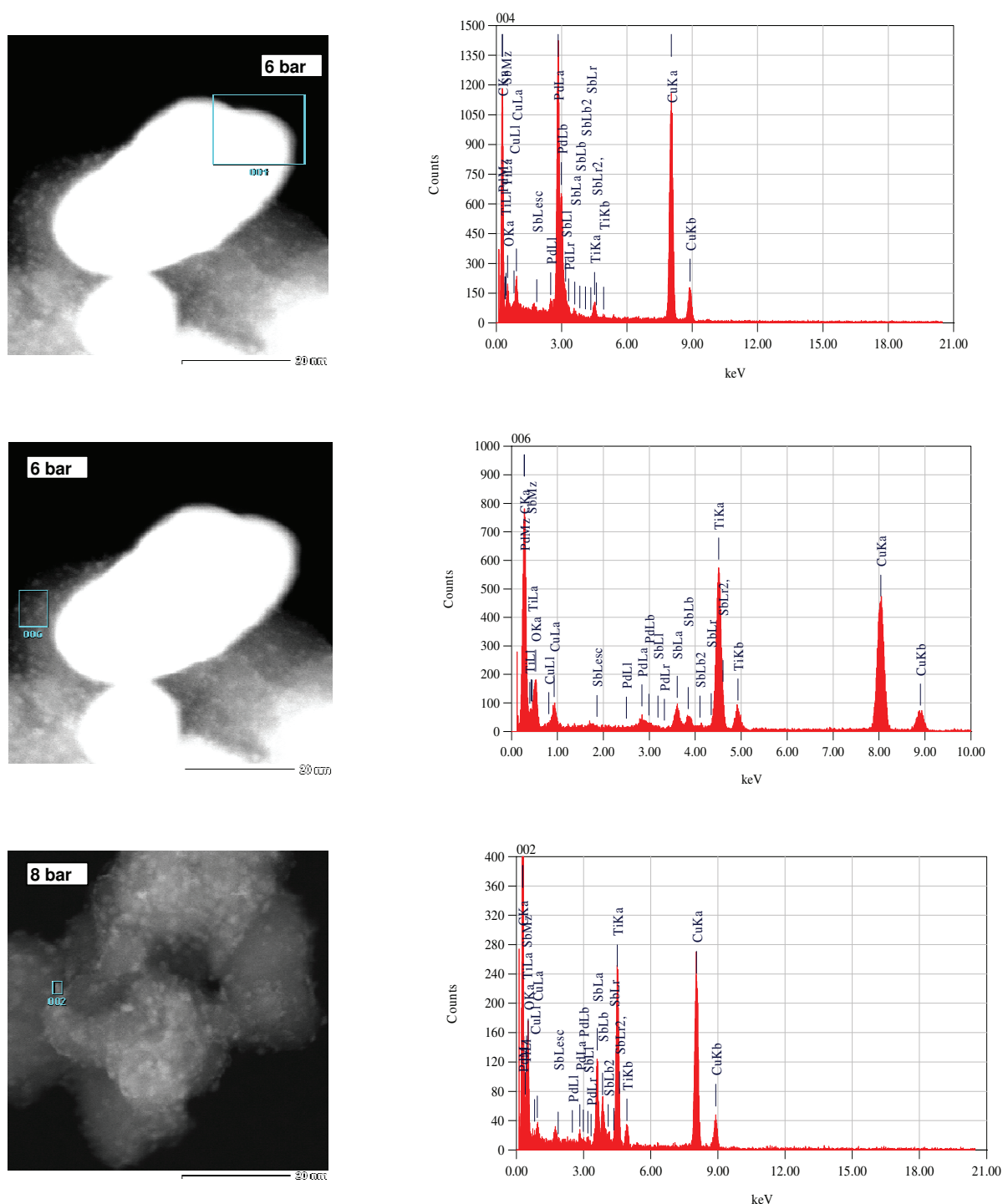


Fig. A7. EDX analysis of the samples of the maximum active $10\text{Pd}16\text{Sb}/\text{TiO}_2$ - He samples treated at 6 and 8 bar reaction pressure

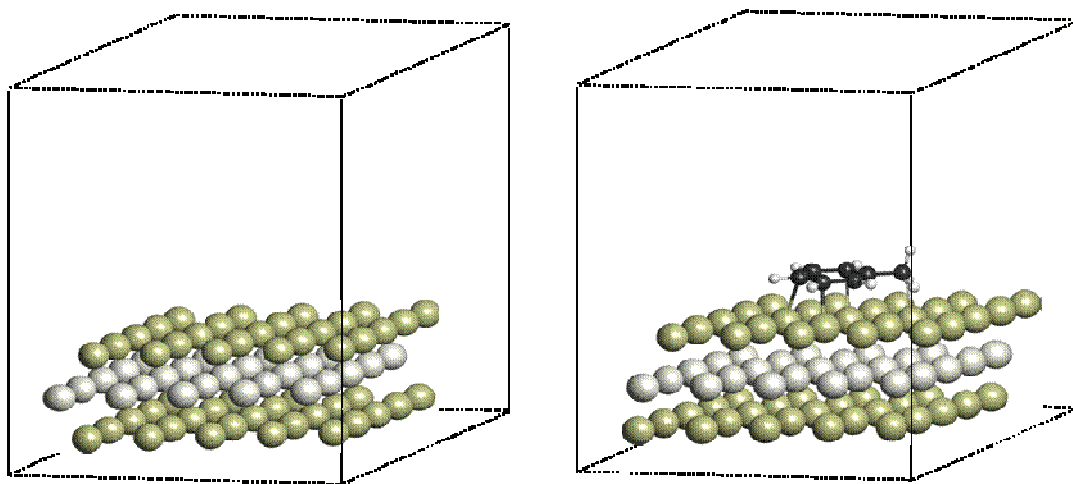


Fig. A8. a) free Pd(111) supercell b) substrate adsorbed on Pd(111) supercell

Table A1. Experiments done with 10Pd16Sb/TiO₂ - He catalyst with varying substituted toluene in presence of acetic acid and oxygen

Expts	Substituent	Feed composition	Organic feed(ml/h)	T (°C)	Pressure (bar)
1	p-xylene	1:4:3:16	1.68	210	2
2	p-xylene	1:4:3:16	1.68	230	2
3	p-xylene	1:4:3:16	1.68	250	2
4	p-xylene	1:4:3:16	1.68	300	2
5	p-xylene	1:4:3:16	1.68	320	2
6	p-xylene	1:4:3:16	1.68	350	2
7	p-xylene	1:4:3:16	1.68	400	2
8	p-xylene	1:4:3:16	1.68	210	4
9	p-xylene	1:4:3:16	1.68	210	6
10	p-xylene	1:4:3:16	1.68	300	4
11	p-xylene	1:4:3:16	1.68	300	6
12	p-xylene	1:4:6:32	0.84	210	2
13	p-xylene	1:4:6:32	0.84	210	2
14	p-xylene	1:4:3:32	0.84	210	2
15	p-xylene	1:4:3:16	0.84	210	2
16	m-xylene	1:4:3:16	1.68	210	2
17	m-xylene	1:4:3:16	1.68	250	2
18	m-xylene	1:4:3:16	1.68	300	2
19	mesitylene	1:4:3:16	1.68	210	2
20	p-chlorotoluene	1:4:3:16	1.68	210	2
21	p-chlorotoluene	1:4:3:16	1.68	230	2
22	p-chlorotoluene	1:4:3:16	1.68	250	2
23	p-chlorotoluene	1:4:3:16	1.68	300	2

24	p-chlorotoluene	1:4:3:16	1.68	320	2
25	p-chlorotoluene	1:4:3:16	1.68	350	2
26	p-chlorotoluene	1:4:3:16	1.68	400	2
27	p-chlorotoluene	1:4:3:16	1.68	210	4
28	p-chlorotoluene	1:4:3:16	1.68	210	6
29	p-chlorotoluene	1:4:3:16	1.68	300	4
30	p-chlorotoluene	1:4:3:16	1.68	300	6
31	p-chlorotoluene	1:4:3:32	0.84	250	2
32	p-fluorotoluene	1:4:3:16	1.68	210	2
33	p-fluorotoluene	1:4:3:16	1.68	250	2
34	p-methoxytoluene	1:4:3:16	1.68	210	2
35	p-methoxytoluene	1:4:3:16	1.68	250	2
36	p-methoxytoluene	1:4:3:16	1.68	300	2
37	m-methoxytoluene	1:4:3:16	1.68	210	2
38	m-methoxytoluene	1:4:3:16	1.68	250	2
39	m-methoxytoluene	1:4:3:16	1.68	300	2
40	o-xylene	1:4:3:16	1.68	210	2
41	o-chlorotoluene	1:4:3:16	1.68	230	2

Table A2. Energy values of the heterolytic cleavage (cationic)

Cationic C-H cleavage (compared to toluene)	$\Delta(\text{Total Energy})$ [kJ/mol]	$\Delta(E)$ [kJ/mol]	$\Delta(G)$ [kJ/mol]	$\Delta(H)$ [kJ/mol]	$\Delta(S)$ [J/mol*K]
o-Fluoro	14	14	13	14	2
o-Chloro	13	12	9	12	7
o-Methyl	-18	-18	-24	-18	12
o-Methoxy	-54	-53	-57	-53	8
m-Fluoro	27	26	25	26	3
m-Chloro	24	22	21	22	3
m-Methyl	-14	-15	-18	-15	6
m-Methoxy	-10	-11	-10	-11	-2
p-Fluoro	-4	-4	-4	-4	1
p-Chloro	-5	-5	-4	-5	-1
p-Methyl	-32	-33	-34	-33	2
p-Methoxy	-75	-74	-75	-74	1

The stabilization energy of the positive charge is especially for substituents in para position favourable. In general methyl (34 kJ/mol) und methoxy (75 kJ/mol) stabilises the positive charge considerably better.

Table A3. Energy values of the heterolytic cleavage (anionic)

Anionic cleavage (compared to toluene)	C-H	$\Delta(\text{Total Energy})$ [kJ/mol]	$\Delta(\text{E})$ [kJ/mol]	$\Delta(\text{G})$ [kJ/mol]	$\Delta(\text{H})$ [kJ/mol]	$\Delta(\text{S})$ [J/mol*K]
o-Fluoro		-16	-15	-16	-15	2
o-Chloro		-31	-29	-31	-29	5
o-Methyl		-6	-6	-7	-6	2
o-Methoxy		9	9	5	9	8
m-Fluoro		-26	-25	-27	-25	3
m-Chloro		-35	-34	-35	-34	2
m-Methyl		0	-1	-5	-1	8
m-Methoxy		-2	-2	-2	-2	1
p-Fluoro		-4	-3	-5	-3	4
p-Chloro		-28	-26	-27	-26	1
p-Methyl		6	10	-3	10	25
p-Methoxy		20	16	22	16	-14

The stabilization energy of the negative charge is on almost all substituents more favorable than on toluene. Especially halogen substituents in meta position are good for an anionic C-H Cleavage.

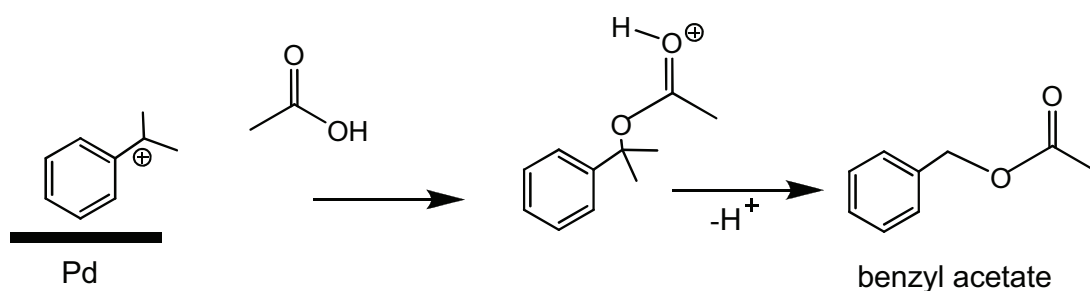
Table A4. Energy values of the homolytic cleavage (radical)

Radical cleavage (compared to toluene)	C-H [kJ/mol]	$\Delta(\text{Total Energy})$ [kJ/mol]	$\Delta(E)$ [kJ/mol]	$\Delta(G)$ [kJ/mol]	$\Delta(H)$ [kJ/mol]	$\Delta(S)$ [J/mol*K]
o-Fluoro	2		2	2	2	2
o-Chloro	3		3	0	3	6
o-Methyl	-1		0	-3	0	6
o-Methoxy	-1		0	-4	0	7
m-Fluoro	1		1	-1	1	3
m-Chloro	1		1	-1	1	3
m-Methyl	-1		-1	-5	-1	9
m-Methoxy	2		2	3	2	-3
p-Fluoro	0		0	-1	0	2
p-Chloro	-1		-1	-1	-1	0
p-Methyl	-2		-2	-3	-2	2
p-Methoxy	-4		-3	-5	-3	3

The stabilization energy doesn't differ substantially from the rests of o, m and p positions. Me and OMe in ortho or para positions stabilize the radical the best

Table A5. Thermodynamic data for the acetoxylation reaction of the various substrates mentioned without catalyst

Thermodynamic of the rxn (compared to Toluene)	$\Delta(\text{Total Energy})$ (kJ/mol)	$\Delta(E)$ (kJ/mol)	$\Delta(G)$ (kJ/mol)	$\Delta(H)$ (kJ/mol)	$\Delta(S)$ (J/molK)
o-Fluoro	4	8	-5	8	26
o-Chloro	5	9	-5	9	29
o-Methyl	1	5	-11	5	32
o-Methoxy	2	5	-9	5	30
m-Fluoro	2	6	-7	6	27
m-Chloro	2	6	-7	6	27
m-Methyl	0	-1	-1	-1	0
m-Methoxy	0	4	-5	4	19
p-Fluoro	0	4	-9	4	26
p-Chloro	1	5	-7	5	24
p-Methyl	-1	3	-10	3	26
p-Methoxy	0	3	-11	3	30

**Scheme A1. Attack of acetic acid on the benzylic cation to form benzyl acetate**

List of Publications

- 1) V.N. Kalevaru, N. Madaan, A. Martin; "Synthesis, characterization and catalytic performance of titania supported VPO catalysts for the ammoxidation of 3-picoline"; *Appl. Catal. A: Gen.*, 391 (2011) 52-62.
- 2) Gatla Suresh, Jörg Radnik, Venkata Narayana Kalevaru, Marga-Martina Pohl, Matthias Schneider, Bernhard Lücke, Andreas Martin, Neetika Madaan and Angelika Brückner; "Tailoring the synthesis of supported Pd catalysts towards desired structure and size of metal particles", *PCCP* 12 (2010) 4833-4842.
- 3) S. Gatla, N. Madaan, J. Radnik, V.N. Kalevaru, M.-M. Pohl, B. Lücke, A. Martin, A. Brückner; "Key properties promoting high activity and stability of supported PdSb/TiO₂ catalysts in the acetoxylation of toluene to benzyl acetate", *Appl. Catal. A: Gen.*, 398 (2011) 104-112.
- 4) N. Madaan, S. Gatla, V. N. Kalevaru, J. Radnik, B. Lücke, A. Brückner, A. Martin. "Deactivation and regeneration studies on PdSb/TiO₂ catalyst in gas phase acetoxylation of toluene", *J. Catal.* (2011), doi:10.1016/j.jcat.2011.06.005.
- 5) N. Madaan, S. Gatla, V.N. Kalevaru, J. Radnik, B. Lücke, A. Brückner, A. Martin; "Optimization of reaction conditions and regeneration procedure of the PdSb/TiO₂ catalyst for acetoxylation of toluene", *Top. Catal.* (2011) accepted
- 6) S. Gatla, N. Madaan, J. Radnik, V.N. Kalevaru, U.Bentrup, B. Lücke, A. Martin, A. Brückner "Role of co-components on the state of Pd and the catalytic performance in the gas phase acetoxylation of toluene", *ChemCatChem* (2011) accepted
- 7) N. Madaan, S. Gatla, V. N. Kalevaru, J. Radnik, B. Lücke, A. Brückner, A. Martin. "Effect of reaction pressure on the performance of 10Pd16Sb/TiO₂ catalyst in gas phase acetoxylation of toluene to benzyl acetate", *Catal. Commun.* (2011) submitted.
- 8) Q. Smejkal, L. Smejkal, N. Madaan, V.N. Kalevaru, A. Martin; "Simplified kinetic study of toluene acetoxylation to benzyl acetate over titania based Pd-containing" (2011) in preparation.
- 9) Gatla Suresh, Neetika Madaan, Jörg Radnik, Venkata Narayana Kalevaru, Marga-Martina Pohl, Bernhard Lücke, Andreas Martin, Angelika Brückner. "Highly selective rutile supported Pd,Sb catalyst in the gas phase acetoxlyation of toluene" *Chem. Commun.* (2011) in preparation.

List of symposia contributions

- 1) 42 Jahrestreffen Deutscher Katalytiker in Weimar, Germany, from 11 to 13 March 2009 "Investigations on the ammoxidation activity of TiO_2 supported VPO catalysts"; N. Madaan, V.N. Kalevaru, A. Martin. (Oral presentation)
- 2) 42 Jahrestreffen Deutscher Katalytiker in Weimar, Germany, from 11 to 13 March 2009 "Influence of synthesis and calcination conditions on composition and particle size of active Pd-containing methyl aromatic acetoxylation catalysts"; G. Suresh, J. Radnik, N. Madaan, V.N. Kalevaru, M.-M Pohl, M. Schneider, B. Lücke, A. Martin, A. Brückner. (Poster presentation)
- 3) 6th World Congress on Oxidation Catalysis, Towards an integrated approach in innovation and development, Lille, France, July 5-10, 2009. "Studies on preparation, characterization and ammoxidation activity of TiO_2 supported VPO catalysts"; N. Madaan, V.N. Kalevaru, A. Martin. (Poster presentation)
- 4) The 10th International Symposium on the "Scientific Bases for the Preparation of Heterogeneous Catalysts" in Louvain-la-Neuve, Belgium, from 11-15 July 2010. "Tuning the active Pd catalysts by thermal treatments: Effect of metal precursors, ammonium additives and calcination atmospheres"; G. Suresh, J. Radnik, N. Madaan, V.N. Kalevaru, M.-M Pohl, M. Schneider, B. Lücke, A. Martin, A. Brückner. (Poster presentation)
- 5) 14th Nordic Symposium on Catalysis, August 29-31, 2010 in Helsingør, Denmark. "Influence of thermal treatment on the catalytic performance of Pd-Sb/ TiO_2 catalyst for acetoxylation of toluene"; N. Madaan, S. Gatla, V.N. Kalevaru, J. Radnik, B. Lücke, A. Brückner, A. Martin. (Poster presentation)
- 6) 9th Congress on Catalysis applied to Fine Chemicals (CAFC9), Zaragoza, Spain, from 13-16 September 2010. "Tailoring the synthesis of supported Pd acetoxylation catalysts towards high stability and selectivity"; S. Gatla, N. Madaan, J. Radnik, V.N. Kalevaru, B. Lücke, A. Martin, A. Brückner. (Oral presentation)
- 7) DECHEMA-Jahrestagung der Biotechnologen und ProcessNet-Jahrestagung 2010., Eurogress Aachen, Germany, from 21-23 September 2010. "Novel preparation routes for PdSb/ TiO_2 catalysts for the acetoxylation of toluene"; G. Suresh, N. Madaan, J. Radnik, V.N. Kalevaru, B. Lücke, A. Martin, A. Brückner. (Poster presentation)

-
- 8) 13th Norddeutsches Doktorandenkolloquium at Ernst-Moritz-Arndt Universität Greifswald, Germany, from 24-25 September 2010 "Improving the performance of promoted Pd/TiO₂ catalysts in the acetoxylation of toluene by tailored synthesis procedures"; S. Gatla, N. Madaan, J. Radnik, V.N. Kalevaru, B. Lücke, A. Martin, A. Brückner. (Oral presentation)
 - 9) 44 Jahrestreffen Deutscher Katalytiker in Weimar, Germany, from 16-18 march "Effect of varying reaction parameters on activation, deactivation and regeneration of PdSb/TiO₂ in gas phase acetoxylation of toluene"; N. Madaan, S. Gatla, V.N. Kalevaru, J. Radnik, B. Lücke, A. Brückner, A. Martin. (Oral presentation)
 - 10) 44 Jahrestreffen Deutscher Katalytiker in Weimar, Germany, from 16-18 march 2011 "Effect of co-components on the performance of Pd based catalysts for the gas phase acetoxylation of toluene"; S. Gatla, N. Madaan, J. Radnik, V.N. Kalevaru, B. Lücke, A. Martin, U. Bentrup, A. Brückner. (Poster presentation)
 - 11) 13th JCF Frühjahrssymposium, Erlangen, Germany, March 23-26 2011 "Investigations on the deactivation and regeneration of PdSb/TiO₂ catalysts in gas phase acetoxylation of toluene"; N. Madaan, S. Gatla, V.N. Kalevaru, J. Radnik, B. Lücke, A. Brückner, A. Martin. (Poster presentation)
 - 12) 2nd Indo-German Catalysis Conference: Catalysis for renewable energy, Rostock, Germany, from 19-22 June 2011. "Effect of total pressure on the catalytic performance of a 10Pd16Sb/TiO₂ catalyst in the gas phase acetoxylation of toluene"; N. Madaan, S. Gatla, V.N. Kalevaru, J. Radnik, B. Lücke, A. Brückner, A. Martin. (Poster presentation)
 - 13) 2nd Indo-German Catalysis Conference: Catalysis for renewable energy, Rostock, Germany, from 19-22 June 2011. "Influence of metals M on the performance of Pd,M/TiO₂ catalysts in the gas phase acetoxylation of toluene to benzyl acetate"; S. Gatla, N. Madaan, J. Radnik, V.N. Kalevaru, B. Lücke, A. Martin, U. Bentrup, A. Brückner. (Poster presentation)
 - 14) 2nd Indo-German Catalysis Conference, Catalysis for renewable energy, Rostock, Germany, from 19-22 June 2011. "Dependence of catalytic performance on the particle size of Pd in acetoxylation of toluene"; V.N. Kalevaru, N. Madaan, S. Gatla, J. Radnik, B. Lücke, A. Brückner, A. Martin. (Keynote lecture)